Dissertation zur Erlangung des Doktorgrades

der Fakultät für Chemie und Pharmazie

der Ludwig-Maximilians-Universität München

# COORDINATION CHEMISTRY OF BARBITURIC ACID, ITS DIETHYL DERIVATIVE AND BENZILDIIMINE WITH TRANSITION METALS
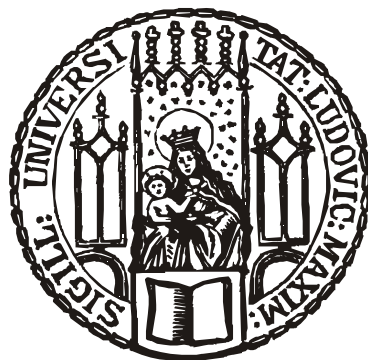
NADERA HAQUE

aus

Dhaka (Bangladesch)

2009

*TO*

*MY FAMILY*

Die vorliegende Arbeit wurde in der Zeit von Januar 2006 bis März 2009 am
Department für Chemie und Biochemie der Ludwig-Maximilians-Universität München
unter Anleitung von


**Prof. Dr. Ingo-Peter Lorenz**


angefertigt.

# TABLE OF CONTENTS

# LIST OF FIGURES

# LIST OF SCHEMES

# List of Abbreviations

| | |
|---|---|
| Ar | Aryl |
| asym. | asymmetric |
| Hdebarb | Diethylbarbiturate monoanion |
| $H_2$debarb | 5,5-Diethylbarbituric acid |
| Cp | $\eta^5$-Cyclopentadienyl |
| Cp* | $\eta^5$-Pentamethylcyclopentadienyl |
| Cq | quaternary carbon atom |
| d | Day |
| decomp. | Decomposition |
| DNA | Deoxyribonucleic acid |
| eq. | equivalent |
| Et | Ethyl |
| h | hour |
| $H_2$BDI | Benzildiimine |
| IR | infrared |
| Me | Methyl |
| MeOH | Methanol |
| Min | Minutes |
| NBA | m-Nitrobenzylalkohol |
| Na[Hdebarb] | Sodium barbiturate |
| NMR | Nuclear Magnetic Resonance |
| NaOMe | Sodium methoxide |
| ORTEP | Oak Ridge Thermal Ellipsoid Plot |
| AgOTf | Silvertrifluoromethylsulfonate |
| Ph | Phenyl |
| *p*-cym/*p*-cymene | 1-isopropyl-4-methylbenzene |
| ppm | parts per million |
| RT | Room temperature |
| sym. | symmetric |
| $Si_2$BDI | Benzil-bis(trimethylsilyl)diimine |

Other symbols and abbriviations used for NMR, IR, Mass spectra and molecular structure analysis are given in the experimental section.

x

# 1   INTRODUCTION

## 1.1   History and importance of Barbituric acid derivatives

The coordination chemistry of organotransition-metal complexes with biologically active ligands has attracted enormous interest over the years. The study of such complexes may lead to a greater understanding of the role of these ligands in biological systems, and may also contribute to the development of new metal-based chemotherapeutic agents. The compounds containing pyrimidine ring play an important role in many biological systems, where they exist in nucleic acids, several vitamins, coenzymes and antibiotics. [1, 2] The nucleic acid is related to antimetabolites used in anticarcinogenic chemotherapy.[3] Metal complexes of pyrimidine have been extensively studied in recent years owing to their great variety of biological activity ranging from antimalarial, antibacterial, antitumoral, antiviral activities etc.[4, 5, 6, 7, 8, 9, 10] Despite the plethora of coordination complexes of pyrimidines, the organometallic chemistry involving these ligands has received limited attention, with most efforts coming from the laboratory of Beck and co-workers.[11, 12]

The derivatives of barbituric acid (2, 4, 6-trioxypyrimidine) (**1**) are known as barbiturates. They are a class of drugs that have diverse applications such as sedatives, hypnotics and anticonvulsants under a variety of conditions and are also employed for anesthesia.[13, 14] For example, phenytoin (5,5-diphenylhydantoin), one of the cyclic ureides related in structure to the barbiturate, was reported to be the least hypnotic, most strongly anticonvulsant and most effective against grand mal. They are also used for the treatment of anxiety, epilepsy and other psychiatric disorders and possess effects on the motor and sensory functions.[15, 16] Barbituric acid is used in the manufacture of plastics and pharmaceuticals products.[17] One of the earliest barbiturates introduced in medical use is 5,5-diethylbarbituric acid ($H_2$debarb) (**2**), also known as barbital, veronal or diemal.[18] First synthesized by E. Fischer in 1903, it is chemically the simplest hypnotic barbiturate.[19] Although many barbiturates display sedative-hypnotic activity, only a few have anticonvulsant properties. Paradoxically many barbiturates cause convulsions at larger doses. Phenobarbital (5-ethyl-5-phenylbarbituric acid) is the drug used most commonly for convulsive disorders and is the drug of choice for infants and young children.[20] Although **2** discontinued as a sedative-hypnotic, the

biological consequence of its low lipid/water partition coefficient makes it interesting.[19] Veronal is usually used as its sodium salt (**3**) which is derived from its tautomeric form and it is water-soluble and more readily absorbed than its parent compound **2**.
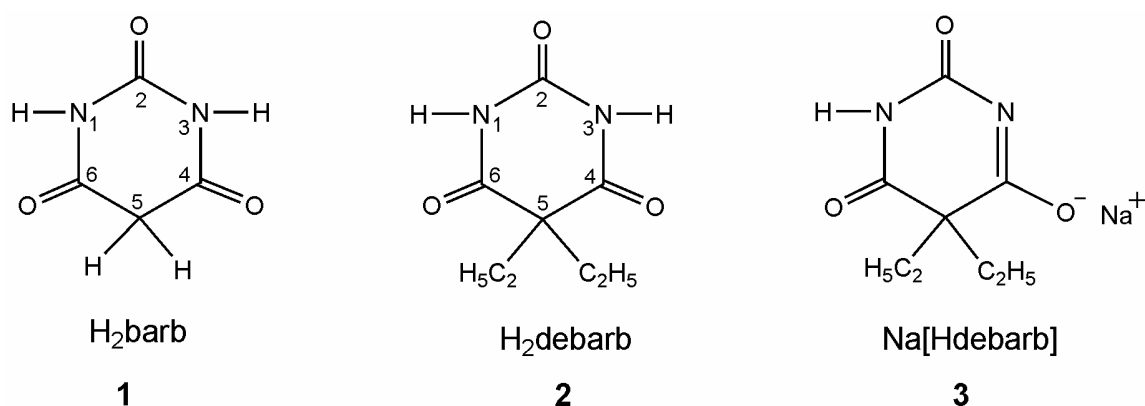


**Figure 1**: Barbiturate ligands used in this study.

Because of the wide range of medicinal applications of barbiturates and their ability to coordinate with transition metals through one or both deprotonated nitrogen and carbonyl oxygen atoms, synthesis of their metal complexes has attracted considerable attention.

## 1.1.1  Synthesis and characteristics of barbiturates

Barbiturates are cyclic ureides and are formed when a dicarboxylic acid reacts with urea. The acids used are generally in the form of ester and are condensed in the presence of sodium ethoxide (i.e., $C_2H_5$-ONa).[21]

Many cyclic ureides are derived from malonic acid or malonic esters. They are collectively known as 'barbiturates' because of their relationship of melonyl urea or barbituric acid. Barbituric acid ($H_2$barb, **1**) is prepared by the interaction of urea and malonyl dichloride or diethyl malonate (Scheme 1).[21]
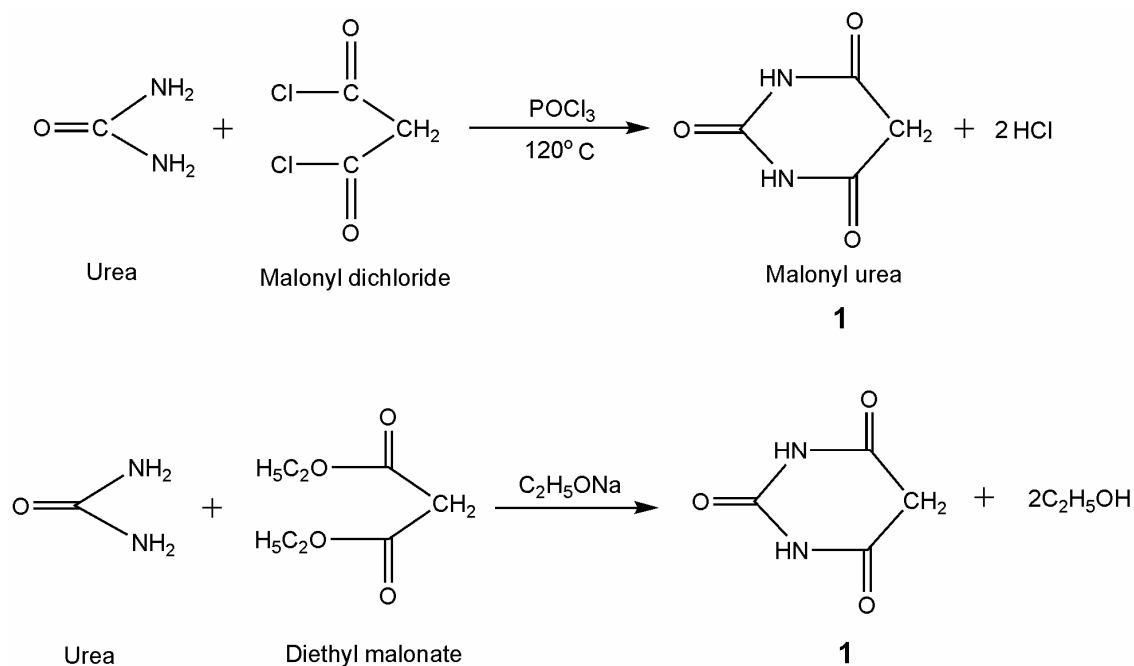
**Scheme 1**: Synthesis of H$_2$barb (**1**).

The cyclic ureides containing a six membered ring are also regarded as derivatives of the fundamental type pyrimidine or 1:3-diazine.

The acidic nature of hydrogens in barbituric acid is ascribed to lactam-lactim tautomerism. As barbituric acid contains three lactam groups, in principle, one, two, or all three groups may take up the structure of the lactim group (Figure 2).[20]
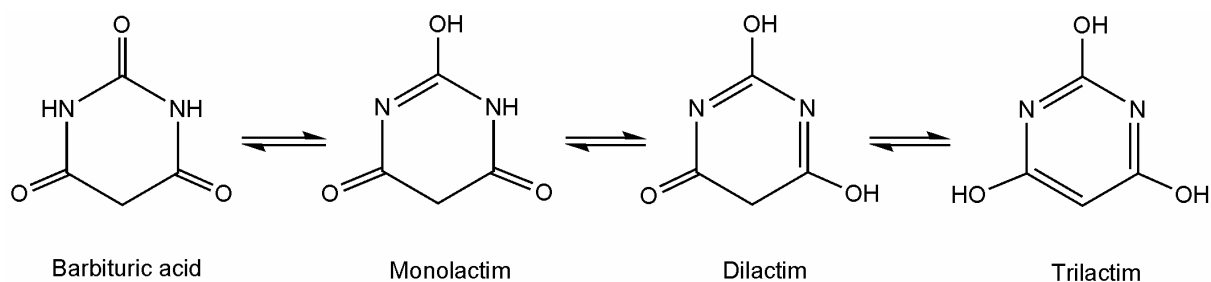


**Figure 2**: Tautomerism observed in **1**.

In the crystalline state, barbituric acid exists as the trioxo tautomer, as shown by X-ray analysis.

3

Condensation reactions are usually used in the preparation of barbituric acid derivatives. These reactions may take place in acidic, neutral or basic media. Veronal (**2**) is prepared by the condensation of urea with diethyl malonoic ester in the presence of sodium ethoxide followed by the elimination of two molecules of ethanol (Scheme 2).[21, 22]
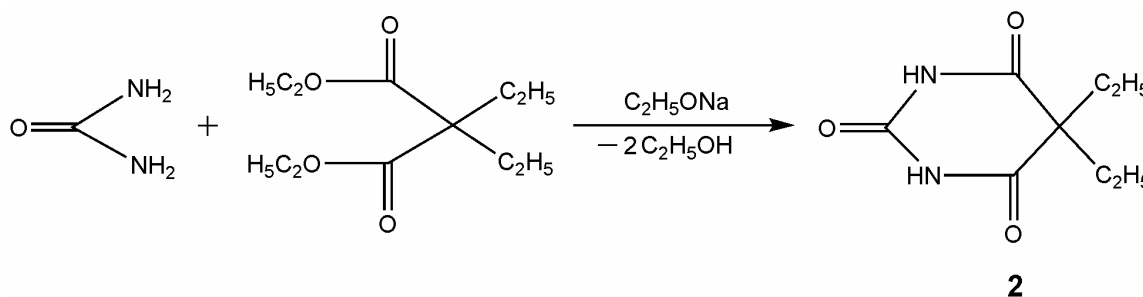


**Scheme 2**: Synthesis of $H_2$debarb (**2**).

However, it is interesting to observe that the barbituric acid itself does not possess any hypnotic properties, but such a characteristic is conferred only when the hydrogen atoms at C-5 are replaced by organic groups (alkyl or aryl). In 1951, Sandberg made his fundamental postulation that, to possess good hypnotic activity, a barbituric acid must be a weak acid and must have a lipid/water partition coefficient between certain limits.[23] Therefore only the 5,5-disubstituted and the 1,5,5-trisubstituted barbituric acids possess acceptable hypnotic, anticonvulsant or anesthetic activity. All other substitution patterns such as 5-monosubstituted barbituric acids, 1,3-disubstituted barbituric acids, or 1,3,5,5-tetrasubstituted barbituric acids are inactive or produce convulsions. As the number of carbon atoms at the fifth carbon position increases, the lipophilic character of the substituted barbituric acids also increases. Branching, unsaturation, replacement of alicyclic or aromatic substituents for alkyl substituents, and introduction of halogen into the alkyl substituents all increase the lipid solubility of the barbituric acid derivatives [22].

The 5,5-disubstituted barbituric acid contains three lactam groups that can undergo pH dependent lactim-lactam tautomerization (Scheme 3). [22]
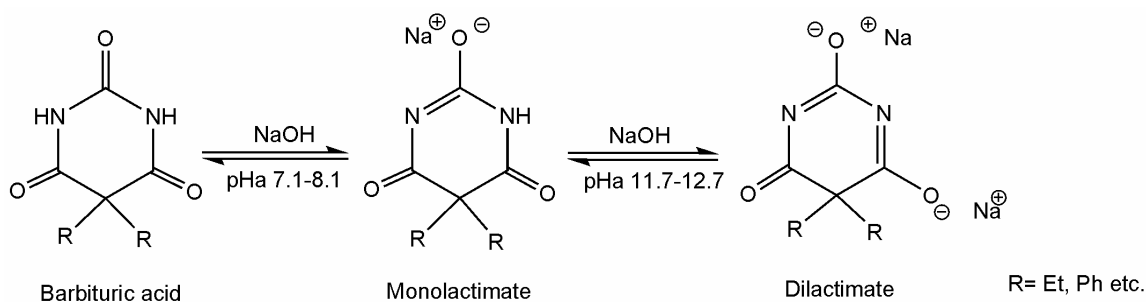
**Scheme 3**: pH dependent tautomerization of disubstituted barbituric acid.

The ultraviolet spectroscopic study of **1** shows that in aqueous solutions it predominates either in the dioxo tautomeric (in alkaline medium) or in the trioxo tautomeric form (in acidic medium).[20] The acidity of barbiturates in aqueous solution depends on the number of substituents attached to the barbituric acid. The dissociation constant (pK) of unsubstituted barbituric acid is 4.12; the pK value of 5,5-disubstituted barbituric acids ranges from 7.1 to 8.1 which indicates that these are relatively weak acids.[22] Although 5,5-disubstituted barbituric acids are weakly acidic because these compounds exist predominantly in the trioxo tautomeric form, salts of these barbiturates are easily formed by the treatment with bases. These acids can undergo a second ionization, when the pKa values are in the range of 11.7-12.7 (Figure 4).[24] So, it can be assumed that if a strong enough base is used then it is possible to prepare the dialkali metal salts of 5,5-disubstituted barbituric acids. Both the mono- and dialkali salts prefer N-substitution rather than O-substitution on the reaction with electrophiles.

The sodium derivative of $H_2debarb$, sodium 5,5-diethylbarbiturate (NaHdebarb, **3**) is prepared by the neutralization of an aqueous solution of **2** with sodium hydroxide and then precipitating the salt by the addition of alcohol (Scheme 4).[21]
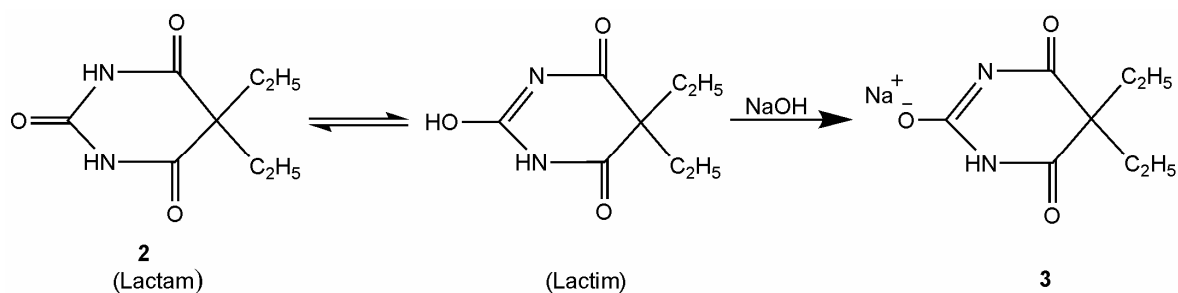


**Scheme 4**: Synthesis of Na[Hdebarb] (**3**).

5

**2** in aqueous solution decomposes at varying rates by base-catalyzed hydrolysis, generating ring-opened salts of carboxylic acids.

The dihydrate barbituric acid (H$_2$barb. 2H$_2$O), which was obtained by crystallization from aqueous solution, was reported by Baeyer in 1863 [25], and the crystal structure of the dihydrate [26] and anhydrous barbituric acid (H$_2$barb) [27] was determined. *Lewis et al* carried out a joint experimental and theoretical study of the possible polymorphs of barbituric acid (**1**), as a molecule where the sequence of hydrogen bond donors and two distinct acceptors gives potential for a variety of hydrogen bonding motifs.[28] Barbituric acid crystallizes easily from aqueous solutions as the dihydrate and the anhydrous compound is obtained as a powder by drying this at 100°C. It is only slightly soluble in alcohol and acetone and is insoluble in many non-polar liquids.[27]

## 1.1.2 The coordination chemistry of barbiturates

*Sinn et al.* reported the crystal structure of [Pd(en)barb](H$_2$O)$_4$, prepared from a solution originally containing [enPd(H$_2$O)$_2$]SO$_4$, barbituric acid, and hydroxide ion in a 1:2:2 molar ratio. In the complex Pd(II) forms bonds to both a deprotonated amide nitrogen and a deprotonated tetrahedral carbon.[29]

Some Mn(II), Zn(II), Cd(II), Co(II), Ni(II), Cu(II), Fe(III), Cr(III) complexes of barbituric acid have been synthesized but the molecular structures of these complexes were not investigated.[30] The X-ray structure analysis of neutral Cu(II) complex, [Cu(Hbarb)$_2$(H$_2$O)$_3$], synthesized by the reaction of sodium barbiturate (NaHbarb) and CuSO$_4$ in water, displays that the Cu(II) ion, in the slightly distorted square-pyramidal geometry, is coordinated by two O atoms of two monodentate barbiturates and three O atoms of three water molecules (**a**, Figure 3). Generally the negative charge of free barbiturate anion (Hbarb$^-$) is mainly located at carbon which is bonded with H atoms, while that of the present coordinated Hbarb$^-$ was mainly centered on one oxygen. This indicated that, in the process of coordination, copper ions induce migration of the negative charge from C to O; in other words, one carbonyl group becomes a hydroxyl anion. This tautomerism is first deserved example for a metal complex of Hbarb$^-$.[31]

The addition of a methanol solution of H$_2$barb to the fourfold excess of PPh$_3$AuCl and sodium methoxide in methanol resulted in the formation of several complexes by the successive elimination of all four hydrogen atoms of **1** (**b**, Figure 3).[32]
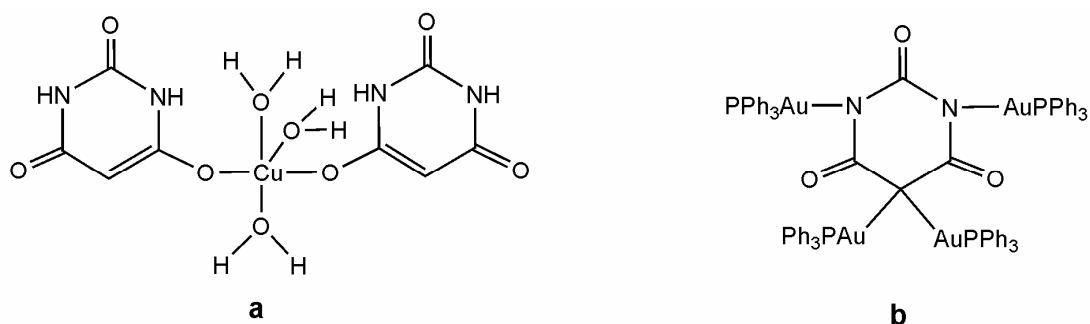


**Figure 3**: Copper (**a**) and gold (**b**) complexes of H$_2$barb (**1**).

Structural properties of barbiturates have received much attention due to their importance in medicine and therefore, the crystal structures of barbital[33] or veronal and its sodium[34] and calcium[35] salts were studied. The relationship between structure and drug action of barbiturates was investigated and the structures, physical and chemical properties and pharmacological activity of a large amount of barbiturates were reviewed by *Doran*.[36]

Most of the reported barbital metal complexes are of general formula M(II)(Hdebarb)$_2$L$_2$ where M is Co, Zn, Cd, Pd, Pt or Cu; Hdebarb is the mono anion of H$_2$debarb and L is an organic base such as ammonia, pyridine or any picoline etc. The first structurally characterized metal complexes of **2** were of [M$^{II}$(Hdebarb)$_2$(im)$_2$] where M$^{II}$ is Co and Zn; im is imidazole [37]. The molecular structure of these two complexes showed that, the donor atom in the barbiturate anion is a deprotonated nitrogen atom. X-ray structures of [Ni(isoamylbarb)$_2$(im)$_2$] [38], [Cu(Hdebarb)$_2$(pic)$_2$].2H$_2$O [39], [Zn(Hdebarb)$_2$(pic)$_2$] [40], [Zn(Hdebarb)$_2$(aepy)$_2$] [41], *cis*-[Cu(Hdebarb)$_2$(en)], and polymeric Cd(II) {[Cd(Hdebarb)$_2$(μ-en)]·2H$_2$O}$_n$ (**c**, **d**, Figure 4) [42], Ag(I) {[Ag$_2$(en)$_3$][Ag$_2$(debarb)$_2$] 2H$_2$O}$_n$ (**e**, Figure 4) [43] complexes (py, pic, en, aepy are pyridine, picoline, ethylenediamine, 2-(2-aminoethyl)pyridine respectively) were studied.

Mn(II), Fe(III), Co(II), Ni(II), Cu(II), Zn(II) and Cd(II) complexes of barbital, thiouracil, adenine, amino acids (methionine, lysine and alanine) and some mixed ligands were

prepared and characterized by elemental analyses, IR, electronic spectra, magnetic susceptibility and ESR spectra.[44]
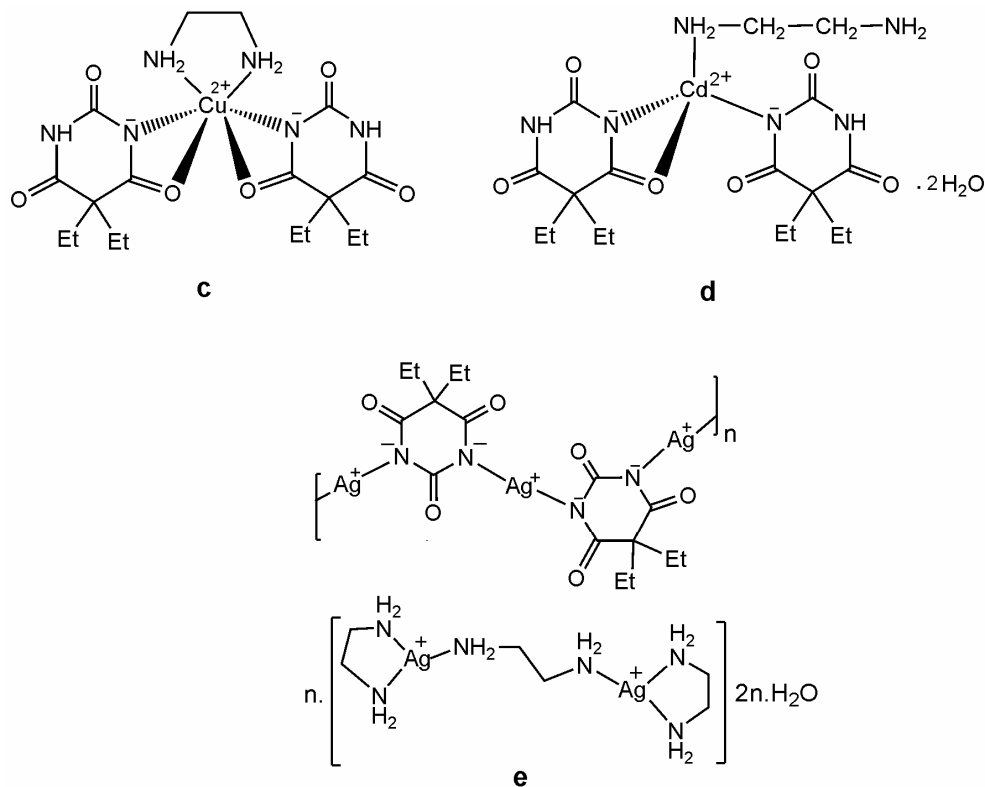




**Figure 4**: Some reported metal complexes (**c-e**) of $H_2$debarb (**2**).

Reaction of barbituric acid (**1**) or its derivatives with $PPh_3AuCl$ in different reaction conditions gave mono-, di-, or tetra-aurated (**b**, Figure 3) derivatives of barbituric acids which were characterized by IR, NMR spectroscopy. An X-ray diffraction study of one complex (**f**, Figure 5) was also carried out.[32] Synthesis and characterisation (NMR, IR, electrospraymass spectrometry, elemental analysis and single crystal X-ray diffraction) of Pt(II) monoamide complexes of **2** and **3** (**g**, Figure 5) derived from platinum(II) halide complexes *cis*-[PtX$_2$L$_2$] [L = PPh$_3$, L$_2$= 1, 2-bis(diphenylphosphino)-ethane (dppe) or 1,1´-bis(diphenylphosphino)ferrocene (dppf)] in different reaction conditions were carried out.[45] *Rudolf et al*. have introduced the CpFe(CO)$_2$ moiety (Cp = $\eta^5$-C$_5$H$_5$) to barbiturates as these type of iron derivatives can be used as IR-detectable marker in carbonylmetalloimmunoassay (CMIA) but they did not reveal the crystal structure of the complexes [46]. Mono- and bis-CpFe(CO)$_2$ complexes of barbiturate anions (**h** and **I**, Figure 5) in moderate yields were formed by the visible-light irradiation of CpFe(CO)$_2$I with the respective barbiturates.
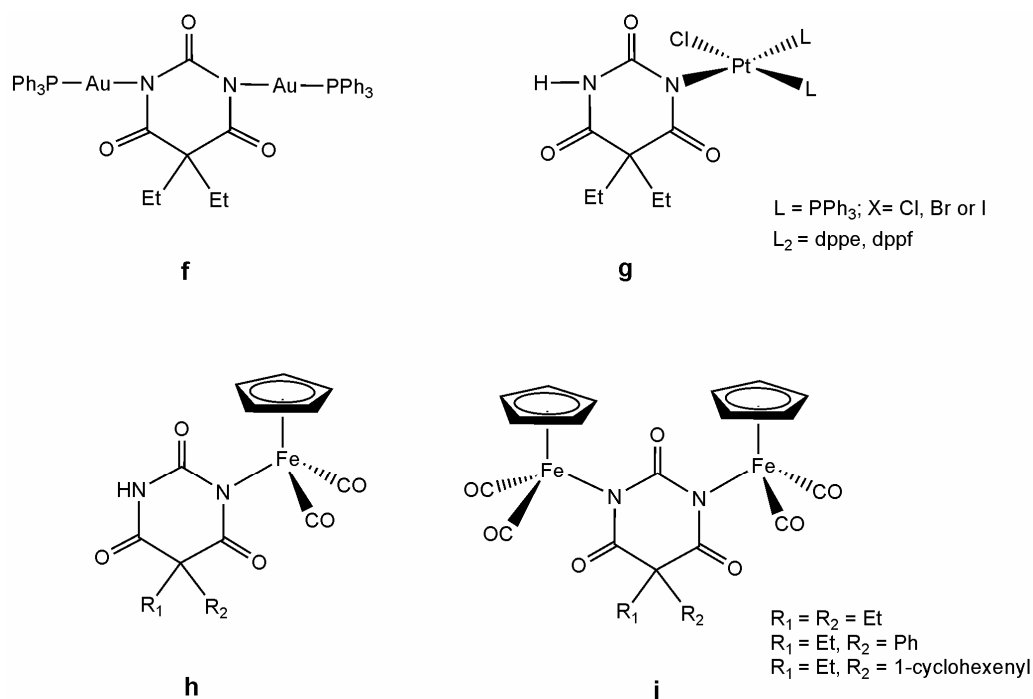
**Figure 5**: Reported examples of barbiturate metal complexes.

The carbonyl stretching frequencies in the IR spectra of the complexes $M(Hdebarb)_2L_2$, $M(Hdebarb)_2$ and $M(II)(debarb)$ or $M(I)_2(debarb)$ (M = Mn(lI), Co(lI), Ni (lI), Cu(lI), Zn(lI), Ag(l), Cd(lI), Hg(lI), Hg-phenyl, Pb(lI); L = imidazole, isobutylamine, pyridine) are assigned and discussed by *Bult et al.*[47]

## 1.1.3  Applications of metal complexes of biologically active ligands

The biological activity of several transition-metal complexes are now well established. Pt, Ag, Zn, and Au complexes have been widely investigated, and some of those complexes are used for therapeutic purposes. The most well known of these compounds is the anticancer therapeutic *cis*-$(NH_3)_2PtCl_2$, a compound that forms complexes with DNA and is a highly effective treatment for growth of certain types of cancers. *Carell et al.* reported that, cisplatin forms 1, 2-d(GpG) DNA intrastrand cross-links (cisplatin lesions) that stall RNA polymerase II (Pol II) and trigger transcription-coupled DNA repair.[48] In investigations aimed at understanding the binding sites of antitumor Pt(II) compounds to nucleic bases, Pd(II) compounds have been also employed. The interest arises from the similarity in the chemical properties of palladium(II) and platinum(II); in fact, both metal ions possess similar ionic radii, prefer nitrogen rather than oxygen donor atoms, and form strongly

tetragonal complexes, but those with Pd(II) react faster. The advantage of the much faster ($10^5$ times) ligand substitution reactions that Pd(II) presents in vitro makes it a good model for studies of reactions in vivo with biological molecules.[49, 50, 51, 52] Moreover, Pd(II) complexes with neutral ligands such as amines pyrimidine, pyridine, pyrazole, aryl groups show antiproliferative and antitumor activities.[53, 54, 55]

Ruthenium complexes have several applications in medicinal chemistry. Apart from applications as anticancer drugs, other medical applications of ruthenium compounds include immunosuppressants , nitric oxide scavengers antimicrobial agents.[56, 57, 58] It has been shown that ruthenium complexes of organic drugs can overcome resistance developed by the microbe to the organic compound alone.[59] Some Ru(II) complexes are currently used in cancer treatment and one important step in the mechanism of action of Ru(III) complexes is thought to be in vivo reduction to Ru(II), which is kinetically more reactive than Ru(III). The arene ligands stabilize Ru(II) and also provide a hydrophobic face for the complexes [60]. So different types of organometallic Ru(II) arene complexes such as [($\eta^6$-arene)Ru(II)(en)X]$^+$, X = halides) have been investigated for their cytotoxicity and were found to be effective inhibitors of the growth of cancer cells and form strong monofunctional adducts with DNA. It was observed that ruthenium(II) complexes of the type [($\eta^6$-arene)RuCl(X)(Y)] (X, Y are monodentate or chelating ligands) are cytotoxic to cancer cells, including cisplatin-resistant cell lines and the complex [($\eta^6$-Bip)-Ru(en)Cl][PF$_6$] is active in vivo against the A2780 xenograft model of human ovarian cancer, and is also active against A2780cis, the cisplatin-resistant xenograft.[61, 62] The cytotoxicity increases with increase in size of the $\eta^6$-arene.

The intercalation of transition metal complexes into DNA has received much attention in the past two decades as the metallointercalators have been used extensively to probe the structural and electronic properties of DNA.[63] For example, bioorganometallic metallointercalators like [($\eta^5$-C$_5$Me$_5$)M(Aa)(dppz)]$^{n+}$ (M = Rh, Ir or Ru, Aa = (S)-amino acids) and [($\eta^5$-C$_5$Me$_5$)M(dppz)(peptide-$\kappa S$]$^{n+}$ (n = 1-3) with $\kappa S$ coordinated methionine-containing peptides, exhibit intercalative binding into DNA.[64, 65, 66]

## 1.2   Benzil-bis(trimethylsilyl)diimine

Benzil-bis(trimethylsilyl)diimine   or   1,2-bis(trimethylsilylimino)-diphenylethane (**4**  =
Si$_2$BDI, Figure **6**) is an interesting model from the view point of the formation of
heterocycles because it possesses two imino groups in 1, 4-relationship and two very labile
Me$_3$Si substitutents in the same molecule.
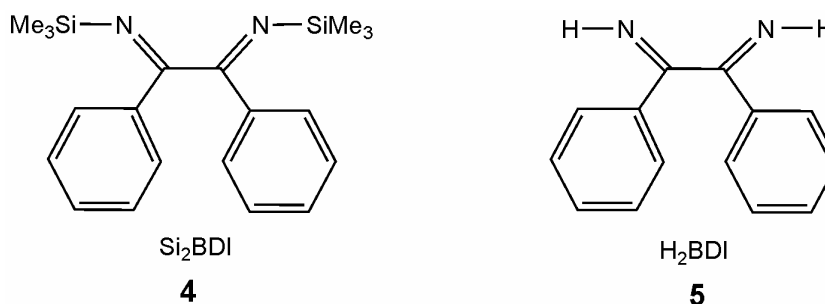


**Figure 6**: Benzil-bis(trimethylsilyl)diimine (**4**) and Benzildiimine (**5**).

## 1.2.1   Synthesis, properties and coordination chemistry of Si$_2$BDI and
H$_2$BDI

Si$_2$BDI (**4**) was prepared according to the modified literature procedure by the reaction of
benzil with two equivalents of sodium- or lithium-bis(trimethylsilyl)amide followed by
quenching with chlorotrimethylsilane (Scheme **5**).[67, 68] The solution of benzil and sodium
bis(trimethylsilyl)amide in benzene was stirred at 70 °C for 7 hours. After the addition of
chlorotrimethylsilane the solution was heated at 60 °C for 5 hours. Then the solution was
filtered and the filtrate was vacuum distilled to yield crystalline solid **4**.
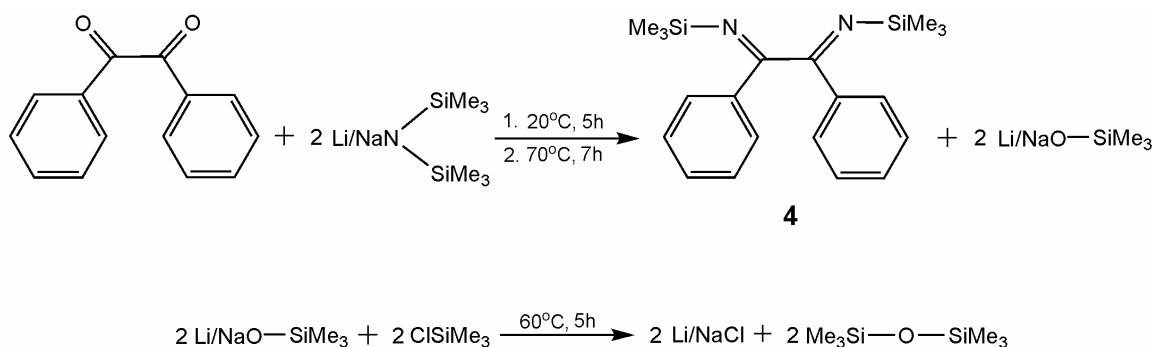


**Scheme 5**: Synthesis of Si$_2$BDI (**4**).

A wide variety of heterocycles such as B,N heterocycles, diazaheteroles, imidazoles, oxazolines and also several coordination complexes were synthesized using **4**.

The synthesis and electronic structure of planar C-S-N rings continue to attract the attention of research groups. So, the reaction between the two bifunctional reagents 1, 2-bis(chlorothio)benzene and **4** in dilute $CH_2Cl_2$ solution was studied which yielded 1,4,5,8-benzodithiadiazocine (by elimination of trimethylchlorosilane) expecting to contain properties of a $14\pi$ electron system (scheme 6).[69]
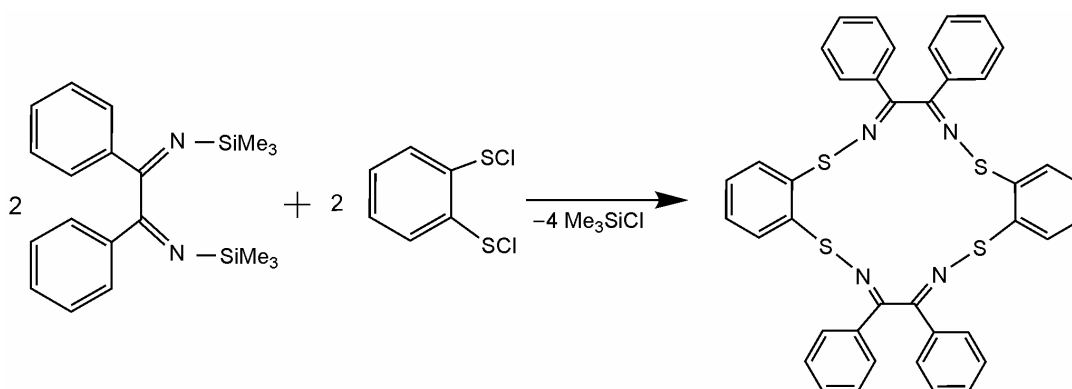


**Scheme 6**: Synthesis of 1,4,5,8-benzodithiadiazocine from **4**.

Different types of five- and ten-membered boron-nitrogen heterocycles such as **j** (4,5-diphenyl-2-diisopropylamino-1,3,2-diazaborole), **k** (2,7-bis(diisopropylamino)-4,5,9,10-tetraphenyl-1,3,6,8,2,7-tetraazadiborecin) can be obtained via silicon-boron exchange reactions between **4** and (diisopropylamino)dichloroborane (scheme 7).[70]
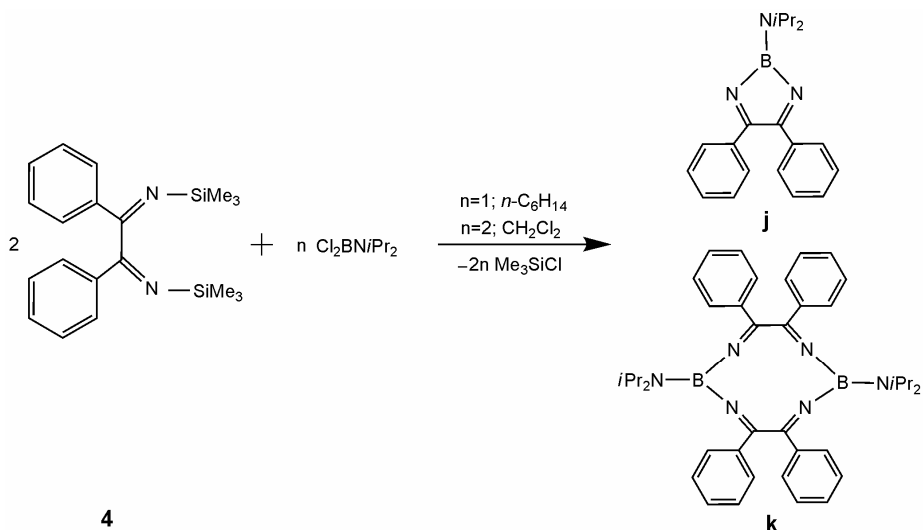
**Scheme 7**: Synthesis of boron-nitrogen heterocycles (**j** and **k**) using **4**.

When **4** is treated with an equivalent amount of aldehydes or diphenylketene in the presence of catalysts ($AlCl_3$ or $(NH_4)_2SO_4$) in benzene under different reaction conditions leads to the formation of imidazole and oxazoline derivatives by the liberation of hexamethyldisiloxane in good yield (scheme 8).[71]
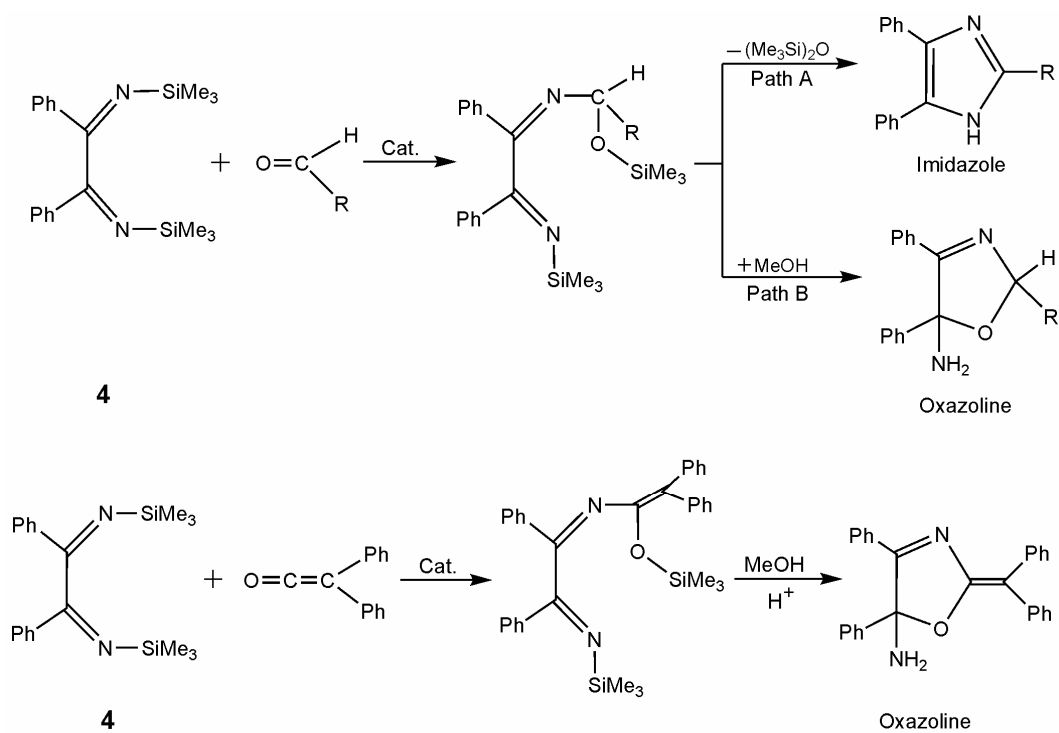


**Scheme 8**: Synthesis of imidazole and oxazoline derivatives starting from **4**.

*Diel et al* synthesized group 15 elements (Sb and Bi) containing diazaheteroles from **4** and phenanthrenequinone-(9,10)-bis(trimethylsilyl)diimine (Si$_2$PDI) (scheme 9) that can be utilized in the preparation of optical materials and provides access to a wide variety of structurally related diazaheteroles.[68] The reaction of **4** and its analogue phenanthrene-9,10-bis(trimethylsilyl)imine (Si$_2$PI) with SeOCl$_2$, SeCl$_4$, TeCl$_4$ results in some chalcogen-diimides (Scheme 10) which may contain electrical conductivity.[72]
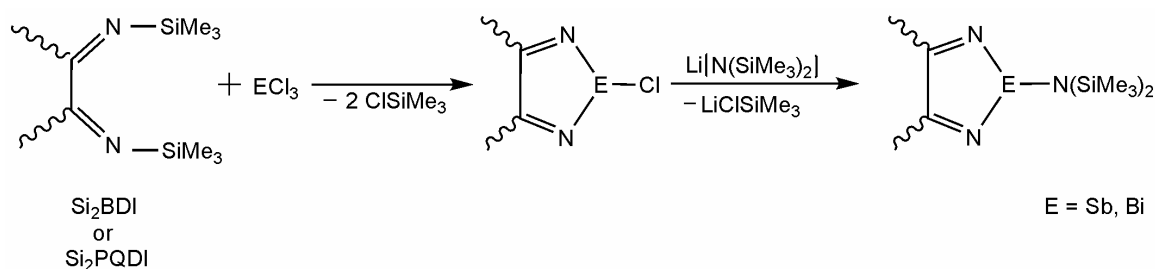


**Scheme 9**: Synthesis of diazaheteroles.
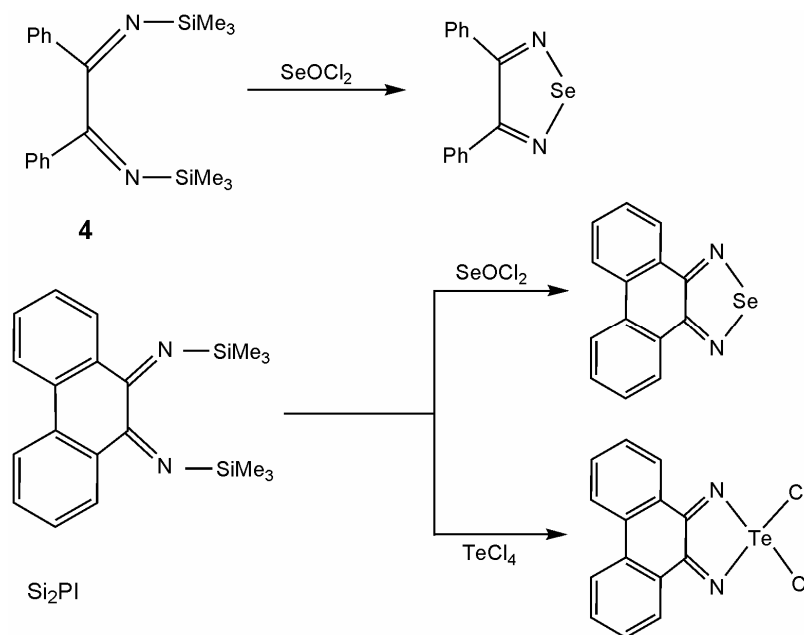


**Scheme 10**: Preparation of chalcogen-diimides from **4**.

Beside the above mentioned reactions there is however only a few metal complexes of **4** known where the two trimethylsilyl (SiMe$_3$) groups stay attached with the ligand. Some complexes with the general formula Mo(CO)$_4$L (where L = **4** or similar phenylimine ligands) were prepared by the thermal substitution reaction of Mo(CO)$_6$ with the respective ligands in refluxing C$_6$H$_6$ (**l**, Figure 7). [73] Only the magnetical and few spectrochemical

properties of these complexes were investigated, the molecular structures however were not reported. The electronic spectrum of **l** has a long wave length which together with its small solvatochromism illustrates it as a high π-acceptor compound.
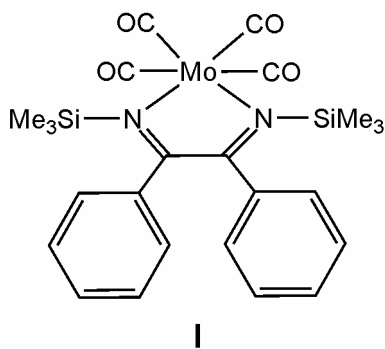


**Figure 7**: Mo complex of **4**.

But, in all reactions presented here with the metal complexes the two SiMe₃ groups are easily cleaved off as the N-SiMe₃ group is very reactive and sensitive to moisture, and sometimes also to chlorinated solvents. After the cleavage, the two SiMe₃ groups are replaced by two H atoms and then the ligand resembles a typical 1, 2-diimine ligand with unsubstituted imino groups. In the present study, we have chosen **5** as the principal ligand, not only because it carries the diimine chromophore (**n**, Figure 9) but also for their different coordination modes.

In all our prepared complexes, **4** is in diimine form (benzildiimine, $H_2BDI$, **5**) which is in good agreement with the complexes synthesized where **4** is bonded with different transition metals to form bis- and tris- chelate complexes (**m**, Figure 8).[74] The complexes are of general formula of $[M(HL)_n](ClO_4)_2$ [HL = benzildiimine, phenanthrenequinonediimine; n = 2, M = Cu; n = 3, M = Fe, Ni] and $[CoL(HL)_2](ClO_4)_2$ and were prepared from the corresponding metal salts and alcoholic HL or alcoholic solution of the corresponding 1,2-bis(trimethylsilylimino) analog. The complexes were characterized by elemental analysis, optical spectra, and magnetic measurements. Similar $Pd(HL)Cl_2$, $[Rh(HL)L]Cl_2$ and $[Rh(HL)_2]Cl_3$ complexes were also prepared from same ligands.[75] The complexes contain considerable π-backbonding in the chelates. The temp.-independent paramagnetism results in unusual magnetic moments for the Fe(II), Co(III), and Rh(III) chelates. But, the complexes were not characterized by X-ray structure analysis.
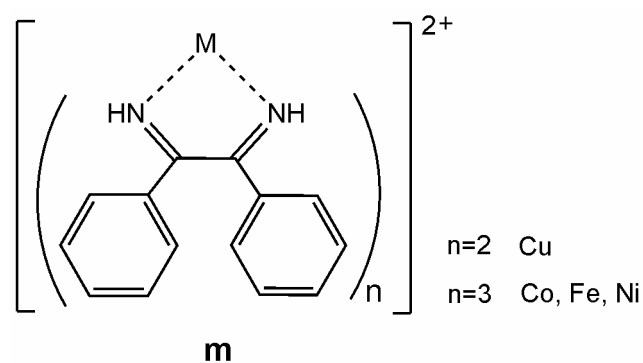
**Figure 8**: Reported complexes of **5**.

We can compare the chemical properties of our chosen ligand with similar diimine ligands. During the past quarter of last century, 1,4-diazabutadienes (α-diimines) have attracted considerable attention as useful reagents in organometallic chemistry due to (i) their variety of coordination modes and reactivity of their coordination complexes; (ii) the applications of such complexes in organic synthesis and catalysis; (iii) the utilization of such complexes as luminescence labels for detection and photochemical cleavage of DNA.[76, 77, 78] In addition, we have already discussed about the utilization and synthesis of selected α-diimines in ring-closure reactions with $SbCl_3$ or $BiCl_3$, to provide the first examples of Sb and Bi containing 1,2,5-pnictadiazoles (Scheme 9). One of the most appealing attributes of the diazabutadienes, which plays a significant role in the physical and chemical properties of the resultant coordination compounds, is their strong π-acceptor ability as a result of the energetically low-lying LUMO.[79]

In spite of these interesting properties, examples of transition metal complexes of **4** are not widely reported and its molecular structure is also unknown till date. So, we were interested to characterize the molecular structure of **4** and synthesize and characterize fully some transition metal complexes of **4**.

Due to the instability and strong reactivity of **4**, it was not possible to isolate the complexes with intact $SiMe_3$ groups. In all the synthesized complexes in this work **5** instead of **4** is bonded to the metal via the nitrogens of imine (=NH) group.

The ruthenium chemistry of diimine ligands such as dioximes is an area of significant current interest. *Das et al* reported the chemistry of some mono- and bis-dioxime (**o**, Figure

9) complexes of ruthenium(II), where triphenylphosphine (PPh$_3$) has been used as the coligand. Triphenylphosphine is also a familiar $\pi$-acceptor ligand and hence its coordination is expected to result in some interesting effect on the $\pi$ interaction with the dioxime ligand as well as on the stereochemistry of the complexes.[80]
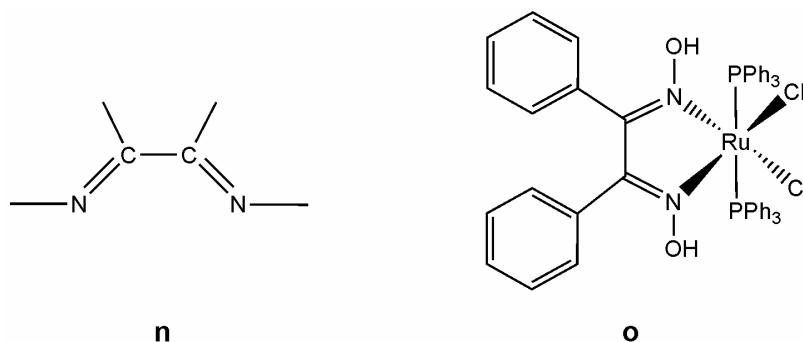


**Figure 9**: Diimine chromophore (**n**) and ruthenium dioxime complex containing a similar chromophore (**o**).

Several types of diimine complexes of ruthenium(II) (Scheme 11) and rhodium(III) of 9,10-phenanthrenequinone (phi) were isolated [78b] which are structurally analogous to complex **20** prepared within this thesis. Both ruthenium(II) and rhodium(III) complexes containing the phi ligand have been found to bind DNA avidly by intercalation between base pairs.[81, 82] Rhodium(II) complexes containing phi have found a particularly wide range of application as photoactivated probes of local DNA helical conformation.[78b]
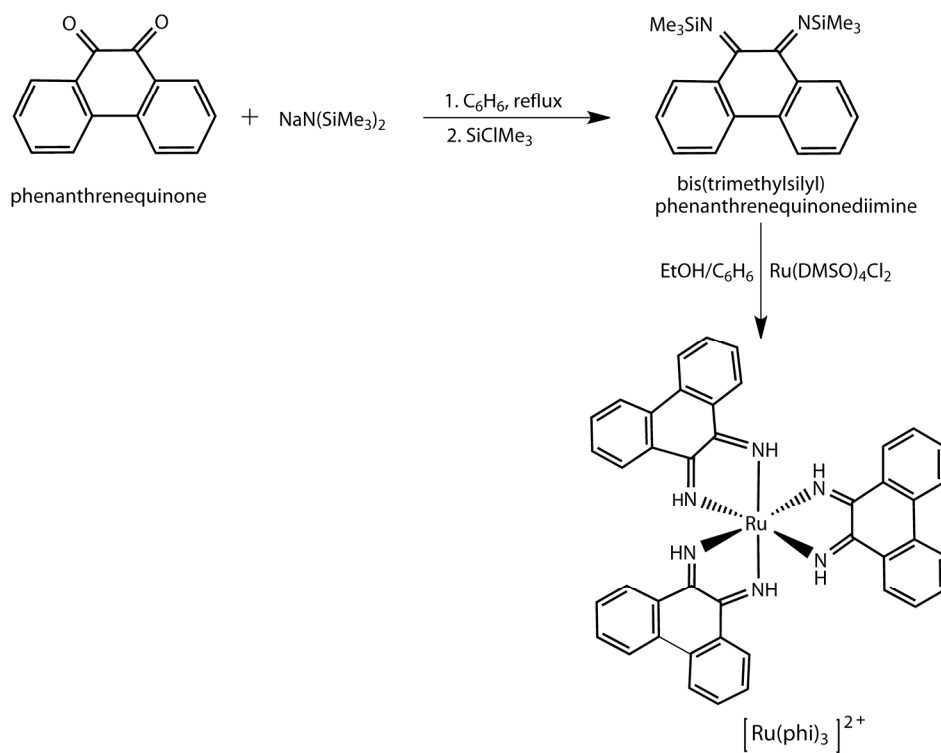
**Scheme 11**: Synthesis of ruthenium(II) complex of 9,10-phenanthrenequinone (phi).

## 1.3  Aim of the study

On the view point of the above discussion (section 1.1.3) it can be concluded that metal complexes of biologically active ligands have versatile applications in medicinal chemistry. In the present study complexes like $(PPh_3)_2PdCl_2$, $(PPh_3)_2Rh(CO)Cl$ and $(PPh_3)_2Cu.BF_4$ were used as precursors in the complexation reactions with barbiturates since it is reported that phosphine ligands by themselves and phosphine complexes of other metals, such as Ag(I), Au(I) and Sn(IV) are anticancer, anti-HIV or anti mitochondrial agents.[83, 84, 85] It is also reported that metals belonging to the same group, such as Au and Cu, have similar chemical properties. Organotransition-metal nitrosyl complexes such as chloro-($\eta^5$-cyclopentadienyl)dinitrosylchromium $[CpCr(NO)_2Cl]$ has been shown to cause endotheliumin-independent relaxation of aortic rings in vitro.[86] To the best of our knowledge till now no Ru, Rh or Ir complex of 5,5-diethyl barbituric acid (**2**) have been synthesized and fully characterized.

Barbituric acid derivatives also exert important action on the central nervous system (CNS) and recently have found totally new biomedicinal applications in fields such as cancer and AIDS therapy.[45] Regarding the therapeutic efficiency and diversity of barbiturates, we decided to synthesize neutral Cr(0), Re(I), Pd(II), Cu(I), Rh(I) and Rh(III), Ir(III), Rh(II) complexes of barbiturates (**1**, **2**, **3** of Figure 1) and to elucidate their structures by IR, NMR, Mass spectra, elemental analysis and single crystal X-ray diffraction.

As discussed in section 1.2.1 that there are only very few reports on the synthesis and coordination modes of metal complexes of benzildiimine (**5**, Figure 6) and benzil-bis(trimethylsilyl)diimine (**4**, Figure 6) and that their structurally analogous metal complexes have a wide variety of applications we were encouraged to synthesize Rh(III), Ir(I), Fe(II) and Cr(III) complexes of **5** and to characterize the new metal complexes by means of IR, mass, $^1$H, $^{13}$C, $^{31}$P NMR spectra, elemental analysis and X-ray diffraction in the second part of this work. In addition, the solid-state structure of **4** was determined here for the first time by single crystal X-ray diffraction study.

# 2  RESULTS AND DISCUSSION

Complexes containing H$_2$debarb (**2**) are not known and therefore, a proton loss from at least one of the amine N atoms is necessary for the complexation of Hdebarb$^-$ or debarb$^{2-}$. In the present work, the anions Hdebarb$^-$ and debarb$^{2-}$ were produced by the addition of excess of triethylamine to H$_2$debarb (**2**) or from Na[Hdebarb] and were used in the preparation of metal complexes. In the case of barbituric acid (H$_2$barb, **1**) complex the Hbarb$^-$ anion was found from the reaction mixture of **1** and NaOMe in methanol.

## 2.1  Chromium complexes of barbiturates

*Cotton et al.* published the crystal structure of the salt Li$_2$Cr(Hdebarb)$_4$.2EtOH which was obtained by the reaction of Cr$_2$(OAc)$_4$.2H$_2$O with lithium diethylbarbiturate.[87] In the complex the ligand binds to the metal center in an *N*-monodentate fashion. Synthesis of barbituric acid complexes derived from Cr(III) salts were carried out.[30]

### 2.1.1  Synthesis of Hdebarb complex of chromium(0)

**(5,5-Diethylbarbiturato-*N*)-($\eta^5$-cyclopentadienyl)-dinitrosyl-chromium(0):**

**(C$_{13}$H$_{16}$CrN$_4$O) (6)**

Addition of an excess of triethylamine to a solution of **2** in chloroform to which 1 mol equivalent of CpCr(NO)$_2$Cl had been added resulted in the formation of **6** within 2 days (Scheme 12). Despite several attempts the synthesis of the dinuclear chromium complex {CpCr(NO)}$_2$(debarb) analogous of complex **9** was not successful. The green compound is soluble in polar organic solvents such as acetone or dichloromethane, but insoluble in non polar pentane and hexane. **6** decomposes in solution when exposed to moist air.
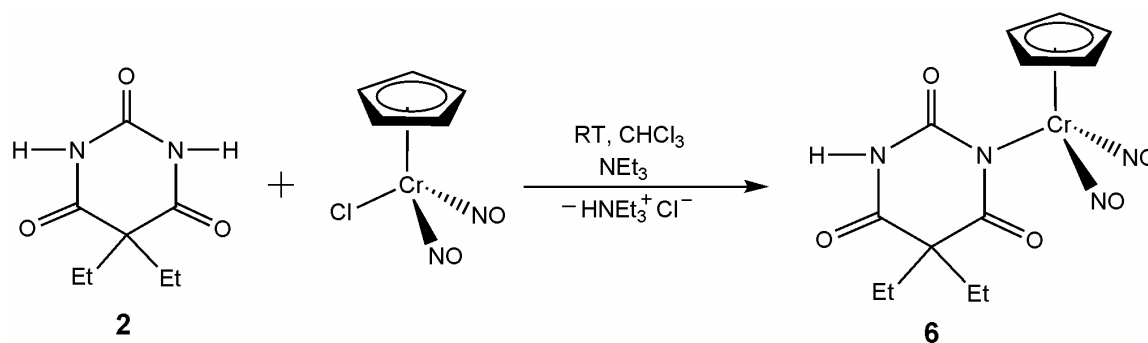
**Scheme 12**: Synthesis of the mono-Hdebarb complex of chromium **6**.

## 2.1.2  Molecular structure of 6

Green crystals of the complex **6** suitable for X-ray diffraction study were obtained by isothermic diffusion of pentane into the solution of the complex in dichloromethane at room temperature within 2 days. It crystallized in the triclinic crystal system and *P*-1 space group. The molecular view of **6** is shown in Figure 10 together with selected bond lengths and angles. The details of the data collection and refinement are given in **Table 5.1** of the crystallographic appendix. The molecular structure possesses a distorted "three-legged piano-stool" geometry around the metal centre with the three N−Cr−N bond angles between 96.0 to 99.9° being typical for pseudotetrahedral configuration and therefore of the same size as found in the starting compound $CpCr(NO)_2Cl$.[88] The angle N(1)−Cr(1)−N(2) 96.0(9)° between both the NO ligands is the smallest one. The average Cr−N−O angle is 169.5°, corresponding to an almost linear $NO^+$ mode of coordination. Whereas, both of the Cr−N bonds with the π-acidic NO ligands are very short (Cr(1)−N(1) 1.709(18) and Cr(1)−N(2) 1.722(18) Å) in comparison to the Cr−$N_{Hdebarb}$ bond (2.055(18) Å), which is a typical Cr−N single bond length value.[89] All Cr−N bond lengths in **2** are very similar to the analogous ones found in $Cp(NO)_2Cr\{N(BF_3)SNSiMe_3\}$.[90] The six-membered ring of Hdebarb is planar (sum of angles at N(3) = 359.9°; C(1)−N(3)−Cr(1) 119.0(13)°; C(4)−N(3)−Cr(1) 119.7(13)°; C(4)−N(3)−C(1) 121.2(16)°). No hydrogen bonds are observed in the crystal packing of the complex.
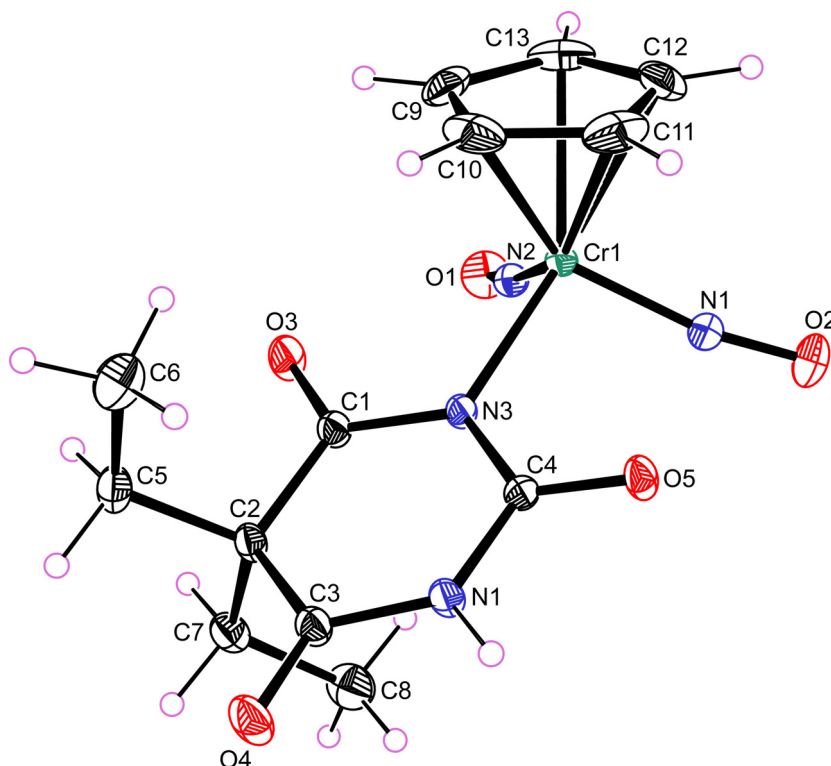
**Figure 10:** Molecular structure of **6**. The thermal ellipsoids are drawn at the 30% probability level.

**Selected bond lengths [Å]:** Cr(1)−N(1) 1.709(18) , Cr(1)−N(2) 1.722(18), Cr(1)−N(3) 2.055(18), O(2)−N(1) 1.167(2), O(1)−N(2) 1.163(2), N(3)−C(1) 1.374(2), N(3)−C(4) 1.366(2), N(4)−C(4) 1.390(3), C(2)−C(5) 1.539(3), C(5)−C(6) 1.519(3), C(7)−C(8) 1.526(3), Cr(1)−C(9) 2.200(2), Cr(1)−C(10) 2.219(2), Cr(1)−C(11) 2.201(2), Cr(1)−C(12) 2.192(2), Cr(1)−C(13) 2.184(3).

**Selected bond angles [°]:** N(1)−Cr(1)−N(2) 96.0(9), N(1)−Cr(1)−N(3) 99.9(8), N(2)−Cr(1)−N(3), 99.3(7), C(4)−N(3)−Cr(1) 119.7(13), C(1)−N(3)−Cr(1) 119.0(13), O(2)−N(1)−Cr(1) 169.4(18), O(1)−N(2)−Cr(1) 169.6(16), N(1)−Cr(1)−C(10) 134.0(11), N(2)−Cr(1)−C(10) 128.3(11), C(3)−C(2)−C(1) 114.5(16), C(3)−N(4)−C(4) 126.4(17), C(4)−N(3)−C(1) 121.2(16), O(3)−C(1)−N(3) 120.6 (18).

## 2.1.3 Spectroscopic characterisation of 6

Complex **6** was fully characterised by the IR, mass, $^1$H, $^{13}$C NMR spectra and elemental analysis. After the coordination of the ligand with the metal complexes the ethyl groups of complex **6** are no longer equivalent in the solid state. Although the ethyl groups are not equivalent, **6** shows simple quartet and triplet in the $^1$H NMR spectrum for the different protons in $CH_2$ and $CH_3$ (Figure 11), respectively, which may be caused by the rotation about the Cr1−N3 axis in solution. These values are in good agreement with the values found in $[Cp(CO)_2Fe(Hdebarb)]$.[46] The signals for $CH_2$ (1.88 ppm) and $CH_3$ (0.75 ppm) hydrogens are shifted slightly upfield in comparison with the same signals found in $H_2$debarb ($^1$H**:** $CH_2$ 1.93 ppm and $CH_3$ 0.84 ppm, recorded in $CD_3OD$). The broad N−H resonance is observed at 8.14 ppm. The single resonance found at 5.66 ppm corresponds to the protons of Cp ligand.

The $^{13}$C NMR spectrum displays three signals (181.19, 174.79 and 156.43 ppm) for the three different carbonyl groups within the coordinated barbiturate moiety (Figure 12). The rest of the carbons of the barbiturate show only one signal for each of $C$Et$_2$ (58.23 ppm), $CH_2$ (32.99 ppm), and $CH_3$ (9.93ppm). The signal observed at 102.8 ppm is due to the carbon of Cp ligand. Beside these signals one additional signal is observed in the $^1$H (5.69 ppm) and $^{13}$C (103.58 ppm) NMR which may arise for the isomer concerning the ethyl groups.

The IR spectrum of **6** (in $CHCl_3$) shows two strong $v$(NO) bands at 1825 and 1720 cm$^{-1}$ and for the three carbonyl groups of the ligand only two $v$(CO) bands at 1621 and 1682 cm$^{-1}$. The band at 1682 cm$^{-1}$ is very weak and more a shoulder of that at 1720 cm$^{-1}$. However, in KBr besides four strong absorptions at 1814, 1727 cm$^{-1}$ (NO) and 1671, 1620 cm$^{-1}$ (CO), one shoulder at 1714 cm$^{-1}$ of medium intensity is additionally observed. This may be assigned to the third $v$(CO) absorption which was concealed by one of the $v$(NO) bands in the solution spectrum.

The mass spectrum showed a peak at *m/z* = 300 which corresponds to the cation formed by the loss of both NO ligands [M−2NO]$^+$. The [MH$^+$] and [MH$^+$ −NO] peaks also observed at *m/z* = 361 and 331 respectively.

**a)**



**b)**



**Figure 11: a)** ^{1}H NMR spectrum of **6** in CD$_2$Cl$_2$. **b)** Quartet and triplet observed for the ethyl groups.
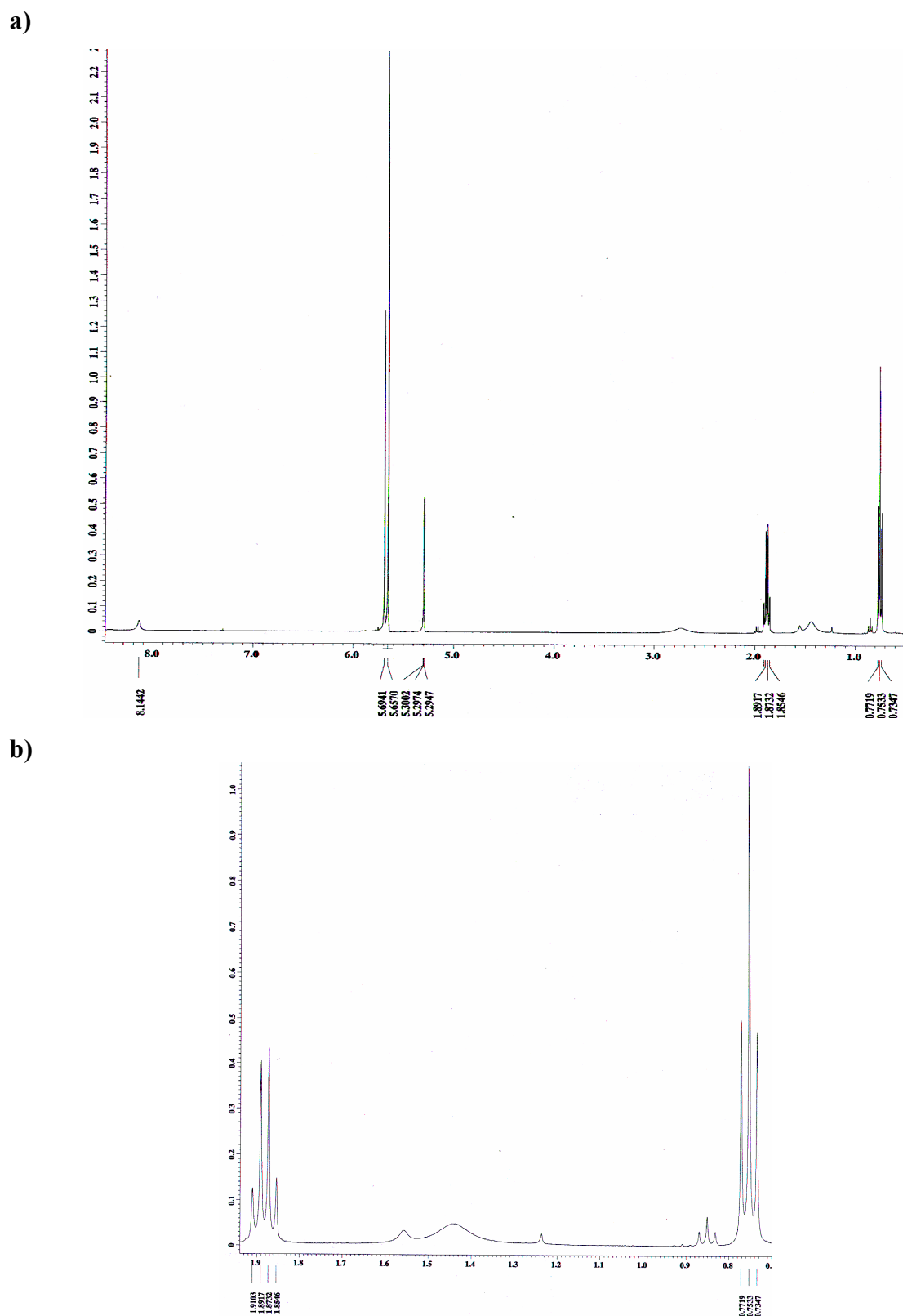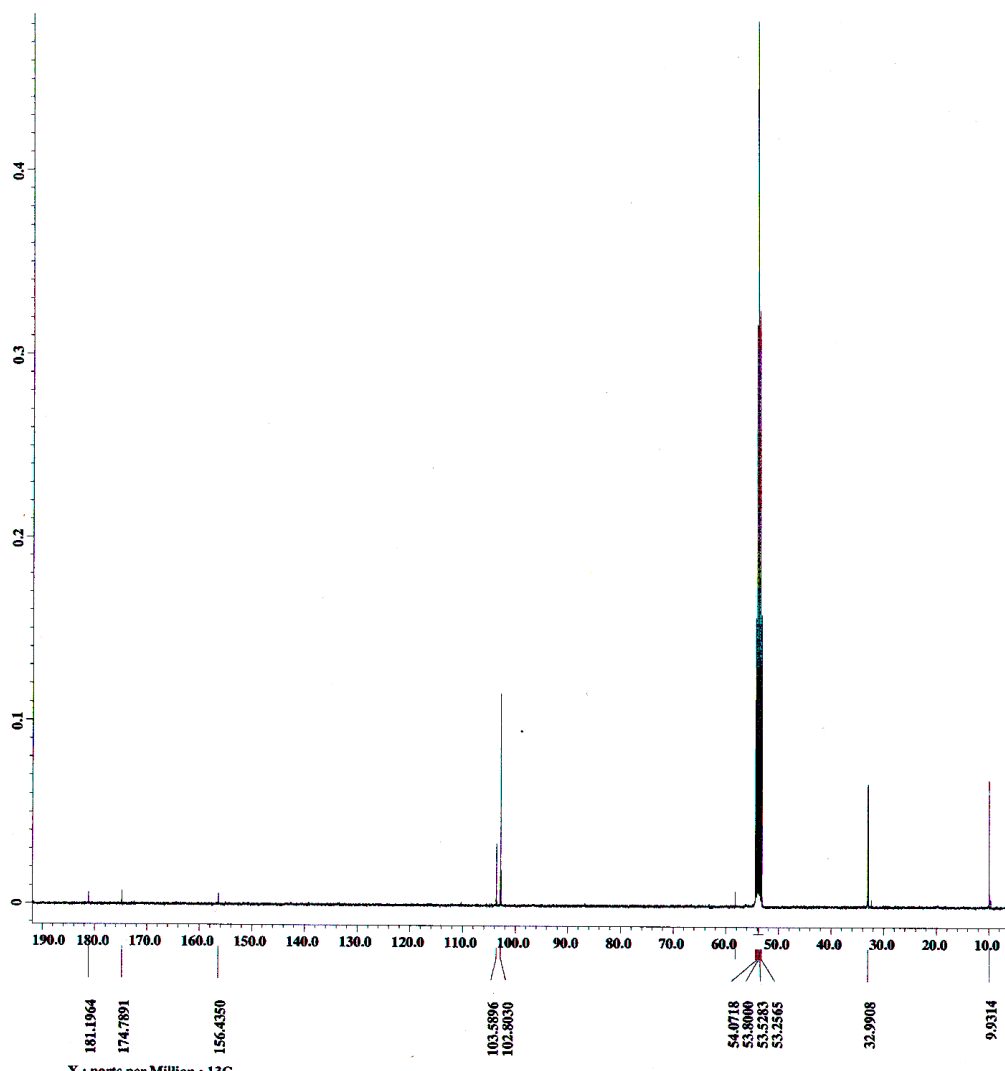
**Figure 12**: $^{13}C$ NMR spectrum of **6** in $CD_2Cl_2$.

## 2.2 Synthesis of Hdebarb complex of rhenium(I)

*cis*-**(5,5-Diethylbarbiturato-*N*)-tetracarbonyl-(triphenylphosphine)-rhenium(I)**
**($C_{30}H_{26}N_2O_7PRe$) (7)**

The rhenium(I) complex $(PPh_3)Re(CO)_4Br$ reacts with the stoichiometric amount (1:1) of the Hdebarb⁻ anion only after the treatment with $AgO_3SCF_3$ (= AgOTf) and separation of the precipitated AgBr, to give the mononuclear barbiturato complexes **7** (Scheme 13). Without the addition of AgOTf no reaction was observed. An excess of triethylamine was also used in this reaction to replace one hydrogen from 5,5-diethylbarbituric acid ($H_2$debarb). Complex **7** is colourless, air stable and soluble in polar organic solvents such as acetone or dichloromethane, but insoluble in non polar pentane and hexane.

25
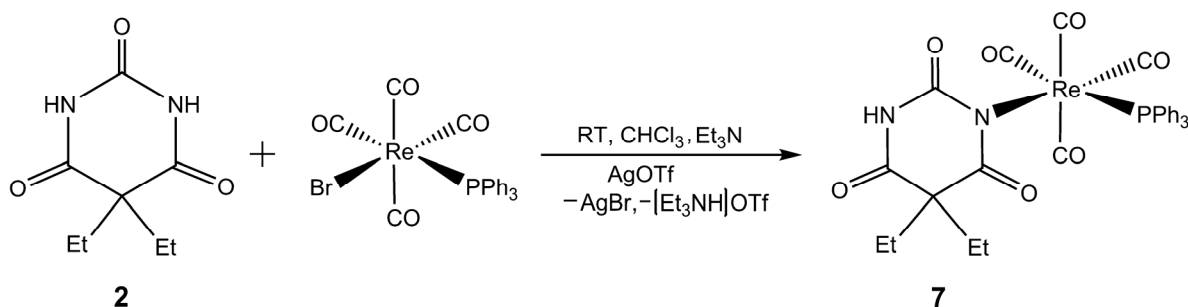
**Scheme 13**: Synthesis of the mono-Hdebarb complex of rhenium(I) **7**.

## 2.2.1  Molecular structure of 7

The colourless crystals of the complex **7** suitable for X-ray diffraction were obtained by isothermic diffusion of pentane into the solution of the complex in $CH_2Cl_2$ at room temperature within 2 days. Complex **7** crystallised in the triclinic crystal system and *P*-1 space group. The molecular structure along with selected bond lengths and angles are presented in Figure 13. Full crystallographic data can be found in appendix, **Table 5.1**. In complex **7** pseudo-octahedral geometry is observed around the rhenium centre. The barbiturate and PPh$_3$ ligand are in *cis*-position as illustrated in Figure 13. The two ethyl groups are inequivalent, one being directed towards the carbonyl ligands and the other towards the phenyl ring of PPh$_3$. The Re1−N1 and Re1−P1 bond lengths are 2.220(2) Å and 2.494(10) Å, respectively and are similar with those of analogous aziridine complexes of Re (e.g: 2.220(4) and 2.496(1) Å).[89] Due to the steric hindrance of the bulkier phenyl group the bond angle N1−Re1−P1 96.2(6)° appears larger than those of Cn−Re1−N1 (n =1−3) with values between 87.2° to 89.5°. The Re1−C4 bond length of 1.926(3) Å is considerably shorter than the M−C bonds of the other carbonyl ligands being *trans*-axial to each other in the complex [1.977(3), 2.002(3) and 2.010(3) Å] indicating greater $\pi$-back-donation to this CO because of the good σ-donor Hdebarb ligand in *trans*-position. For the same effect the bond length of O4−C4 (1.149(4) Å) is longer than the other O−C bond lengths (1.129(4), 1.130(4), 1.134(3) Å). The C4−Re1−N1 bond angle of 176.87(10)° is slightly deviated from 180° and the plane of the ligand is approximately perpendicular to the equatorial co-ordination plane containing the PPh$_3$ and 3 CO ligands and turned out from the plane given by P1, C1 and C4 [torsion angles: C4−Re1−N1−C5 and C4−Re1−N1−C8 are 77.2(18)° and −94.6(18)° respectively]. This is in good agreement with the corresponding torsion angles of *cis*-[PtCl(Hdebarb)(PPh$_3$)$_2$].[45]
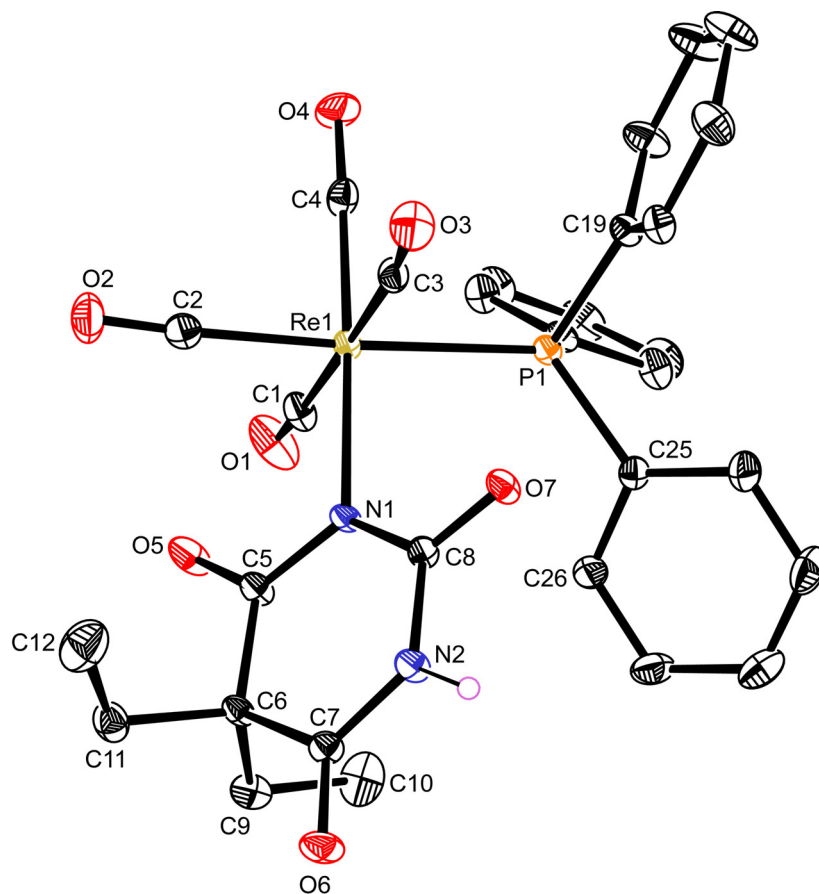
**Figure 13:** Molecular structure of **7**. The thermal ellipsoids drawn at the 30% probability level. Hydrogen atoms of ethyl and phenyl groups are omitted for clarity.

**Selected bond lengths [Å]:** Re(1)−N(1) 2.220(2), Re(1)−P(1) 2.494(10), Re(1)−C(1) 2.010(3), Re(1)−C(2) 1.977(3), Re(1)−C(3) 2.002(3), Re(1)−C(4) 1.926(3), O(1)−C(1) 1.130(4), O(2)−C(2) 1.129(4), O(3)−C(3) 1.134(3), O(4)−C(4) 1.149(4), N(1)−C(5) 1.374(3), N(2)−C(8) 1.388(3), C(5)−C(6) 1.527(4).

**Selected bond angles [°]:** N(1)−Re(1)−P(1) 96.2(6), C(1)−Re(1)−N(1) 89.3(11), C(2)−Re(1)−N(1) 87.2(10), C(3)−Re(1)−N(1) 89.5(10), C(4)−Re(1)−N(1) 176.8(10), C(5)−N(1)−Re(1) 117.2(17), C(8)−N(1)−Re(1) 121.8(17), C(5)−N(1)−C(8) 120.4(2), C(8)−N(2)−C(7) 126.9(2), C(7)−C(6)−C(5) 113.8(2).

**Torsion angles [°]:** C(4)−Re(1)−N(1)−C(5) 77.2(18), C(4)−Re(1)−N(1)−C(8) −94.6(18).

**Hydrogen bond:** N(2)−H(2)···O(7) 0.88, 2.030, 2.908, 176.0(6).

Intermolecular hydrogen bonding is observed in the complex. The molecules of Hdebarb are connected to each other by N−H···O bond, involving the amine hydrogen atom of one Hdebarb and the carbonyl oxygen atom of another Hdebarb ligand.

### 2.2.2 Spectroscopic characterisation of 7

The complex was fully characterised by the IR, mass, $^1$H, $^{13}$C, $^{31}$P NMR spectra and elemental analysis. After coordination of the ligand with the metal complexes the ethyl groups of the complex are no longer equivalent. So, in the $^1$H NMR spectra of **7** the CH$_2$ resonances show diastereotopism and appear as multiplets, rather than the expected quartet. For the two different CH$_2$ there is one set of multiplet. This may arise as the differences in chemical shifts are very small and they coincide with one another. The signals of complex **7** are shifted more downfield compared to the signals of **6** and also of **8**, **9** indicating an electron-enriched system, because of the more electron-donating triphenylphosphine ligand. The signals for CH$_2$ (1.77 ppm) and CH$_3$ (0.65 ppm) hydrogens are shifted slightly upfield in comparison with the same signals found in H$_2$debarb ($^1$H: CH$_2$ 1.93 ppm and CH$_3$ 0.84 ppm recorded in CD$_3$OD). The broad N−H resonance is observed at 7.76 ppm.

The $^{13}$C NMR spectrum of **7** displays three signals for the three different carbonyl groups within the coordinated barbiturate moiety at 181.08, 173.33, 156.59 ppm and three signals for the carbonyl ligands attached with rhenium at 188.39, 187.16 and 184.26 ppm. The rest of the carbons of the barbiturate show only one signal for each of CEt$_2$ (56.17 ppm), CH$_2$ (32.05 ppm) and CH$_3$ (9.46 ppm). The phenyl carbon atoms of the PPh$_3$ ligand show multiplets at 133.35−128.79 ppm with doublet character because of the P−C coupling.

In the $^{31}$P NMR spectrum the signal of PPh$_3$ is found at 11.64 ppm.

In the IR spectrum of **7** (in CHCl$_3$) the stretching vibrations of the carbonyl groups of Hdebarb appear as three bands at 1718, 1681 and 1619 cm$^{-1}$ (Figure 14), almost similar to those observed for di-substituted barbiturate complexes.[32, 91] The carbonyls of rhenium show three strong absorptions (2105, 2010, 1946 cm$^{-1}$) which are typical for σ-donor-π-acceptor ligand. As complex **7** possesses C$_S$ or *pseudo*-C$_{2V}$ symmetry one would expect four absorptions for the carbonyls of rhenium. However, only three main absorptions are observed in CHCl$_3$ but in KBr with three bands at 2106, 2020, 1926 cm$^{-1}$ there is one shoulder at 1999 cm$^{-1}$ comparable to analogous aziridine RePPh$_3$(CO)$_4$ complex.[89] The spectrum (KBr disc) also exhibits weak absorptions for the N–H stretching vibrations in the range of 3177–3053 (3390 in CHCl$_3$) cm$^{-1}$. The characteristic bands for the *v*(C−H) (2961–

2880 cm$^{-1}$), $v$(C–C and C−H$_{deformation}$) (1484–1316 cm$^{-1}$) and $v$(C–N) (1237 cm$^{-1}$) vibrations are observed in the expected region.

The mass spectrum shows no unexpected behaviour and is easily interpreted because of the metal isotope distribution. The FAB$^{+}$ mass spectrum exhibited the parent signal for the intact molecule at $m/z$ = 743. The fragmentation pattern is characterized by the successive loss of the CO ligands.
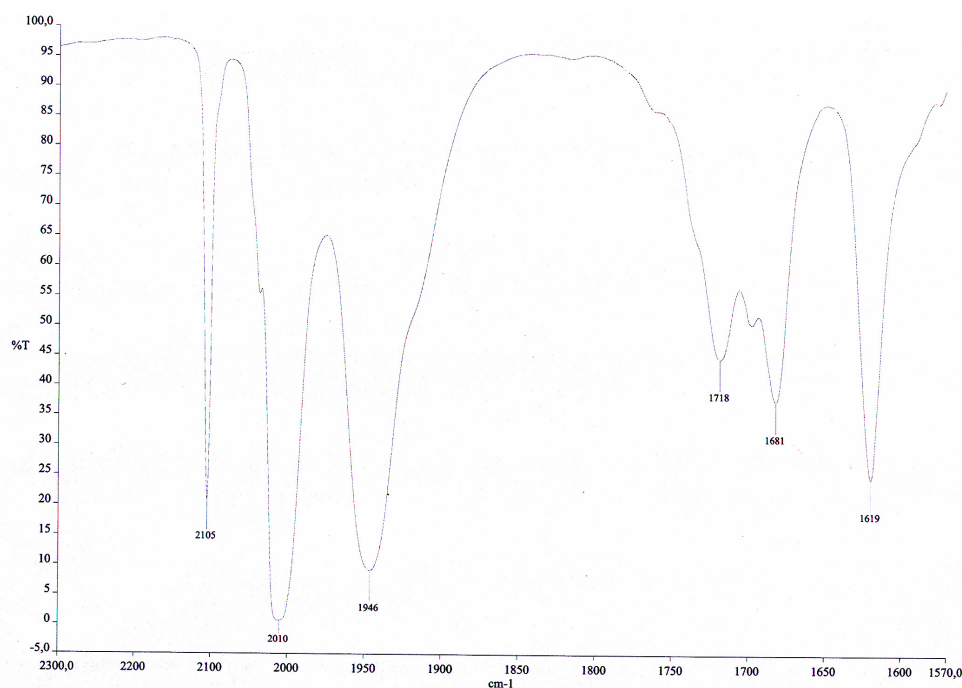


**Figure 14**: Carbonyl absorptions observed in **7**.

## 2.3   Synthesis of mono- and di-nuclear rhenium(I) complexes of H$_2$debarb

**(5,5-Diethylbarbiturato-*N*)-pentacarbonyl-rhenium(I), (C$_{13}$H$_{11}$N$_2$O$_8$Re) (8)**
**and**
**(*µ*-Diethylbarbiturato-*N*,*N'*)bis[pentacarbonyl-rhenium(I)], (C$_{18}$H$_{10}$N$_2$O$_{13}$Re$_2$) (9)**

1 mol of Re(CO)$_5$Br reacts with 1 mol of Hdebarb$^-$ anion only after the treatment with AgO$_3$SCF$_3$ (= AgOTf) and separation of the precipitated AgBr, to give the mononuclear complex **8** (Scheme 14). Without the addition of AgOTf no reaction is observed. When the twofold excess of Re(CO)$_5$Br was used, the dinuclear complex {Re(CO)$_5$}$_2$(debarb) (**9**) with the dianionic debarb$^{2-}$ was formed. An excess of triethylamine was always used in these reactions to replace one or both hydrogens from H$_2$debarb. The colourless compounds **8** and **9** are air stable over extended periods. They are soluble in polar organic solvents such as acetone or dichloromethane, but insoluble in non polar pentane and hexane.
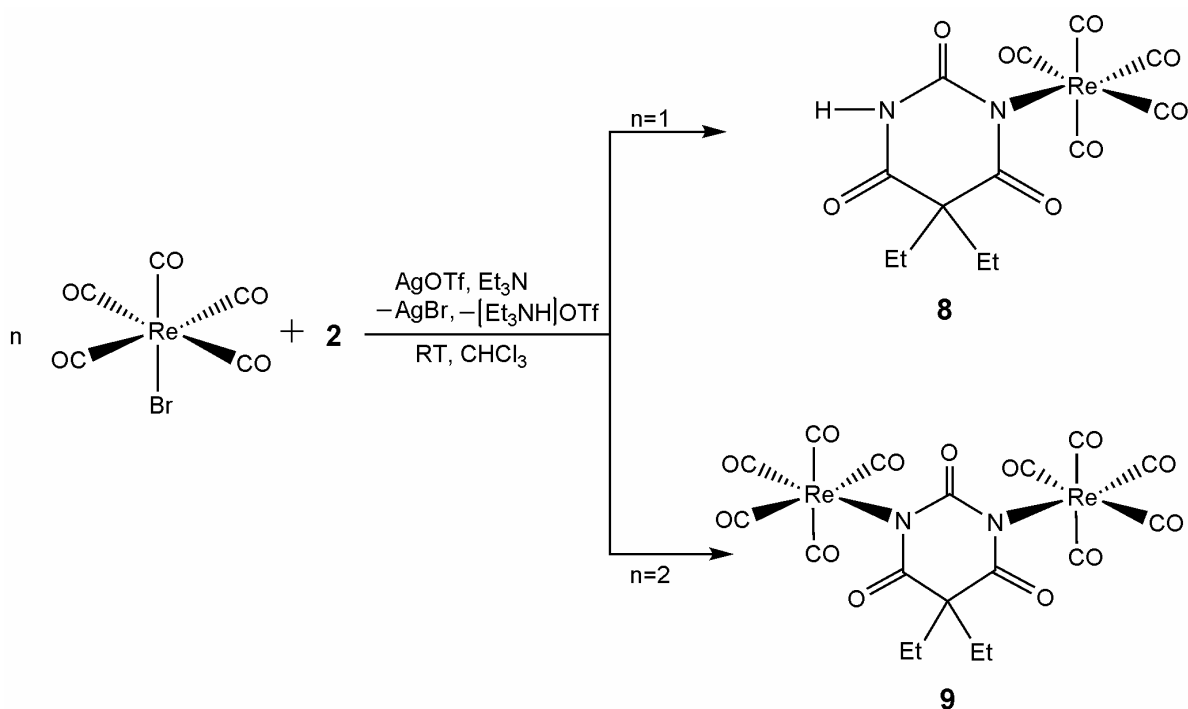


**Scheme 14**: Synthesis of mono- (Hdebarb) and dinuclear (debarb) rhenium(I) complexes **8** and **9**.

### 2.3.1  Molecular structure of 8 and 9

**8** and **9** were crystallised by isothermic diffusion of pentane into the solution of the complexes in $CH_2Cl_2$ at room temperature within 2 days. The colourless crystals isolated were suitable for X-ray crystallographic analysis. Complex **8** crystallises in the monoclinic crystal system $P2_1/c$ while complex **9** crystallises in the triclinic crystal system $P1$ respectively. The molecular structure of **8** and **9** are depicted in Figure 15 and Figure 16 respectively along with selected bond lengths and angles. Full crystallographic data for both compounds can be found in appendix, **Table 5.2**. Both of the complexes show pseudo-octahedral geometry around the rhenium centre. Like complex **7**, the Re−C(CO) bond distances in these complexes (1.936−1.943 Å) *trans* to the barbiturato-*N*-ligand are also shorter than the rest of the Re−C(CO) distances (2.007−2.058 Å). The *trans*-axial bond angles N−Re−C are slightly deviated from 180° (**8**: C(3)−Re(1)−N(1) 176.8(2)°; **9:** C(5)−Re(1)−N(1) 175.7(4)° and C(18)−Re(2)−N(2) 178.0(4)°) which may be attributed to the less steric factor in comparison to complex **7** with its bulky PPh₃ ligand in *cis*-position. The plane of the ligand in **8** is slightly turned out from the plane containing the Re−CO [torsion angles: C1−Re1−N1−C6 and C1−Re1−N1−C9 are 133.3(4)° and −47.6(4)° respectively].

In complex **9** Re1−(CO)₅ and Re2−(CO)₅ are almost in the same plane [torsion angles: Re1−N1−C6−N2 and Re2−N2−C6−N1 are 176.1(7)° and 179.9(7)° respectively] and show eclipsed situation. Furthermore, the X-ray structure analysis of **9** shows that although equivalent Re(CO)₅ moieties are bonded with the nitrogen atoms of the same ligand but their bond lengths and angles in both complex fragments are not exactly same. This indicates that the two rhenium atoms interact with the ligand in slightly different manner and therefore Re(1)−N(1) and Re(2)−N(2) bond lengths differ by 0.03 Å. No hydrogen bonds are observed in the crystal packing of the complexes.
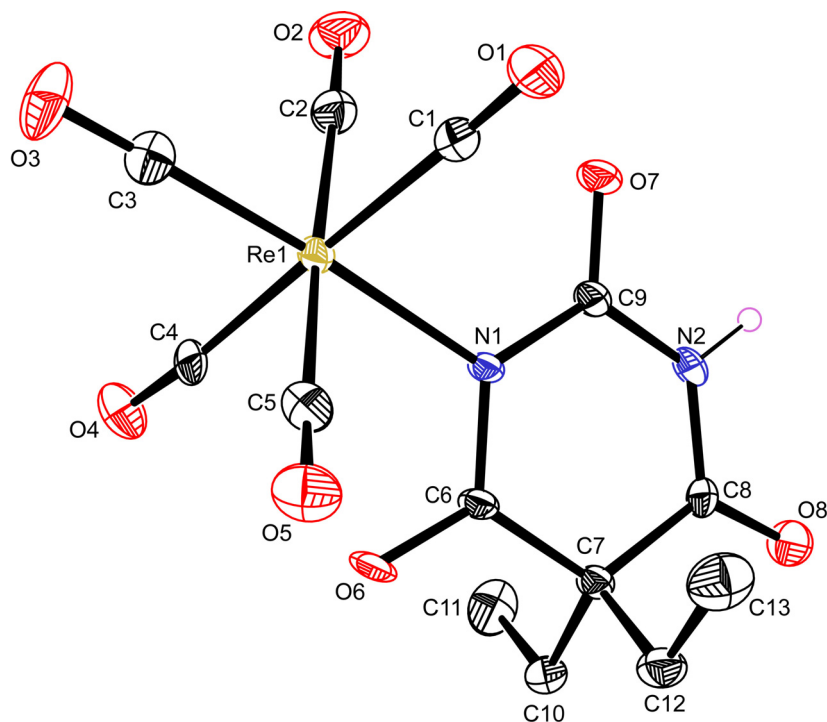
**Figure 15:** Molecular structure of **8**. The thermal ellipsoids are drawn at the 30% probability level. The disordered protons of the ethyl groups are omitted for clarity.

**Selected bond lengths [Å]:** Re(1)−N(1) 2.197(4), Re(1)−C(3) 1.943(6), Re(1)−C(5) 2.019(6), Re(1)−C(4) 2.020(6), Re(1)−C(1) 2.021(6), Re(1)−C(2) 2.023(5), C(3)−O(3) 1.129(7), C(4)−O(4) 1.121(6), C(1)−O(1) 1.108(6), C(2)−O(2) 1.116(6).

**Selected bond angles [°]:** C(3)−Re(1)−N(1) 176.8(2), C(5)−Re(1)−N(1) 87.88(19), C(1)−Re(1)−N(1) 89.55(18), C(2)−Re(1)−N(1) 91.02(18), C(4)−Re(1)−N(1) 88.64(17) C(6)−N(1)−Re(1) 119.5(3), C(9)−N(1)−Re(1) 119.6(3), C(4)−Re(1)−C(2) 91.6(2), C(3)−Re(1)−C(4) 88.7(2), C(4)−Re(1)−C(1) 178.0(2), O(3)−C(3)−Re(1) 177.5(5), C(6)−N(1)−C(9) 120.8(4), N(1)−C(9)−N(2) 119.4(4), C(5)−Re(1)−C(2) 176.9(2).

**Torsion angles [°]:** C(1)−Re(1)−N(1)−C(6) 133.3(4)°, C(1)−Re(1)−N(1)−C(9) −47.6(4)°.
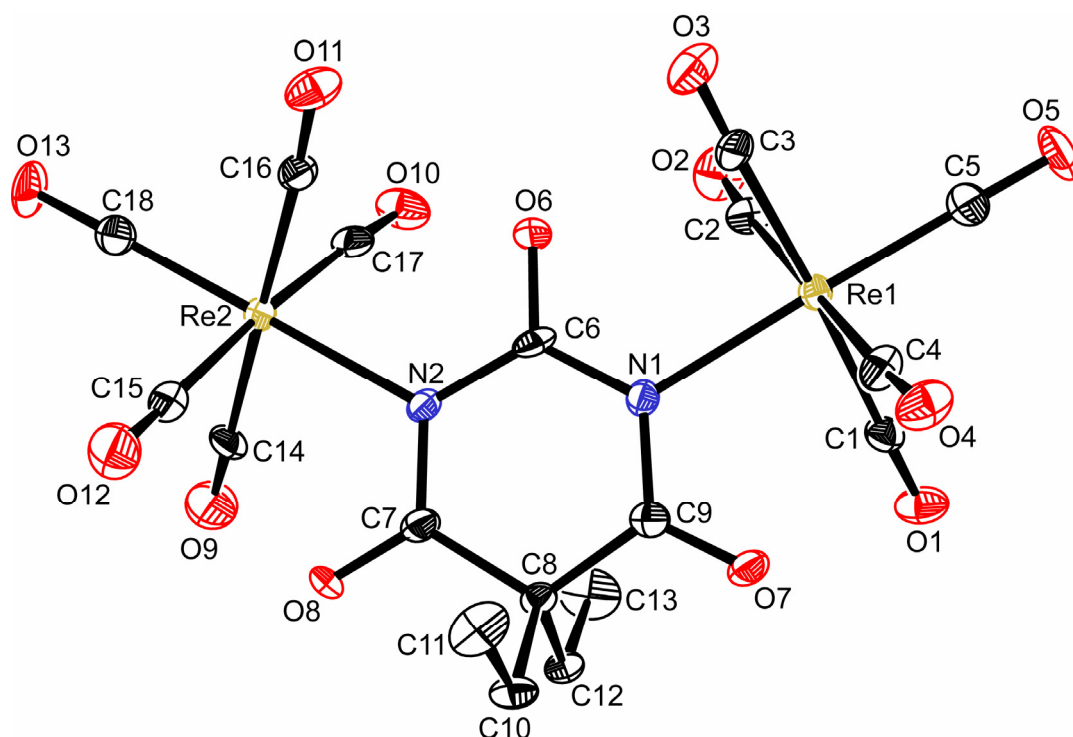
**Figure 16:** Molecular structure of **9**. The thermal ellipsoids are drawn at the 30% probability level. The disordered protons of two ethyl groups and one molecule of the complex are omitted for clarity.

**Selected bond lengths [Å]:** Re(1)−N(1) 2.208(8), Re(2)−N(2) 2.181(8), Re(1)−C(1) 2.049(11), Re(1)−C(2) 2.058(11), Re(1)−C(3) 2.029(12), Re(1)−C(4) 2.020(11), Re(1)−C(5) 1.936(11), Re(2)−C(14) 2.007(11), Re(2)−C(15) 2.031(12), Re(2)−C(16) 2.019(11), Re(2)−C(17) 2.009(13), Re(2)−C(18) 1.937(12), C(5)−O(5) 1.142(14), C(18)−O(13) 1.169(14), N(1)−C(6) 1.378(13), N(1)−C(9) 1.360(13), N(2)−C(6) 1.407(14), N(2)−C(7) 1.345(13),

**Selected bond angles [°]:** C(5)−Re(1)−N(1) 175.7(4), C(18)−Re(2)−N(2) 178.0(4), C(9)−N(1)−Re(1) 118.7(6), C(6)−N(1)−Re(1) 118.6(7), N(1)−C(6)−N(2) 121.3(9), C(7)−N(2)−C(6) 121.4(8), C(9)−N(1)−C(6) 122.5(9).

**Torsion angles [°]:** Re(1)−N(1)−C(6)−N(2) 176.1(7)°, Re(2)−N(2)−C(6)−N(1) 179.9(7)°.
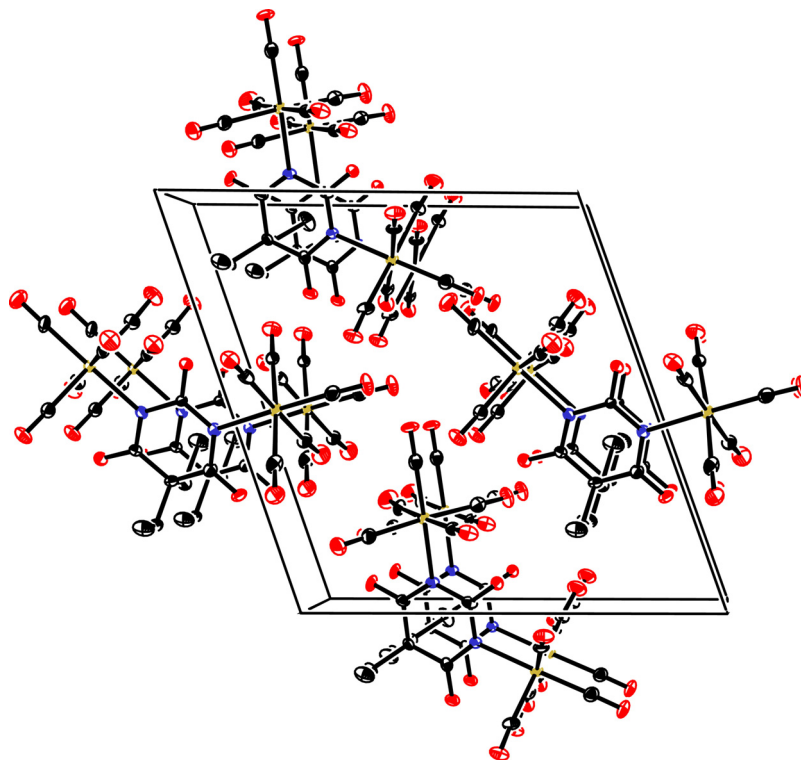
**Figure 17:** View of the unit cell of **9**.

## 2.3.2 Spectroscopic characterisation of 8 and 9

After coordination of the ligand with the metal complexes the ethyl groups of the complexes are no longer equivalent. Although the ethyl groups are not equivalent, complex **8** and **9** show in the $^1$H NMR spectra simple quartet and triplet for the protons of $CH_2$ and $CH_3$, respectively. These values are in good agreement with the values found in [Cp(CO)$_2$Fe(Hdebarb)] [46]. As the complex **9** is almost symmetrical, it shows no multiplet for the two ethyl groups. The signals for $CH_2$ (1.92(**8**), 1.93 (**9**) ppm) and $CH_3$ (0.74 (**8**), 0.75 (**9**) ppm) hydrogens of the complexes are shifted slightly upfield in comparison with the same signals found in **2** ($^1$H**:** $CH_2$ 1.93 ppm and $CH_3$ 0.84 ppm recorded in $CD_3OD$).

The $^{13}$C NMR spectra of **8** and **9** display three signals for the three different carbonyl groups within the coordinated barbiturate moiety and in addition show three signals for the carbonyl ligands attached with rhenium in **8**. In **9**, however some weak unresolved signals (181.31−156.22 ppm) were observed for all thirteen carbonyl carbons of complex **9**. In all the complexes the rest of the carbons of the barbiturate show only one signal for each of $C$Et$_2$ (56.17 (**8**), 57.18 (**9**) ppm), $CH_2$ (33.17 (**8**), 32.83 (**9**) ppm) and $CH_3$ (9.86 (**8**), 9.51 (**9**) ppm). On the other hand, in the case of complex **9** it was not possible to identify the signal

for $C$Et$_2$ carbon as the signal was in the same region of the signal of CD$_2$Cl$_2$. When the NMR of this complex was measured in CDCl$_3$ then the signal of $C$Et$_2$ was detected at 55.69 ppm. The broad N−H resonance of **8** is observed at 8.33 ppm.

In the IR spectra of **8** and **9** (in CHCl$_3$) the stretching vibrations of the carbonyl groups of Hdebarb and debarb appear as three bands in the range of 1723−1586 cm$^{-1}$, almost similar to those observed for di-substituted barbiturate complexes.[32, 91] The carbonyls of rhenium in both complexes show three bands in the range 2145−1987 cm$^{-1}$ (in CHCl$_3$) due to their pseudo-C$_{4v}$ symmetry (2A$_1$+E) in all the complexes which are typical for this σ-donor-π-acceptor ligand.

The mass spectra of the complexes show no unexpected behaviour and are easily interpreted because of the metal isotope distribution. The FAB$^+$ mass spectra exhibited the parent signals for the intact molecules at $m/z$ = 509 (**8**) and 834 (**9**). The fragmentation pattern is characterised by the successive loss of the CO ligands.

## 2.4  Palladium(II) complexes of barbiturates

*Sinn et al.* reported the crystal structure of bis[ethylenediamine(barbiturato-$C,N$)-palladium]-4-water which is a dimeric complex of dianionic barbituric acid (**1**) and was prepared from a solution originally containing [enPd(H$_2$O)$_2$]SO$_4$, barbituric acid, and hydroxide ion in a 1:2:2 molar ratio and has the formula [Pd(en)barb]$_2$(H$_2$O)$_4$. In the complex Pd(II) is coordinated to both a deprotonated amide nitrogen and the deprotonated tetrahedral carbon in 1,3-position.[29]

## 2.4.1 Synthesis of Hbarb complex of palladium(II)

*trans*-[Chlorido-(barbiturato-*N*)-bis-(triphenylphosphine)-palladium(II)]

C$_{40}$H$_{33}$ClN$_2$O$_3$P$_2$Pd (10)

Equivalent molar of **1** and [*trans*-PdCl$_2$(PPh$_3$)$_2$] were reacted in methanol in the presence of sodium methoxide (1 equivalent). After heating the reaction mixture at 50°C for 1 hour, it was allowed to cool to room temperature and stirred for 2 days to obtain the complex **10** (Scheme 15). The product was dissolved in dichloromethane and the solution was filtered to remove sodium chloride. The yellow compound is air stable and readily soluble in polar solvents, insoluble in H$_2$O and non-polar solvents.
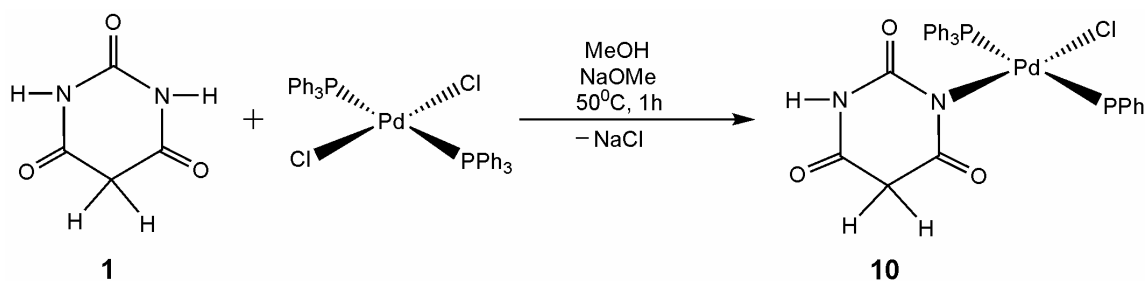


**Scheme 15**: Synthesis of Hbarb complex of palladium(II) **10**.

### 2.4.1.1 Molecular structure of 10

Yellow crystals of **10** (orthorhombic, space group *Pbca*) suitable for the X-ray analysis were grown by slow isothermic diffusion of *n*-pentane into the solution of the complex in CH$_2$Cl$_2$ within 1 day. The molecular structure of **10** together with selected bond lengths and angles are presented in Figure 18. The details of the data collection and refinement are given in **Table 5.3** of the crystallographic appendix. The crystal structure shows the d$^8$ Pd(II) center to be in a usual square planar geometry, assembled by the deprotonated amide nitrogen atom of the H$_2$barb, chlorido and two PPh$_3$ ligands which are trans to each other. However, the deviation of P1–Pd–P2 (177.48(4)°) and the Cl1–Pd–N1 (179.57(10)°) angles from linearity indicates the presence of a slight distortion of the Pd atom stereogeometry which may arise from the steric interaction between the Hbarb (deprotonated **1**) ligand and the two bulky ancillary PPh$_3$ ligands. The short Pd–N1 bond [2.030(3) Å] suggests a strong interaction between the metal and the amide nitrogen atom. A slight *trans* differential effect is also visible as the Pd–N1 bond *trans* to the Pd1−Cl1 bond [2.3049(11) Å] is shorter than both of

**Figure 18:** Molecular structure of **10**. The thermal ellipsoids are drawn at the 30% probability level. Hydrogen atoms of phenyl groups are omitted for clarity.

The N2a and C3a atoms are disordered. So, more accurate values were used to modify a better drawing of the structure.

**Selected bond lengths [Å]**: Pd(1)−N(1) 2.030(3), Pd(1)−Cl(1) 2.3049(11), Pd(1)−P(1) 2.3145(12), Pd(1)−P(2) 2.3325(12), N(1)−C(1) 1.367(6), N(1)−C(4) 1.344(6).

**Selected bond angles [°]**: Cl(1)−Pd(1)−N(1) 179.57(10), Cl(1)−Pd(1)−P(1) 88.77(4), Cl(1)−Pd(1)−P(2) 88.96(4), P(1)−Pd(1)−P(2) 177.48(4), P(1)−Pd(1)−N(1) 90.96(9), P(2)−Pd(1)−N(1) 91.31(9), Pd(1)−N1−C(1) 117.8(3), Pd(1)−N1−C(4) 118.3(3), C(1)−N(1)−C(4) 123.7(4).

**Torsion angles [°]**: P(1)−Pd(1)−N(1)−C(1) 77.2(3), P(1)−Pd(1)−N1−C(4) −107.4(3).

**Hydrogen bonds [Å] and angles [°]**: C(12)−H(12)···Cl(1) 0.950, 2.760, 3.465(5), 132.00; C(18)−H(18)···O(1) 0.9500, 2.5700, 3.446(6), 153.00; C(34)−H(34)···Cl(1) 0.9500, 2.7200, 3.434(5), 133.0.

the Pd–P bond distances [Pd1−P1 2.314(12) Å and Pd1−P1 2.332(12) Å]. The bond lengths and angles are within the expected values and are comparable to those found in complex **11** and other structurally analogous complexes.[32, 49, 92]

The Hbarb ligand is sandwiched between two phenyl rings of different PPh$_3$ ligands and is approximately perpendicular to the palladium co-ordination plane. This is illustrated by the torsion angles P1−Pd1−N1−C1 and P1−Pd1−N1−C4 which are 77.2(3)° and −107.4(3)° respectively. The pyrimidine ring of the Hbarb ligand is essentially planar (the sum of the angle around the N atom is 359.8°). Two phenyl rings which are closer to Hbarb ligand than the other phenyl rings are involved in π-π stacking. The distance between the centroids of stacked phenyl and Hbarb rings are 3.63 and 3.92 Å and the closest C–C distance is 3.315 Å.

In the crystal packing the molecules are characterised by three different intermolecular hydrogen bonds. One is between one oxygen (O1) atom of the Hbarb molecule and one H atom of adjacent phenyl ring. The rest two hydrogen bonds links two hydrogen atoms of phenyl ring with the Cl atom.

## 2.4.1.2 Spectroscopic characterisation of 10

The $^1$H NMR spectrum reveals the presence of the aromatic rings of the phenyl ligands in the range 7.83−7.36 ppm. The broad signal of N–H was observed at 8.01 ppm. The resonance due to methylene protons (2.14 ppm) was shifted to upfield with respect to the free ligand (N–H: 11.13 ppm and CH$_2$: 3.4 ppm recorded in DMSO).[2]

The aromatic carbon signals have been observed in the range 134.89−128.36 ppm. A considerable shift takes place in the position of the carbonyl carbons C=O (171.57, 168.18, 154.69 ppm) and methylene carbon CH$_2$ (singlet at 37.66 ppm), as compared with the free ligand (C=O: 166.8, 150.7 ppm and CH$_2$: 38.4 ppm recorded in DMSO).[93]

In the $^{31}$P NMR spectrum a single signal observed at 22.39 ppm is clearly indicative of both phosphorus nuclei to be present in equal magnetic environments.

In the IR spectrum of complex **10**, the weak absorption bands at 3371 cm$^{-1}$ and in the range of 3075–2986 cm$^{-1}$ correspond to the $v$(NH) and $v$(C–H) vibrations respectively. The $v$(C=O) stretching vibration bands for the three carbonyl groups appear at 1766, 1720 and 1696 cm$^{-1}$ in the case of H$_2$barb, while in **10** these bands are shifted towards lower energy at 1720 (s), 1683 (s) and 1615 cm$^{-1}$. The bands with strong intensity between 1480 and 1347 cm$^{-1}$ correspond to the C–H deformation and C–C vibrations and the two very strong bands at 1251 and 523 cm$^{-1}$ are attributed to the C–N stretching and Pd–N vibration.

The ion-positive FAB mass spectrum of **10** displays the molecular ion peak at $m/z$ = 793 with the expected isotopic distribution and a peak at 757 corresponding to the loss of the coordinated chloride.

## 2.4.2 Synthesis of Hdebarb complex of Pd(II)

*trans*-[Chlorido-(5,5-diethylbarbiturato-*N*-)-bis-(triphenylphosphine)-palladium(II)]

C$_{44}$H$_{41}$ClN$_2$O$_3$P$_2$Pd (11)

1 equivalent of **2** was reacted with 1 equivalent of [*trans*-PdCl$_2$(PPh$_3$)$_2$] in methanol in the presence of sodium methoxide (1 equivalent). After heating the reaction mixture at 50°C for 1 h, it was allowed to cool to room temperature and stirred for 2 days to obtain the complex **11** (Scheme 16). The product was dissolved in dichloromethane and the solution was filtered to remove sodium chloride. The yellow compound is air stable and slightly soluble in alcohols and readily soluble in other polar solvents, insoluble in H$_2$O, acetone and non-polar solvents.
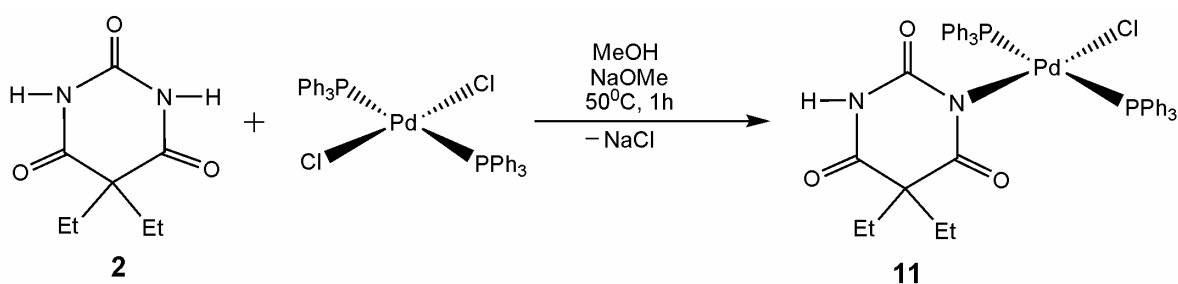


**Scheme 16**: Synthesis of Hdebarb complex of palladium(II) **11**.

## 2.4.2.1 Molecular structure of 11

Yellow crystals of **11** suitable for the X-ray analysis were grown by slow isothermic diffusion of *n*-pentane into a solution of the complex in $CH_2Cl_2$ within 2 days. The complex crystallises in the monoclinic crystal system $P2_1/n$. The molecular structure of the complex with the selected bond lengths and angles are shown in Figure 19. The details of the data collection and refinement are given in **Table 5.3** of the crystallographic appendix. The palladium centre displays slightly distorted square planar coordination: two *trans* corners of the square plane are occupied by the phosphorus atoms of two triphenylphosphines. The chloride atom and the deprotonated nitrogen atom of the Hdebarb ligand are *trans* to each other. The angles P1–Pd–P2 [171.5(2)°], and Cl1–Pd-N1 to [176.6(5)°] indicate that the distortion from the planarity is larger than that of **10** as two ethyl groups are present here to apply stronger steric interaction. The distance Pd1-Cl1 [2.3017(6) Å] is shorter than the distances of Pd−P [(2.3155(5) and 2.3392(5) Å)]. The Pd1-N1 bond length of 2.030(15) Å is similar to what was previously found in **10** and other structurally analogous palladium complexes.[32, 49, 92] Again, the Hdebarb ligand is sandwiched between two phenyl rings of both PPh$_3$ ligands and is almost perpendicular to the palladium co-ordination plane. This is illustrated by the torsion angles P1−Pd1−N1−C1 and P1−Pd1−N1−C4 which are −89.2(14)° and 90.4(15)° respectively. The environment around amide nitrogen atom is trigonal planar (sum of angles = 360°). The molecules of Hdebarb are connected to each other by N−H···O bond, involving the amine hydrogen atom of one Hdebarb and the carbonyl oxygen atom of another Hdebarb ligand. Moreover two carbon atoms of the phenyl rings of one molecule are also bonded via C−H···Cl and C−H···O with another molecule.
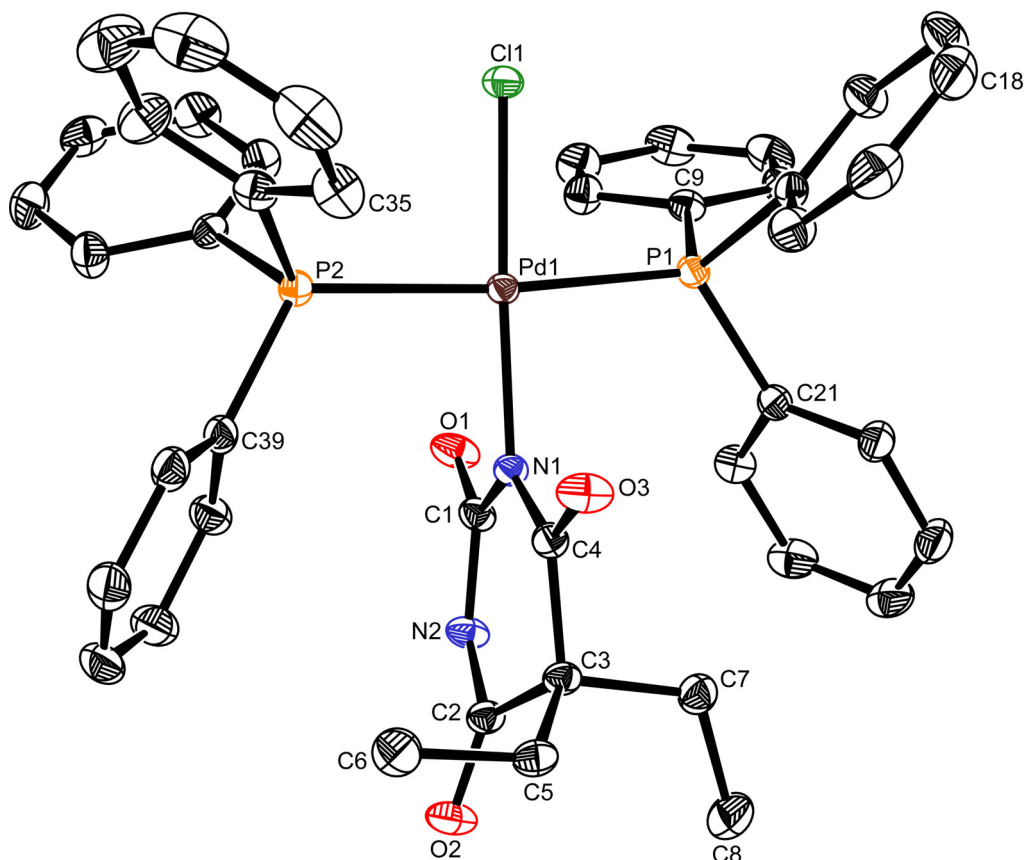
**Figure 19:** Molecular structure of **11**. The thermal ellipsoids are drawn at the 30% probability level. Hydrogen atoms are omitted for clarity.

**Selected bond lengths [Å]**: Pd(1)−N(1) 2.030(15), Pd(1)−Cl(1) 2.301(6), Pd(1)−P(1) 2.315(5), Pd(1)−P2 2.339(5), N(1)−C(1) 1.356(3), N(1)−C(4) 1.364(3), O(1)−C(1) 1.227(3), O(2)−C(2) 1.212(3), O(3)−C(4) 1.223(2), C(3)−C(4) 1.531(3), C(2)−C(3) 1.517(3).

**Selected bond angles [°]**: C(1)−Pd(1)−P(1) 86.13(2), Cl(1)−Pd(1)−P(2) 89.18(2), Cl(1)−Pd(1)−N(1) 176.67(5), P(1)−Pd(1)−P(2) 171.54(2), P(1)−Pd(1)−N(1) 92.31(5), P(2)−Pd(1)−N(1) 92.73(5), Pd(1)−N(1)−C(1) 115.10(13), Pd(1)−N(1)−C(4) 121.50(12), C(1)−N(1)−C(4) 123.40(17).

**Torsion angles [°]**: P(1)−Pd(1)−N(1)−C(4) 90.4(15), P(1)−Pd(1)−N(1)−C(1) −89.2(14).

**Hydrogen bonds [Å] and angles [°]**: N(2)−H(2)···O(1) 0.83(3), 2.04(3), 2.815(2), 156(2), C(18)−H(18)···Cl(1) 0.9500, 2.740, 3.683(3), 171.0, C(32)−H(32)···Cl(1) 0.950, 2.740, 3.475(2), 135.00, C(35)−H(35)···O(2) 0.950, 2.590, 3.213(3), 124.0.

## 2.4.2.2 Spectroscopic characterisation of 11

In the $^1$H NMR spectrum of **11** revealed a multiplet between 7.13 and 7.77 ppm due to the presence of the protons in the aromatic rings of the PPh$_3$ ligands. The protons of the ethyl groups show one set of signals, quartet at 1.87 ppm for CH$_2$ and triplet at 0.95 ppm for CH$_3$.

In the $^{13}$C NMR spectrum Hdebarb carbon signals appears at $\delta$ = 183.9, 175.04, 154.58 (CO), 56.8 (CEt$_2$), 29.76 (CH$_2$), and 9.33 (CH$_3$) as singlets. The CO signals shifted to downfield and rest of the C signals to upfield in comparison to the free ligands (C=O: 174.9, 150.3, CEt$_2$: 58.6, CH$_2$: 32.9, CH$_3$: 9.7 ppm recorded in CD$_3$OD). The phenyl carbon signals have been observed in the range 134.9−127.9 ppm.

The $^{31}$P NMR spectrum contains only one main resonance with a chemical shift of 22.77 ppm indicating two PPh$_3$ groups in a *trans* arrangement. Small amount of *cis* complex is also produced in the reaction which is observed in the spectrum (34.19, (d) and 28.2 (d) ppm).

The X-ray structure of **11** showed that palladium is coordinated to the deprotonated imidic nitrogen atom of the ligand. Further evidence for the coordination comes from the lowered C=O stretching frequencies, from 1763, 1715 and 1676 cm$^{-1}$ in H$_2$debarb to 1707, 1670 and 1613 cm$^{-1}$ in the IR spectrum (KBr) of the complex, which reflects the longer carbonyl bonds due to deprotonation of the N−H group.[49] The N−H vibration band is not prominent in KBr but in CHCl$_3$ the band is observed at 3398 cm$^{-1}$. The bands observed in the range 3055–2849 and 1459-1327 cm$^{-1}$ are characteristic of the $v$(C−H) stretching and deformation and $v$(C=C) vibrations (PPh$_3$) respectively. The band found at 1252 cm$^{-1}$ is assigned to the C–N stretching vibration and at 523 cm$^{-1}$ to the Pd−N vibration.

In the positive-ion FAB mass spectra of **11** the [MH$_2$$^{2+}$] peak was observed at *m/z* = 851. Other peaks resulting from the fragmentation of **11** are observed at *m/z* = 813, 551 and 289 assigned to [M$^+$−Cl], [M$^+$−Cl−PPh$_3$], [M$^+$−Cl−2PPh$_3$] respectively.

## 2.5   Copper complexes of barbiturates

Levi and Hubley have studied the reaction of copper with twelve different barbiturates in the presence of pyridine and, on the basis of IR spectral data, have suggested that the barbiturate ligand is bound to the copper through oxygen atoms.[94] *Caira et al* reported the first crystal structure of the complex [Cu(Hdebarb)$_2$(py)$_2$] which was prepared by mixing aqueous solutions of sodium barbital, pyridine and copper(II) chloride in the molar ratio 2:2:1, at room temperature. [95]

### 2.5.1   Synthesis of Hdebarb complex of copper(I)

**5,5-Diethylbarbiturato-*N*-bis(triphenylphosphine)-copper(I)**
**C$_{44}$H$_{41}$CuN$_2$O$_3$P$_2$ (12)**

One molar equivalent of **2** was treated first with an excess of triethylamine in CHCl$_3$ to produce the Hdebarb anion. Addition of equivalent molar of [(PPh$_3$)$_2$CuBH$_4$] to this mixture and heating the solution at 50°C for 4 hours resulted in the formation of **12** within 1 day (scheme 17). The colourless complex is air stable and soluble in common solvents (CH$_2$Cl$_2$, CHCl$_3$, acetone etc) but insoluble in H$_2$O, methanol, pentane, hexane etc.
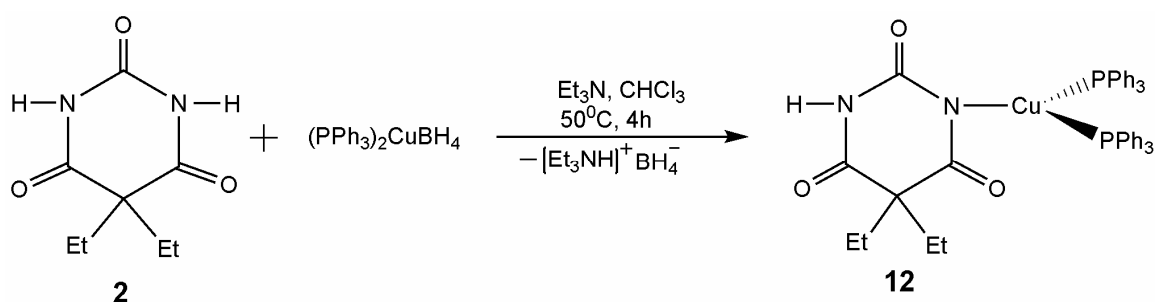


**Scheme 17:** Synthesis of Hdebarb complex of copper(I) **12**.

### 2.5.2   Molecular structure of 12

Colourless crystals were obtained by slow isothermic diffusion of *n*-pentane into a solution of the complex in chloroform within 1 day. The molecular structure of the title compound is shown in Figure 20 along with the relevant bond distances and angles. The complex crystallises in the triclinic crystal system *P*-1. The details of the data collection and refinement are given in **Table 5.4** of the crystallographic appendix.
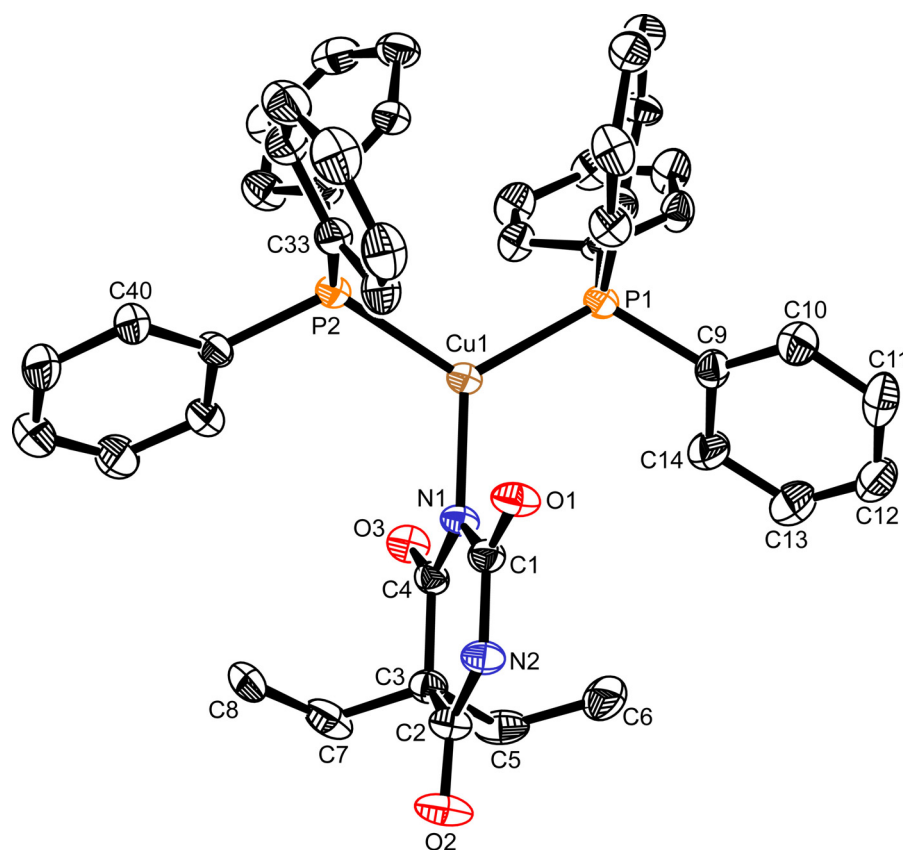
**Figure 20:** Molecular structure of **12**. The thermal ellipsoids are drawn at the 30% probability level. Hydrogen atoms, one molecule of the complex connected by the hydrogen bonds and $CHCl_3$ molecules of crystallisation are omitted for clarity.

**Selected bond lengths [Å]**: Cu(1)−N(1) 1.978(7), Cu(1)−P(1) 2.249(2), Cu(1)−P(2) 2.249(2), O(1)−C(1) 1.246(10), O(2)−C(2) 1.207(10), N(1)−C(4) 1.376(10), N(1)−C(1) 1.333(10), O(1)−C(1) 1.246(10), O(3)−C(4) 1.210(9), O(3)−C(4) 1.210(9).

**Selected bond angles [°]**: P(1)−Cu(1)−P(2) 118.91(9), P(1)−Cu(1)−N(1) 120.99(18), P(2)−Cu(1)−N(1) 119.84(18), Cu(1)−N(1)−C(4) 126.9(5), Cu(1)−N(1)−C(1) 110.8(5), C(1)−N(1)−C(4) 122.3(7).

**Hydrogen bonds [Å] and angles [°]**: N2−H2···O5 0.880, 2.060, 2.907(8), 162.0; N4−H4···O1 0.880, 1.910, 2.786(8), 174.0; C38−H38···O1 0.9500, 2.550, 3.485(10), 169.0; C60−H60···O4 0.950, 2.470, 3.387(10), 161.0; C62−H62···Cl7 0.950, 2.680, 3.343(12), 128.0; C89−H89···O6 1.000, 2.060, 3.046(16), 170.0; C90−H90···O3 1.000, 2.080, 2.992(16), 151.0.

In the crystal one molecule of the complex is bonded with another molecule via hydrogen bond and along with these two molecules there are three CHCl$_3$ solvent molecules in the crystal which explain rather poor R value. Complex **12** has a trigonal planar coordination around Cu(I) (sum of angles = 359.74°) which is bonded to the Hdebarb ligand via deprotonated nitrogen atom and with two PPh$_3$-ligands in an almost ideal sp$^2$−hybridized situation [P1−Cu1−P2 = 118.91(9)°] and with essentially identical Cu−P distances [2.249(2) Å]. The Cu1-N1 distance (1.978(7) Å) is shorter than the Cu−P bond distances as expected and consistent to those found in bis{(5,5-Hdebarb)-pyridine}Cu(II) complex [1.983(5) Å].[96] All the above mentioned bond lengths and angles along with the six independent P−C$_{Ph}$ bonds (1.816−1.833 Å) and Cu−P−C angles (107.9−118.6°) are in good agreement with those found in other copper triphenylphosphine complexes.[97, 98, 99, 100]

One complex molecule of [(PPh$_3$)$_2$Cu(Hdebarb)] (**12**) is bonded through N−H···O hydrogen bonds with the adjacent molecule (Figure 21) and phenyl ring is bonded with the solvent CHCl$_3$ molecule by the C−H···Cl bond to form an extensive layer network of hydrogen bonds.
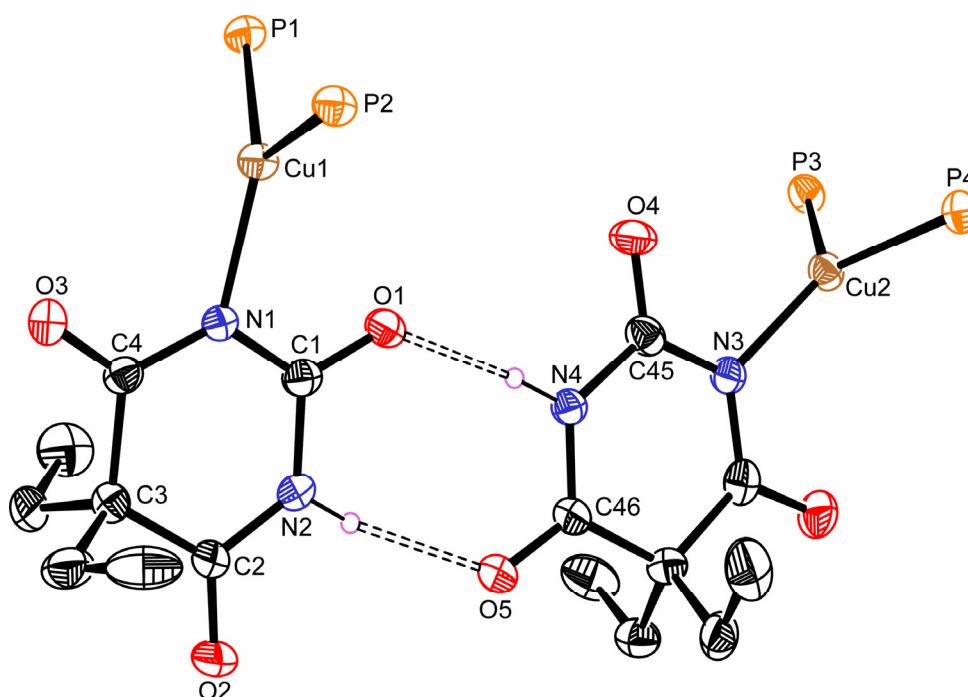


**Figure 21:** One set of hydrogen (N−H···O) bonding in **12**. The phenyl ligands and hydrogen atoms are omitted for clarity.

## 2.5.3 Spectroscopic characterisation of 12

The $^1$H NMR of **12** revealed a multiplet between 7.18 and 7.33 ppm due to the presence of the protons in the aromatic rings of the PPh$_3$. The signals observed at 7.62, 1.77 and 0.46 ppm are assigned to the NH, CH$_2$ and CH$_3$ protons.

The $^{13}$C NMR spectrum displays three signals for the three different carbonyl groups at 181.09, 176.36, 156.51 ppm. The rest of the carbons of the barbiturate show one signal for each of $C$Et$_2$ (57.02 ppm), CH$_2$ (32.08 ppm) and CH$_3$ (9.46 ppm) carbons. The phenyl carbon atoms of the PPh$_3$ ligand show multiplets at 133.35−128.79 ppm. The signals of the carbonyl groups are shifted to downfield and other signals observed for the carbon and hydrogen atoms of Hdebarb ligand are shifted to upfield in comparison to the free ligand (**2**). ($^1$H**:** CH$_2$ 1.93 ppm and CH$_3$ 0.84 ppm, **2** recorded in CD$_3$OD) and (C=O: 174.9, 150.3, $C$Et$_2$: 58.6, CH$_2$: 32.9, CH$_3$: 9.7 ppm, **2** recorded in CD$_3$OD).

The $^{31}$P NMR spectrum contains only one resonance with a chemical shift of −0.850 ppm.

In the IR spectrum (KBr disc) the relatively weak bands absorption in the frequency range 3170−2930 cm$^{-1}$ are attributed to the $v$(NH) vibrations of the amine and C−H stretching vibrations of the ethyl group of the Hdebarb. For the three carbonyl groups two strong $v$(CO) bands at 1670 and 1595 cm$^{-1}$ and one weak band at 1711 cm$^{-1}$ were observed. The bands with strong intensity between 1435 and 1316 cm$^{-1}$ correspond to the C−H deformation vibrations and the band centered around 1252 cm$^{-1}$ is attributed to the C−N stretching vibrations.[94]

In the mass spectrum (FAB$^+$) of **12,** instead of molecular peak [M]$^+$ the [M−H]$^+$ with $m/z =$ 770 is present. The molecular peak is missing which is in line with the fact, that **12** is neutral, and therefore the loss of an anion or hydrogen ion is necessary to reach a fragment which is detectable in the FAB-MS. The peaks at 509 [M−PPh$_3$]$^+$ and at 325 [Cu(PPh$_3$)$_2$]$^+$ are also detected in the FAB-MS

## 2.6 Rhodium complexes of barbiturates

## 2.6.1 Synthesis of Hdebarb complex of rhodium(I)

*trans*-[Carbonyl-5,5-diethylbarbiturato-*N*-bis(triphenylphosphine)rhodium(I)] C$_{45}$H$_{41}$N$_2$P$_2$O$_4$Rh (13)

A solution of RhCl(CO)(PPh$_3$)$_2$ in CHCl$_3$ was treated with AgOTf and stirred for 1h until the AgCl had precipitated. After centrifugation and separation of the solution by decantation, **2** was added to the solution followed by triethylamine. The yellow solution was stirred at room temperature for 2 days to obtain the complex **13** (scheme 18). The complex is air stable and soluble in common polar solvents, but insoluble in H$_2$O, sparingly soluble in methanol and insoluble in pentane and hexane etc.
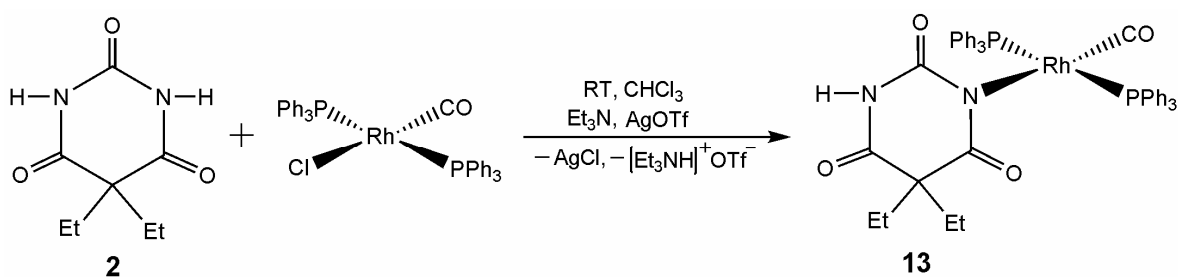


**Scheme 18:** Synthesis of Hdebarb complex of rhodium(I) **13.**

## 2.6.1.1 Molecular structure of 13

Pale yellow twin crystals were grown by slow isothermic diffusion of *n*-pentane into a solution of the complex in CH$_2$Cl$_2$ within 2 days. Attempts to obtain single crystals of **13** from numerous solvent mixtures resulted only in twinned crystals whose structure nevertheless could be solved. The structure is shown in Figure 22 together with selected bond lengths and angles. The details of the data collection and refinement are given in **Table 5.4** of the crystallographic appendix. It crystallises in the triclinic crystal system *P*-1 and with one molecule of dichloromethane but there are no close contacts between them. The molecular structure shows the d$^8$ Rh(I) center to be in a slightly distorted square planar geometry, having the ligands CO and Hdebarb in a *trans* arrangement and completing the coordination with the two PPh$_3$ ligands in *trans* position to each other. The Rh1−C9 (1.804(9) Å) bond *trans* to the Hdebarb ring is shorter than the Rh1−N1 (2.141(6) Å) and

the Rh1−P bonds. The Rh1−P1 bond (2.352(2) Å) is slightly longer than that of Rh1−P2 (2.325(2) Å). Possibly steric constraints imposed by the two PPh$_3$ ligands and monodented Hdebarb ligand causes the lengthening of the Rh1−P1 bond and the deviation of P1−Rh1−P2 (165.6(8)°) and N1−Rh1−C9 (178.9(3)°) bond angles from linearity. These bond lengths and angles along with the other bond angles around Rh (P−Rh−N: 92.6−94.4°; P1−Rh1−C9: 85.9−86.8°) are consistent with other literature reports for Rh(I) complexes.[101, 102, 103] The plane of the ligand is approximately perpendicular to the Rh(I) co-ordination plane. This is illustrated by the torsion angles: P1−Rh1−N1−C1 (72.9(5)°), P1−Rh1−N1−C4 (−101.9(7)°), P2−Rh1−N1−C4 (90.7(7)°), P2−Rh1−N1−C1 (−94.6(5)°). It seems reasonable that tipping of the barbiturate ligand out of perpendicularity occurs as a result of a steric interaction with the phenyl rings.

The Hdebarb ligand is essentially planar (the sum of the angles around the N atom is 359.8°) with normal bond distances and angles. There are intermolecular hydrogen bonds between the amino N−H of one molecule of the Hdebarb and the amide oxygen of an adjacent molecule and a second type is between the C−H of phenyl ring of one molecule with the amide oxygen of an adjacent molecule.
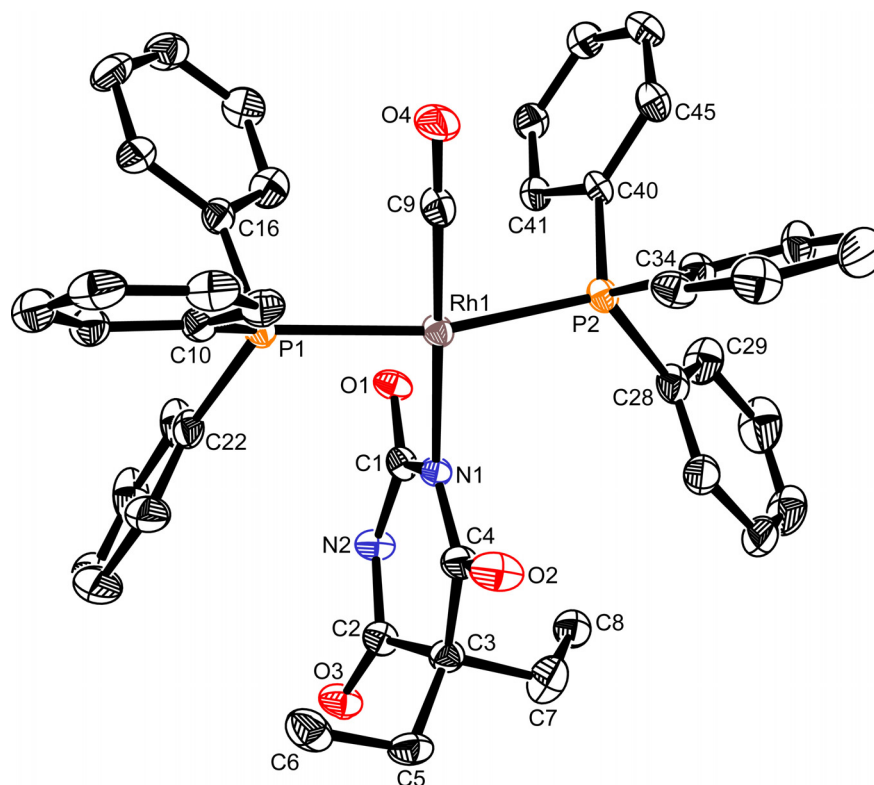
**Figure 22:** Molecular structure of **13** (only one molecule is shown). The thermal ellipsoids are drawn at the 30% probability level. Hydrogen atoms and the enclosed $CH_2Cl_2$ molecule are omitted for clarity.

The crystal was a twinned one, however, the twin integration failed, which explains the rather poor R-values. The disorder in an ethyl group was handled by a split model. The dichloromethane molecules have been refined isotropically.

**Selected bond lengths [Å]**: Rh(1)−N(1) 2.141(6), Rh(1)−C(9) 1.804(9), Rh(1)−P(1) 2.352(2), Rh(1)−P(2) 2.325(2), O(4)−C(9).1.164(11), O(1)−C(1) 1.234(11), O(2)−C(4) 1.227(11), O(3)−C(2) 1.209(10), N(1)−C(4) 1.356(11), N(1)−C(1) 1.354(10).

**Selected bond angles [°]**: P(1)−Rh(1)−P(2) 165.61(8), P(1)−Rh(1)−N(1) 92.61(17), P(1)−Rh(1)−C(9) 86.8(3), P(2)−Rh(1)−N(1) 94.49(17), P(2)−Rh(1)−C(9) 85.9(3), N(1)−Rh(1)−C(9) 178.9(3), Rh(1)−N(1)−C(1) 114.1(5), Rh(1)−N(1)−C(4) 124.3(5), C(1)−N(1)−C(4) 121.4(7).

**Torsion angles [°]**: P(1)−Rh(1)−N(1)−C(1) 72.9(5), P(1)−Rh(1)−N(1)−C(4) −101.9(7), P(2)−Rh(1)−N(1)−C(4) 90.7(7), P(2)−Rh(1)−N(1)−C(1) −94.6(5).

**Hydrogen bonds [Å] and angles [°]**: N2−H2···O1 0.880, 1.980, 2.839(9), 166.0; N4−H4···O5 0.880, 1.9500, 2.805(8), 164.0; C13−H13···O7 0.950, 2.280, 3.208(13), 165.00; C17−H17···O1 0.950, 2.550, 3.409(12), 151.00; C41−H41···O1 0.950, 2.4300, 3.365(10), 169.0; C53−H53···O6 0.980, 2.590, 3.230(19), 123.0; C78−H78···O5 0.9500, 2.4400, 3.364(10), 164.00.

## 2.6.1.2 Spectroscopic characterisation of 13

The $^1$H NMR spectrum contains four groups of signals. In the region 7.72−7.36 ppm there are signals of phenyl protons of PPh$_3$ ligands. A singlet at 7.07 ppm (NH), quartet at 2.03 ppm (CH$_2$) and a triplet at 0.22 ppm (CH$_3$) are due to the presence of the protons of the Hdebarb ligand.

In the $^{13}$C NMR spectrum, a triplet at 181.91 ppm (Rh−CO) and three individual singlets at 179.62, 174.79, 155.29 ppm (Hdebarb−CO) are assigned to the carbonyl carbons. The remaining Hdebarb carbon atoms show one signal for each of CEt$_2$ (56.02 ppm), CH$_2$ (27.7 ppm) and CH$_3$ (8.9 ppm).

The $^{31}$P NMR spectrum shows a doublet at 31.79 ppm with the coupling constant $^1J$ (Rh–P) 135.5 Hz, indicating the *trans* arrangement of the phosphine ligands.

The IR spectrum of **13** (KBr disc) shows four strong to medium intensity absorption bands at 1975 (Rh–CO), 1717, 1664 and 1601 (H$_2$debarb–CO) cm$^{-1}$ for the four carbonyl groups. The spectrum also has resonances at 3159 (3397 in CHCl$_3$), 1435 and 1264 cm$^{-1}$, assigned to $v$(N–H), $v$(P–Ph) and $v$(C–N), respectively. Moreover, typical $v$(C−H) and $v$(C=C) vibrations (PPh$_3$) are observed in the range of 3055–2854 and 1460-1312 cm$^{-1}$. The strong bands at 692 and 518 cm$^{-1}$ are indicative of Rh-PPh$_3$ ligation in the complexes.[104]

In the mass spectra (FAB$^+$) the [MH$^+$] peak appears at $m/z$ = 839. Other peaks observed at 810, 548 and 286 correspond to the cations formed by the loss of CO and successive loss of both PPh$_3$ ligands.

## 2.7   Synthesis of Hdebarb complexes of Rh(III), Ir(III) and Ru(II)

*Bis*-(5,5-diethylbarbiturato-*N,O*)-(5,5-diethylbarbiturato-*N*)-
($\eta^5$-pentamethylcyclopentadienyl)-rhodium(III)
$C_{26}H_{37}N_4O_6Rh$ (14)

Chlorido-($\eta^5$-pentamethylcyclopentadienyl)-(5,5-diethylbarbiturato-*N,O*)-
iridium(III)
$C_{18}H_{26}ClIrN_2O_3$ (15)

*Bis*-(5,5-diethylbarbiturato-*N,O*)-(5,5-diethylbarbiturato-*N*)-($\eta^6$-*p*-
isopropyl(methyl) benzene)-ruthenium(II)
$C_{26}H_{36}N_4O_6Ru$ (16)

Chlorido-($\eta^6$-*p*-isopropyl(methyl)benzene)-(5,5-diethylbarbiturato-*N,O*)-
ruthenium(II)
$C_{18}H_{25}ClRuN_2O_3$ (17)

The dinuclear pentamethylcyclopentadienyl complexes [{($\eta^5$-C$_5$Me$_5$)MCl$_2$}$_2$] (M = Ir, Rh) and the arene ruthenium complex [{($\eta^6$-arene)RuCl$_2$}$_2$] (arene = *p*-Pr$^i$C$_6$H$_4$Me) react with either two molar or four molar equivalents of the Na[Hdebarb] (**3**) in CHCl$_3$/MeOH mixture to form the neutral pentamethylcyclopentadienyl iridium and rhodium complexes [($\eta^5$-C$_5$Me$_5$)Rh(Hdebarb)$_2$] (**14**) (Scheme 19), [($\eta^5$-C$_5$Me$_5$)IrCl(Hdebarb)] (**15**) (Scheme 20), and the arene ruthenium complexes [($\eta^6$-arene)Ru(Hdebarb)$_2$] (**16**) and [($\eta^6$-arene)RuCl(Hdebarb)] (**17**) (Scheme 21). In all the four reactions first the metal complexes dissolved in CHCl$_3$ were heated for 15-30 minutes and then appropriate molar solutions of **3** in MeOH was added with it and the mixture was heated for 4-5 hours at 50°C. The solutions were allowed to cool to room temperature and stirred for 2 days to complete the reaction. In complex **14** one molecule of Hdebarb is coordinated with Rh through chelate *N,O* and another molecule via N atom. But, in **15** only one chelating *N,O*- ligand is bonded with Ir. In the case of {($\eta^6$-arene)RuCl$_2$}$_2$ synthesis of two different types of complexes (**16**, **17**) using different molar ratios (1:1 and 1:2) of metal complex and **3** was successful. In one of the two complexes (**16**) the coordination mode is similar to complex **14** and the coordination in

second complex **17** resembles to **15**. Treatment of $\{(\eta^5\text{-}C_5Me_5)RhCl_2\}_2$ and **3** in 1:1 and $\{(\eta^5\text{-}C_5Me_5)IrCl_2\}_2$ and **3** in 1:2 molar ratio always produce only complex **14** and **15** respectively. The crystals of **15** and **16** were physically separated from the few crystals of unreacted metal complex with the aid of a microscope. The complexes **14−17** are orange-yellow, non-hygroscopic and air-stable. They are sparingly soluble in water, soluble in polar organic solvents and insoluble in pentane and hexane.
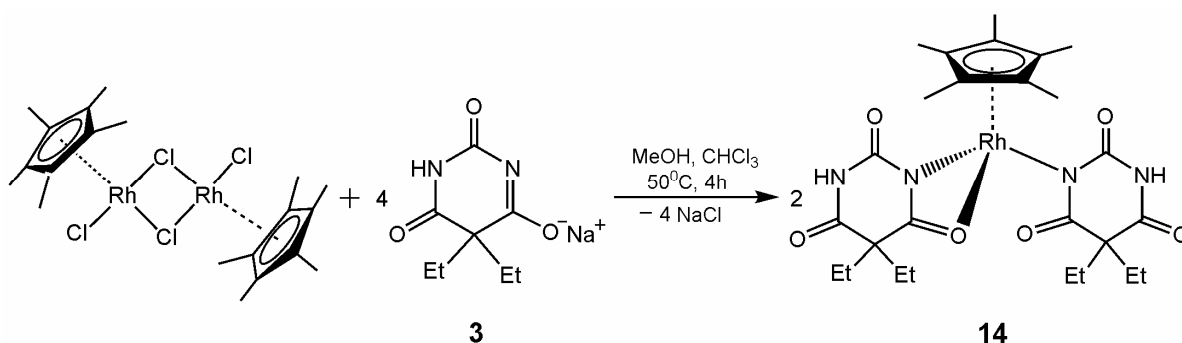


**Scheme 19:** Synthesis of bis (Hdebarb) complex of rhodium(III) **14**.
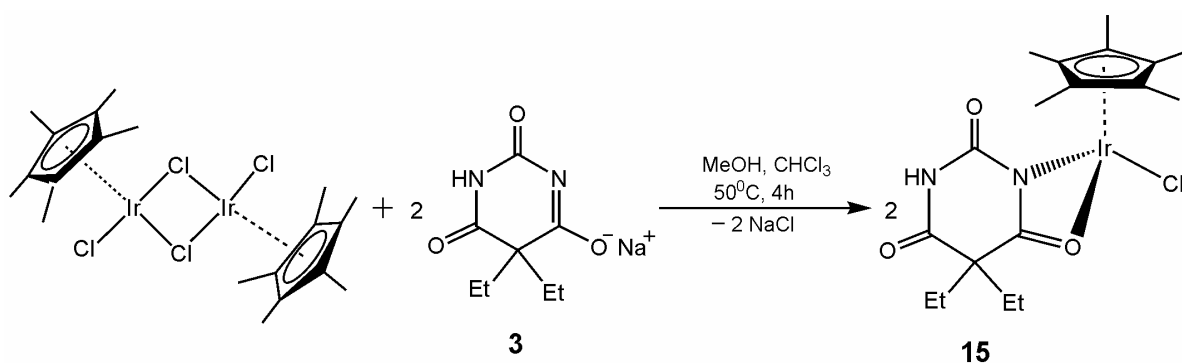


**Scheme 20:** Synthesis of mono-Hdebarb complex of iridium(III) **15**.
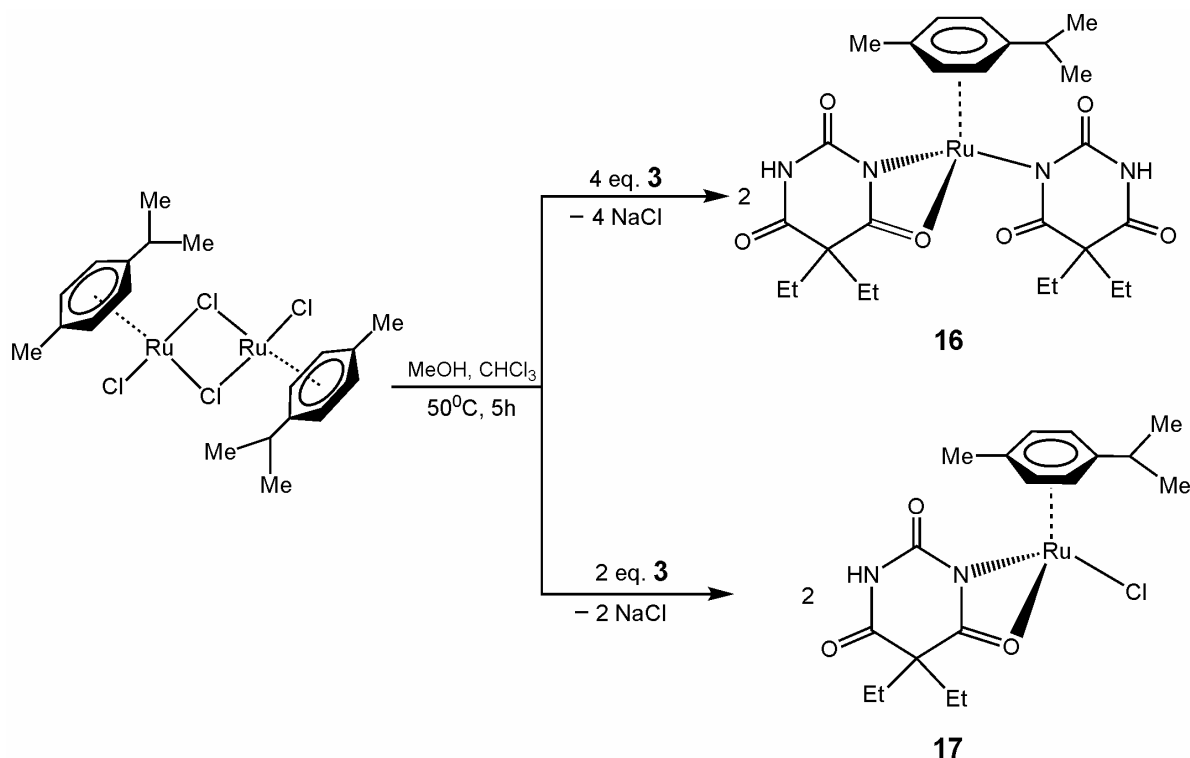
**Scheme 21:** Synthesis of mono- and bis (Hdebarb) complexes of ruthenium(II) **16** and **17**.

## 2.7.1  Molecular structure of 14

Orange crystals of the complex suitable for X-ray analysis were grown by slow diffusion of pentane into a solution of **14** in dichloromethane at room temperature. The molecular structure and selected bond lengths and angles are presented in Figure 23. The details of the data collection and refinement are given in **Table 5.5** of the crystallographic appendix. The complex crystallizes in the monoclinic crystal system *C2/c*. The molecular structure of **14** shows a pseudo octahedral or better a piano-stool geometry with the Rh(III) centre coordinated by the $\eta^5$-bonded Cp* ligand, a chelating *N,O*- and a monodented-*N*-barbiturato ligand. Due to the geometric requirements of the four membered chelate ring the $\eta^2$-coordinated N-O barbiturate group forms a small N1−Rh1−O1 angle of 59.67(7)°. The deprotonated N of the second barbiturate ligand forms also small angles N3−Rh1−N1/O1 (N3−Rh1−N1 86.59(8)° and N3−Rh1−O1 83.62(7)°). As one of the three angles is the smallest, one can assume that the total hindrance is reduced, so that the Cp* ligand can approach somewhat more closely to the metal at a distance of 1.747 Å (Rh1−Cp*$_{centroid}$) to be compared with the similar complexes (1.764, 1.782 Å). [105, 106] The Rh−Cp* bonds (2.097−2.156 Å) are within the range previously described in the literature.[107] The distance Rh1−N3 (2.118(2) Å) is similar to that of **16** (Ru1−N3 2.114(4) Å). On the other hand the

53

distances Rh1−N1 and Rh1−O1 (2.130(2) and 2.2714(18) Å respectively) of **14** are somewhat longer than the distances Ru1−N1 and Ru1−O1 (2.102(4) and 2.213(3) Å respectively) of **16**. It is noteworthy that the Rh1−N3 bond is the shortest of all the other Rh−N and Rh−O bonds just mentioned.

Both the coordinated N1 and N3 atoms have a planar environment since the average sum of the bond angles around these atoms is 360°. It was found that as a result of deprotonation, the internal ring angle at N1 closes from 126.4° in $H_2$debarb to 119.2° in its anion.[34] It is observed in **14** that the C1−N1−C4 and C9−N3−C12 bond angles of the coordinated N atoms range between 121.4°−122.8° which are close to the values of Hdebarb anion rather than the values of $H_2$debarb molecule.

The packing diagram of the complex **14** is governed by N−H···O hydrogen bonds involving the amino hydrogen atoms of the two Hdebarb ligand and the carbonyl O atoms of the Hdebarb ligands of the adjacent units, resulting in a three dimensional network. The first hydrogen bond connects via N2 atom of one Hdebarb molecule to O1 atom of another *N,O*−chelate Hdebarb ring and the second hydrogen bond connects N4 atom of one *N*−bonded Hdebarb ring with the O4 atom of free C=O bond of another Hdebarb molecule. The distances and the angles of the hydrogen bonds are in good agreement with other hydrogen bond containing Hdebarb complexes.[33, 37, 40, 41]
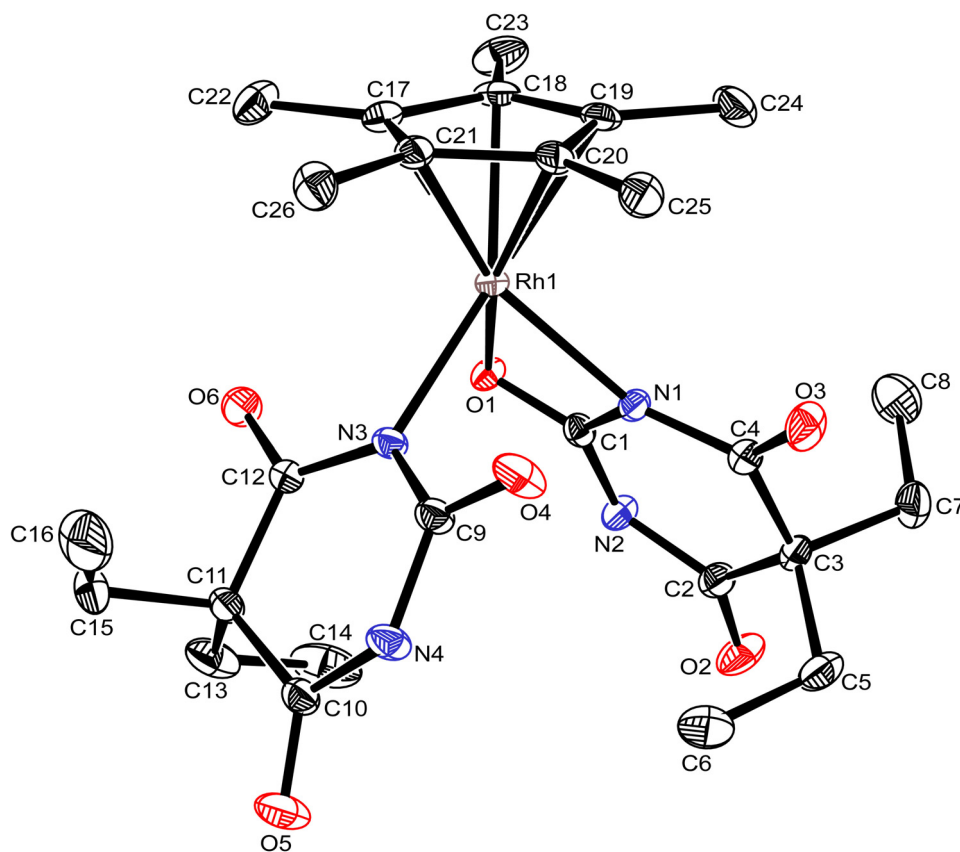
**Figure 23:** Molecular structure of **14**. The thermal ellipsoids are drawn at the 30% probability level. Hydrogen atoms are omitted for clarity.

**Selected bond lengths [Å]**: Rh(1)−N(3) 2.118(2), Rh(1)−N(1) 2.130(2), Rh(1)−O(1) 2.271(18), Rh(1)−C(21) 2.135(2), Rh(1)−C(20) 2.097(2), Rh(1)−C(19) 2.137(3), Rh(1)−C(17) 2.137(3), Rh(1)−C(18) 2.156(2), N(3)−C(9) 1.362(3), N(3)−C(12) 1.363(3), N(1)−C(1) 1.332(3), N(1)−C(4) 1.372(3), C(1)−O(1) 1.249(3), C(2)−O(2) 1.213(3), C(4)−O(3) 1.214(3), C(9)−O(4) 1.221(3), C(10)−O(5) 1.212(3), C(12)−O(6) 1.226(3), Rh(1) $\cdots$ C$_{centroid}$ 1.747.

**Selected bond angles [°]**: N(1)−Rh(1)−O(1) 59.67(7), N(3)−Rh(1)−N(1) 86.59(8); N(3)−Rh(1)−O(1) 83.62(7), N(3)−Rh(1)−C(21) 96.36(9), C(1)−N(1)−C(4) 122.8(2), C(1)−N(1)−Rh(1) 93.96(15), C(4)−N(1)−Rh(1) 143.24(17), C(9)−N(3)−Rh(1) 117.78(16), C(12)−N(3)−Rh(1) 120.85(16), C(9)−N(3)−C(12) 121.4(2).

**Hydrogen bonds [Å] and angles [°]**: N(2)−H(2)$\cdots$O(1) 0.88(4), 1.95(4), 2.822(3), 167(3); N(4)−H(4)$\cdots$O(4) 0.81(4) 2.02(4), 2.824(3), 174(4).

## 2.7.1.1 Spectroscopic characterisation of 14

The $^1$H and $^{13}$C NMR spectra of **14** showed two inequivalent ethyl substituents, consistent with the molecular structure where the protons of ethyl groups are in magnetically distinct environments. Two of four groups are directed towards the CH$_3$ groups of Cp* and other two towards the *N, O* atoms of the ligand. So, the $^1$H NMR spectrum showed a quartet at 2.03 ppm, a broad signal at 1.86 ppm due to the CH$_2$ protons and two triplets (0.87 and 0.81 ppm) for the CH$_3$ protons of the ethyl groups. These signals are relatively weaker than the signals found in complexes **6-13**. A sharp singlet at 1.57 ppm is observed for the CH$_3$ protons of the Cp* moiety.

In the $^{13}$C NMR spectrum, two signals for each of the CH$_2$ (32.10 and 29.68 ppm), CH$_3$ (9.89 and 9.73 ppm) and one for the *C*Et$_2$ (57.59 ppm) carbons were observed. The *C*H$_3$(Cp*) was observed at 9.64 ppm and $C_q$(Cp*) at 93.70 ppm as a doublet ($J_{Rh-C}$ 22 Hz). The carbonyl signals are found at 174.40, 172.38, and 151.89 ppm.

The signals of the Hdebarb in both of the spectra shifted slightly than the signals observed in free ligand. ($^1$**H:** CH$_2$ 1.93 ppm and CH$_3$ 0.84 ppm recorded in CD$_3$OD), (C=O: 174.9, 150.3, CEt$_2$: 58.6, CH$_2$: 32.9, CH$_3$: 9.7 ppm recorded in CD$_3$OD)

The IR spectrum (KBr disc) of **14** shows two medium and one strong intensive absorptions of $v$(C=O) at lower frequency (1723, 1684 and 1630 cm$^{-1}$) than that of the free ligand, for the six carbonyl groups of the complex. The lower frequency shift and the presence of three different types of carbonyl groups suggest the bidentate coordination (N, O) of Hdebarb with Rh. The spectrum also exhibits weak absorptions for the N–H stretching vibrations in the range of 3185–3085 (3388, in CHCl$_3$) cm$^{-1}$, as well as the characteristic bands for the $v$(C−H) (2965–2847 cm$^{-1}$), $v$(C–C and C−H$_{deformation}$) (1483–1312 cm$^{-1}$) and $v$(C–N) (1242 cm$^{-1}$) vibrations.

The FAB$^+$ mass spectra of **14** showed a peak at *m/z* = 421 which corresponds to the cation formed by the loss of one Hdebarb ligand.

## 2.7.2 Molecular structure of 15

Complex **15** crystallizes by slow diffusion of pentane into a solution of the compound in $CH_2Cl_2$ at room temperature. The orange crystals isolated were suitable for X-ray crystallographic analysis. Half a molecule of unreacted Na[Hdebarb] also crystallised with each of the complex. The molecular structure and selected bond lengths and angles are given in Figure 24. The details of the data collection and refinement are presented in **Table 5.5** of the crystallographic appendix. Complex **15** crystallized in the monoclinic crystal system and *C*2/*c* space group. It shows the usual three-legged piano stool coordination environment as the Ir(III) atom is bound to one Cp*, the bidentate barbiturate and one chlorido ligand.

The Ir1−N1 bond length (2.111(3) Å) is comparable to the M−N lengths of the other complexes in this work [**14**: Rh1−N3 = 2.118, **16:** Ru1−N1 = 2.102(4), **17:** Ru1−N1 = 2.106(19) Å)], while the Ir1−O3 (2.322(3) Å) bond is longer than that of Ru1−O3 (2.223(19) Å). There is no significant difference between the M−Cl bond lengths in **15** (Ir1−Cl2 = 2.374 Å) and **17** (Ru1−Cl2 = 2.372 Å)

The angle N1−Ir1−O3 of 58.46(13)° within the four-membered chelate is significantly smaller than the "open" angles N1−Ir1−Cl2 (87.76(11)°) and O3−Ir1−Cl2 (85.77(6)°) and these angles are consistent with the similar angles of **14** and **16**.

The distance between the Ir atom and the centre of the Cp* ligand is 1.753 Å, the corresponding distances between Ir and the C atoms of Cp* (2.122−2.157 Å) are within the range previously described in the literature.[106, 104] Due to the steric effect the Hdebarb and the Cp* ligand tend to stay away from each other. So, the Ir1−C12 bond length (2.157(5) Å) which lies at the same side of the disubstituted barbiturate ligand is slightly longer than the rest of the Ir−C bonds.

The Hdebarb ligand is planar (the sum of the angles around N is 359.6°). In contrast to the bond angles observed in **14** and **16**, the C4−N1−C1 bond angle (124.2(4)°) in **15** is more close to the corresponding angle in the neutral $H_2$debarb molecule (126.4°). The C−C bond lengths of the ethyl groups of the Hdebarb ligand are almost same in the complexes, with the only exception of **15** where the bond lengths (C7−C8 1.415(9) and C5−C6 1.402(11) Å) are significantly shorter than other similar bonds of **14**, **16** and **17**.
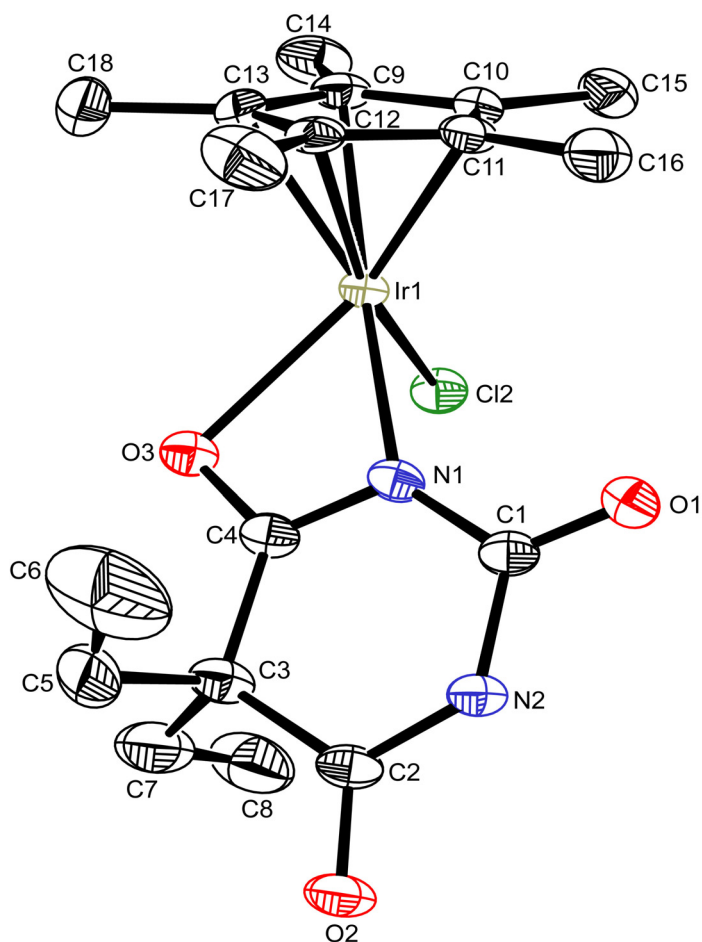
**Figure 24:** Molecular structure of **15**. The thermal ellipsoids are drawn at the 30% probability level. Hydrogen atoms and half a molecule of unreacted **2** are omitted for clarity.

**Selected bond lengths [Å]:** Ir(1)−N(1) 2.111(3), Ir(1)−O(3) 2.322(3), Ir(1)−Cl(2) 2.374(13), Ir(1)−C(9) 2.136(4), Ir(1)−C(10) 2.124(4), Ir(1)−C(11) 2.122(4), Ir(1)−C(12) 2.157(5), Ir(1)−C(13) 2.129(4), N(1)−C(4) 1.328(6), N(1)−C(1) 1.365(6), C(3)−C(7) 1.516(8) , C(7)−C(8) 1.415(9), C(5)−C(6) 1.402(11), C(3)−C(5) 1.566(8), C(1)−O(1) 1.214(5),C(4)−O(3) 1.264(5), C(2)−O(2) 1.216(5), Ir(1) $\cdots$ C$_{centroid}$ 1.753.

**Selected bond angles [°]:** N(1)−Ir(1)−Cl(2) 87.76(11), O(3)−Ir(1)−Cl(2) 86.60(9), N(1)−Ir(1)−O(3) 58.46(13), C(1)−N(1)−Ir(1) 137.7(3), C(4)−N(1)−C(1) 124.2(4), C(4)−N(1)−Ir(1) 97.7(3).

**Hydrogen bonds [Å] and angles [°]:** N(2)−H(2)$\cdots$Cl(2) 0.88(4), 2.48(4), 3.350(4), 166(4); N(81)−H(81)$_{Hdebarb}$$\cdots$O(2) 0.96(5), 1.91(5), 2.843(5), 166(5).

N−H···Cl and N−H···O hydrogen bonds link together two Hdebarb rings in the crystal packing of **15** forming a three dimensional network. Here the amine H atom (H2) is bonded with the Cl2 ligand of another Hdebarb molecule and the amine H atom of unreacted half molecule of Hdebarb is bonded with the O atom of an adjacent complex.

The Ir1−O3 bond is remarkably longer than that of Ir1−N1 and it makes the octahedral coordination slightly distorted along the O atom. Also the C−O distances in the complex involving the hydrogen bonding are longer than the rest of the free C−O distances as expected.

## 2.7.2.1 Spectroscopic characterisation of 15

Although the ethyl groups are not in equivalent environment, the $^1$H NMR spectrum of **15** showed simple quartet and triplet for the protons in $CH_2$ (2.03 ppm) and $CH_3$ (0.88 ppm), respectively. A sharp singlet at 1.74 ppm is observed for the protons of Cp*. A broad N−H resonance is observed at 7.96 ppm.

The $^{13}$C NMR spectrum displays two signals (172.03 and 151.78 ppm) for the carbonyl groups within the coordinated barbiturate moiety. The rest of the carbons of the barbiturate show one signal for each of $CEt_2$ (58.13 ppm), $CH_2$ (32.10 ppm), and $CH_3$ (9.93 ppm). The signals at 88.92 and 9.36 ppm corresponds to the Cp* ligand.
The signals found for the Hdebarb in both of the spectra shift slightly than the signals of uncomplexed ligand. ($^1$H**:** $CH_2$ 1.93 ppm and $CH_3$ 0.84 ppm recorded in $CD_3OD$), (C=O: 174.9, 150.3, $CEt_2$: 58.6, $CH_2$: 32.9, $CH_3$: 9.7 ppm recorded in $CD_3OD$)

The IR spectrum of **15** (in $CHCl_3$) shows two prominent $v$ (CO) bands at 1701 and 1636 for two different carbonyl groups. In addition, the typical $v$(C−H) vibrations of the ethyl moieties are observed in the range of 2922−2878 cm$^{-1}$ and 1458−1313 cm$^{-1}$ and $v$(C–N) at 1251 cm$^{-1}$.

The positive-ion FAB mass spectrum of **15** displays a peak at $m/z$ = 511 corresponding to the loss of the coordinated chloride with the expected isotopic distribution (ca. 22% $^{191}$Ir and 39% $^{193}$Ir).

### 2.7.3  Molecular structure of 16

Yellow crystals of the complex suitable for X-ray analysis were grown by slow diffusion of pentane into a solution of **16** in dichloromethane at room temperature. The molecular structure and selected bond lengths and angles are presented in Figure 25. The details of the data collection and refinement are given in **Table 5.6** of the crystallographic appendix. The complex **16** crystallizes in the monoclinic crystal system and space group $P2_1/c$. One molecule of unreacted $H_2$debarb (**2**) also crystallizes along with the complex. Inspite of using NaHdebarb (**3**) as a starting compound the unreacted part of it has changed to $H_2$debarb. Probably heating and the presence of methanol influence this transformation. The molecular structure shows a pseudo octahedral or a piano-stool geometry with the metal centre coordinated by the $\eta^6$-bonded *p*-cymene, a chelating *N,O*- and a monodented-*N*-Hdebarb ligand. Due to the geometric requirements of the Hdebarb ligands the $\eta^2$-coordinated N−O group forms a small N1−Ru1−O1 angle of 61.04(13)° in the metallacycle. The deprotonated N atom of the second Hdebarb ligand also makes smaller N3−Ru1−N1/O1 angles [(N1−Ru1−N3 86.51(15)° and N3−Ru1−O1 81.83(13)°] than 90°. As one of the three angles being smaller, one can assume that the total hindrance is reduced, so that the cymene ligand can approach somewhat more closely to ruthenium at a distance of 1.639 Å to be compared with 1.666 Å in a similar complex.[108]

The bond length Ru1−N3 (2.114(4) Å) in **16** is similar to that of **14** (Rh1−N3 2.118(2) Å). On the other hand the Rh1−N1 and Rh1−O1 bonds (2.130(2) and 2.2714(18) Å respectively) of **14** are longer than those of Ru1−N1 and Ru1−O1 bonds (2.102(4) and 2.213(3) Å respectively) of **16**. Again the Ru1−N1/3 bond lengths are shorter than that of Ru1−O1. The coordinated N1 and N3 atoms have a planar environment (the sum of the bond angles = 359.9°). It was found that as a result of deprotonation, the internal ring angle at N1 closes from 126.4° in $H_2$debarb to 119.2° in its anion.[34] We observe in the complex the bond angles of the coordinated N atoms are C9−N3−C12 121.8° and C1−N1−C4 122.3°, closes to the values of Hdebarb ion rather than to those of neutral $H_2$debarb molecule. The packing diagram of the complex is governed by N−H⋯O hydrogen bonds which are almost similar to those found in complex **14**. In addition to the common hydrogen bonds here the amine H atoms of the enclosed $H_2$debarb are also bonded with the O3 and O6 atoms of the complex.
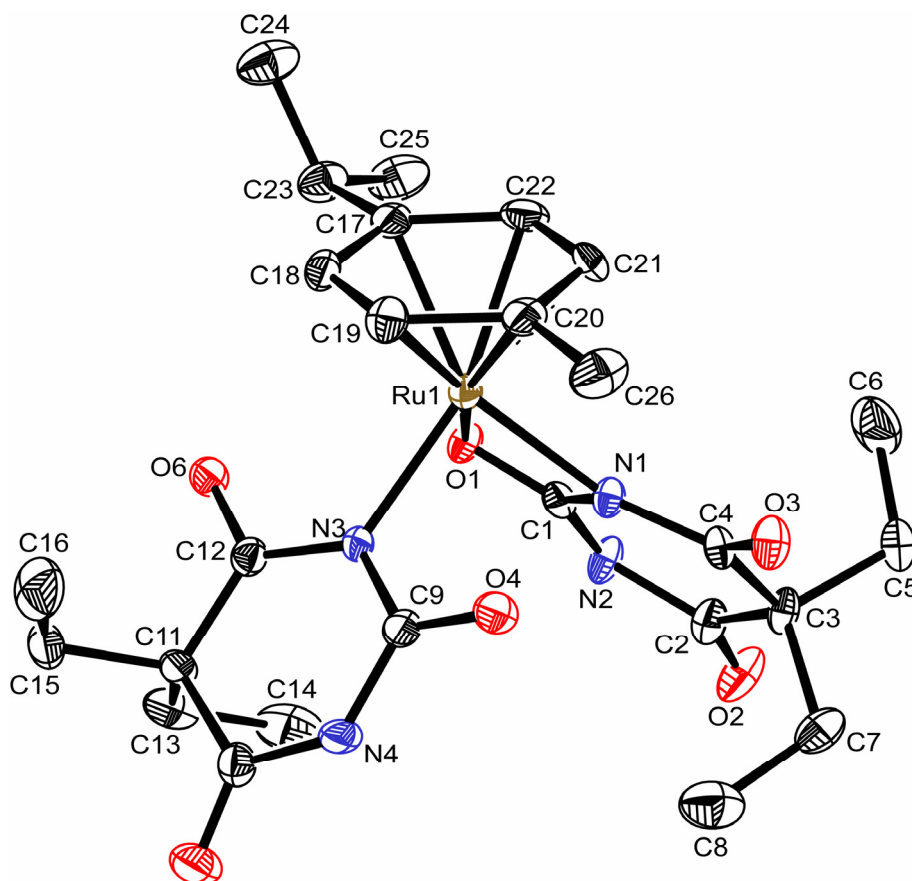
**Figure 25:** Molecular structure of **16**. The thermal ellipsoids are drawn at the 30% probability level. Hydrogen atoms, disordered pentane and one molecule of unreacted **2** are omitted for clarity.

**Selected bond lengths [Å]**: Ru(1)−N(1) 2.102(4), Ru(1)−N(3) 2.114(4), Ru(1)−O(1) 2.213(3), Ru(1)−C(17) 2.168(5) , Ru(1)−C(18) 2.164(5), Ru(1)−C(19) 2.154(5), Ru(1)−C(20) 2.171(5), Ru(1)−C(21) 2.155(5), Ru(1)−C(22) 2.164(5), N(1)−C(1) 1.347(5), N(1)−C(4) 1.354(5), N(2)−C(1) 1.361(6), C(1)−O(1) 1.254(5), C(4)−O(3) 1.218(5), C(2)−O(2) 1.193(6), N(3)−C(9) 1.354(6), N(3)−C(12) 1.370(5), Ru(1) $\cdots$C$_{centroid}$ 1.639, C(3)−C(7) 1.538(7), C(7)−C(8) 1.513(7), C(3)−C(5) 1.537(6), C(5)−C(6) 1.504(8)

**Selected bond angles [°]**: N(1)−Ru(1)−N(3) 86.51(15), N(1)−Ru(1)−O(1) 61.04(13), N(3)−Ru(1)−O(1) 81.83(13), C(1)−N(1)−C(4) 122.3(4), C(1)−N(1)−Ru(1) 93.2(3), C(4)−N(1)−Ru(1) 144.3(3), C(9)−N(3)−C(12) 121.8(4), C(9)−N(3)−Ru(1) 116.1(3), C(12)−N(3)−Ru(1) 122.0(3).

**Hydrogen bonds [Å] and angles [°]**: N(2)−H(2)$\cdots$O(4) 0.88, 1.92, 2.748(5), 156.8 4; N(4)−H(4)$\cdots$O(1) 0.88, 2.19, 2.999(5), 151.7; N(81)−H(81)$_{H2debarb}\cdots$O(3) 0.88, 1.98, 2.834(5), 163.7; N(82)−H(82) $_{H2debarb}\cdots$O(6) 0.88, 2.14, 3.020(5), 173.2.

### 2.7.3.1 Spectroscopic characterisation of 16

In complex **16** the ethyl groups of Hdebarb are not symmetrical, two of them are directed to the *p*-cymene ring and other two are to the Hdebarb ring. So, in the NMR spectrum two different sets of signals are observed for the Hdebarb ethyl group. For the *p*-cymene protons and carbons one set of signals is present in the NMR.

In the $^1$H NMR spectrum the methyl (singlet) and the isopropyl protons (one doublet) of the *p*-cymene ligand appear at 2.25 and 1.32 ppm, respectively. The isopropyl CH proton appears as a septet at 2.94 ppm. The *p*-cymene ring protons ($C_6H_4$) are observed at 5.75 and 5.65 ppm as two doublets (4H). The signals of $CH_2$ protons of Hdebarb appear as multiplet (0.82 ppm, for 9 protons) and triplet (0.53 ppm, for 3 protons). But, the signal of $CH_2$ protons is unresolved and appears as a broad signal at 1.85 ppm. The signals of Hdebarb are shifted to upfield as compared to the uncomplexed ligand ($^1$H**:** $CH_2$ 1.93 ppm and $CH_3$ 0.84 ppm, **2** recorded in $CD_3OD$).

In $^{13}$C NMR spectrum the *p*-cymene resonances are observed in four distinctive resonances of 103.0, 95.8 ($Ar_{p\text{-cym}}$-Cq) and 78.4, 78.1 (*p*-cym *C*H), 29.6 (*C*H($CH_3$)$_2$), 19.1 (s, CH($CH_3$)$_2$) and 19.1 (s, 3H, $CH_3$) ppm. The other spectral features due to Hdebarb ligand appear in expected region [$\delta$ = 174.1, 172.8 and 154.9 (CO), 57.5, 57.4 (*C*Et$_2$), 31.5, 31.3 ($CH_2$), 9.6, 9.4 ($CH_3$)].

The IR spectrum (in $CHCl_3$) shows the absorptions for the $v$(N−H) stretching vibration at 3387 cm$^{-1}$ and $v$(C−H) vibrations at the expected range of 2941−2833 and 1458−1311 cm$^{-1}$, as well as the characteristic bands of the Hdebarb and *p*-cymene ligands in the fingerprint region (1254−643 cm$^{-1}$). It also exhibits two prominent $v$(CO) bands at 1700 and 1629 cm$^{-1}$ and one very weak band at 1717 cm$^{-1}$ for the five free carbonyl groups.

The FAB$^+$ mass spectra of **16** showed a peak at $m/z$ = 418 which corresponds to the cation formed by the loss of one Hdebarb ligand.

## 2.7.4 Molecular structure of 17

Yellow crystals of the complex suitable for X-ray analysis were grown by slow diffusion of pentane into a solution of **17** in $CH_2Cl_2$ at room temperature. The complex crystallizes in the triclinic crystal system and space group *P*-1. The details of the data collection and refinement are given in **Table 5.6** of the crystallographic appendix. The molecular structure and selected bond lengths and angles are given in Figure 26.

Complex **17** has the characteristic "piano-stool" geometry of Ru(II) arene complexes, with an $\eta^6-\pi$ bonded arene ring forming the seat and three other metal-to-ligand bonds forming the legs of the stool. The Ru1−N1 (2.106(19) Å) distance is comparable to that of **15** (Ir1−N1= 2.111(3) Å). This distance is also similar with Rh1−N3 (**14**) and Ru1−N1 (**16**), while the distance Ir1−O3 (2.322(3) Å) is longer than that of Ru1−O3 (2.223(19) Å). There is no significant difference in the M−Cl bond lengths in **15** (Ir1−Cl2: 2.374(13) Å) and **17** (Ru1−Cl2: 2.372(10) Å).

The bond angle N1−Ru1−O3 (60.06(7)°) is significantly smaller than those of N1−Ru−Cl2 (87.02(6)° and O3−Ru−Cl2 (86.60(9)°) angles and these values compare well with the values found in **14** and **16**. The distance between the Ru metal and the arene centroid in **17** is 1.644 Å which is somewhat shorter than the reported values.[105]

The M−C distances of the *p*−cymene ring lie between 2.148 to 2.195 Å. Within these distances the Ru−C bonds attached with the substituted carbons (Ru1−C9, Ru1−C12 2.195(2) and 2.184(3) respectively) are longer than the other Ru−C bonds. The longest Ru−C bond to the isopropyl substituted C(9) of **3** (Ru1−C9 2.195(2) Å) is 0.047 Å longer than the other Ru−C bonds of *p*−cymene ring.

The barbiturato ligand is planar (the sum of the angles around N1 is 359.9°). In contrast to the bond angles observed in the complexes **14** and **16** the C4−N1−C1 bond angle in **17** (123.31(19)°) is closer to the corresponding angle of protonated barbital molecule (126.4°).
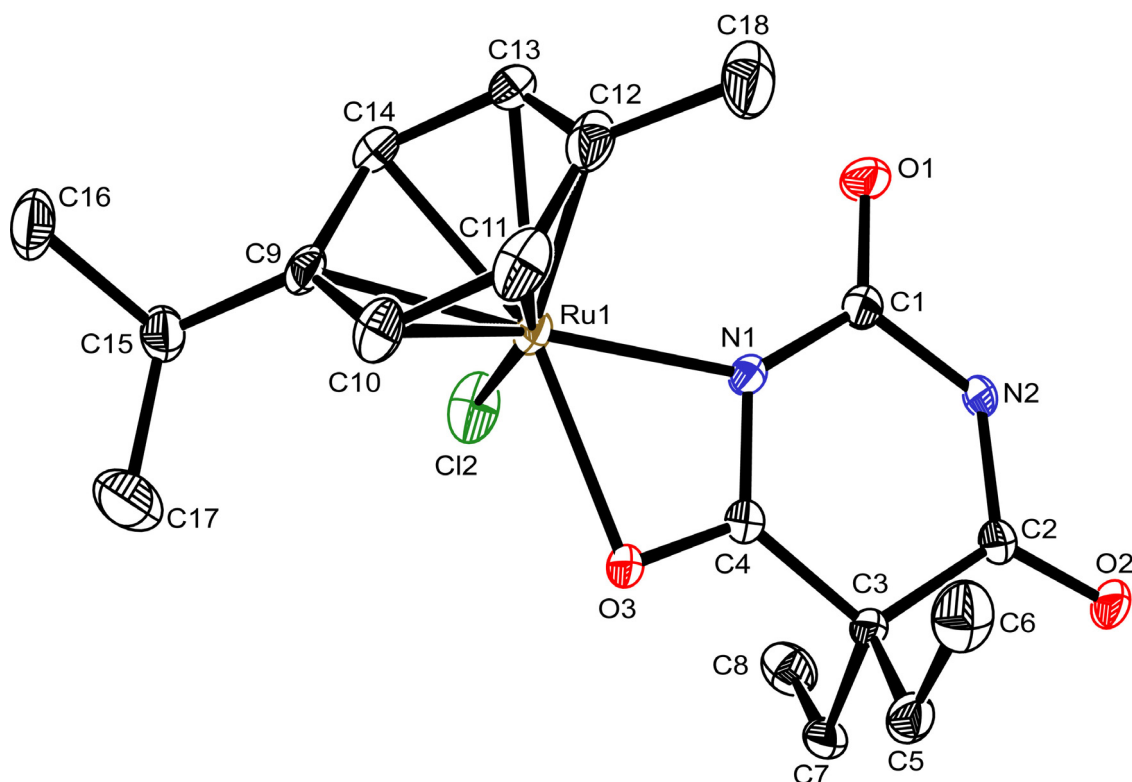
**Figure 26:** Molecular structure of **17**. The thermal ellipsoids are drawn at the 30% probability level. Hydrogen atoms are omitted for clarity.

**Selected bond lengths [Å]**: Ru(1)−N(1) 2.106(19), Ru(1)−O(3) 2.223(19), Ru(1)−Cl(2) 2.372(10), Ru(1)−C(9) 2.195(2), Ru(1)−C(10) 2.162(2), Ru(1)−C(11) 2.174(3), Ru(1)−C(12) 2.184(3), Ru(1)−C(13) 2.148(3), Ru(1)−C(14) 2.151(2), C(4)−N(1) 1.331(3), N(1)−C(1) 1.368(3), C(7)−C(8) 1.514(4), C(5)−C(6) 1.515(4), C(4)−O(3) 1.262(3), C(1)−O(1) 1.207(3), C(2)−O(2) 1.221(3), N(2)−H(2) 0.70(2), Ru(1) ⋯C$_{centroid}$ 1.644.

**Selected bond angles [°]**: N(1)−Ru(1)−O(3) 60.06(7), N(1)−Ru(1)−Cl(2) 87.02(6), O(3)−Ru(1)−Cl(2) 85.77(6), C(1)−N(1)−Ru(1) 141.80(15), C(4)−N(1)−Ru(1) 94.87(14), C(4)−N(1)−C(1).123.31(19).

**Hydrogen bonds [Å] and angles [°]**: N(2)−H(2)⋯O(2) 0.70(2), 2.19(2), 2.886(3), 177(3).

64

N−H···O hydrogen bonds link two Hdebarb rings in the crystal packing of **17** forming into a three dimensional network. Here the amine H atom (H2) is bonded with the O2 atom of free C2=O2 bond of another Hdebarb ligand.

In all four complexes (**14−17**) the M−O distances are longer than the M−N distances and it makes the octahedral coordination slightly distorted along the O atoms. Also the C=O distances in these complexes involving the hydrogen bonding are longer than the rest of the free C=O distances as expected. In **14** and **16** the metal atom is coordinated with the N1 and C1 atoms of one Hdebarb while in **15** and **17** they are coordinated with N1 and C4 atoms.

## 2.7.4.1 Spectroscopic characterisation of 17

The $^1$H and $^{13}$C NMR spectra of **17** showed two inequivalent ethyl substituents, consistent with the molecular structure where the protons of ethyl groups are in magnetically distinct environments. One of the ethyl groups is directed towards the $CH_3$ group of *p*-cymene and the second one towards to the Cl anion. So, the $^1$H NMR spectrum showed two multiplets at 1.82 and 0.77 ppm due to the $CH_2$ and $CH_3$ protons of the two different ethyl groups. These signals are shifted to upfield as compared to the free ligand ($^1$H**:** $CH_2$ 1.93 ppm and $CH_3$ 0.84 ppm, recorded in $CD_3OD$). The *p*-cymene ring protons ($C_6H_4$) are present as two doublets, at $\delta$ 5.71 (1H) and 5.56, and one triplet at 5.64 ppm (the latter may be arise from two different doublets as their differences in chemical shifts are small and they coincide with one another). The isopropyl CH proton appears as a septet at 2.96 ppm. The methyl (singlet) and the isopropyl protons (two doublets) of the *p*-cymene ligand appear at 2.28 and 1.35 and 1.30 ppm, respectively.

$^{13}$C NMR spectrum exhibits two singlets for each of the inequivalent $CH_2$ (32.1, 31.6 ppm) and $CH_3$ (9.9, 9.2 ppm) carbons and a singlet at 57.8 ppm for the $CEt_2$ carbon. Two singlets observed at 22.5 and 22.4 ppm can be assigned to the two methyl carbons of $CH(CH_3)_2$ which are now in a magnetically different environment. Another two singlets at 30.9 and 19.2 ppm are due to the $CH(CH_3)_2$ and *p*-cymene $CH_3$ carbons respectively. While the six carbon atoms of the *p*-cymene ring appear at 79.3–78.1 ($Ar_{p\text{-cym}}$-$CH$) ppm and at 101.1, 94.4

($Ar_{p\text{-cym}}$-$C$q). The complex shows the expected two carbonyl resonances at 173.16 and 152.9 ppm.

In the IR spectrum the absorptions observed for the $v$(N−H), $v$(C−H) and $v$(C=C) vibrations are consistent with those of complex **16**. A medium intensive band observed at 1250 cm$^{-1}$ is assigned to the C−N vibration. It also exhibits two prominent $v$(CO) bands at 1701 and 1630 cm$^{-1}$ which are due to the presence of two free carbonyl groups.

The FAB$^+$ mass spectrum showed a peak at $m/z$ = 454 with the correct isotope pattern for [M]$^+$. Furthermore, another peak at 418, arising from the loss of Cl anion was also observed.

## 2.8   Synthesis of benzil-bis(trimethylsilyl)diimine

### $C_{20}H_{28}N_2Si_2$ (4)

**4** was prepared according to the literature procedure by the reaction of benzil and sodium bis(trimethylsilyl)amide in benzene.[68] The solution was stirred at 70°C for 7 hours. After the addition of chlorotrimethylsilane the solution was heated at 60°C for 5 hours. Then the solution was filtered and the filtrate was vacuum distilled to yield crystalline solid **4**. It is well soluble in common polar solvents, sparingly soluble in non-polar solvents.

### 2.8.1   Molecular structure of 4

Yellow crystals of **4** suitable for X-ray analysis were isolated when the vacuum distilled yellow liquid was allowed to cool to room temperature after the synthesis. **4** crystallizes in the triclinic crystal system and *P*-1 space group. The molecular structure and selected bond lengths and angles are given in Figure 27. The details of the data collection and refinement are given in **Table 5.7** of the crystallographic appendix. As shown in Figure 27 the chemically equivalent bonds and angles of the two equal parts of the Si$_2$BDI (**4**) molecule have similar values of bond lengths and angles and compare well with those found in structurally analogous compounds.[109, 110] The bond lengths C−N (N1−C1 1.268(19) and N2−C2 1.270(19) Å), Si−N (Si1−N1 1.737(14) and Si2−N2 1.746(13)) and C−C [C1−C2 = 1.523(2), C1−C3 = 1.490(2), C2−C9 = 1.493(2) Å] fall within the expected range of ideal C=N double, Si-N and C-C single bonds. The sum of angles around C1 and C2 is 359.99°, as expected for a $sp^2$ hybridized carbon. The phenyl ligands are planar (the sum of the angles around C3 and C9 are 359.99° and 359.97° respectively) and nearly perpendicular to each other with a torsion angle C3−C1−C2−C9 of 86.82°. The atoms N1 and N2 attached with the Si(CH$_3$)$_3$ groups are in the opposite side to each other and to the phenyl ring as required by the imposed steric interaction of the bulky groups (torsion angles: N1−C1−C2−N2 87.90, N1−C1−C2−C9 −92.81, C3−C1−C2−N2 −92.46°). This may be the reason that **4** can not act as bidentate ligand and is easily cleaved by hydrolysis to form cissoidal **5** which can coordinated with metal atoms as a chelating ligand.
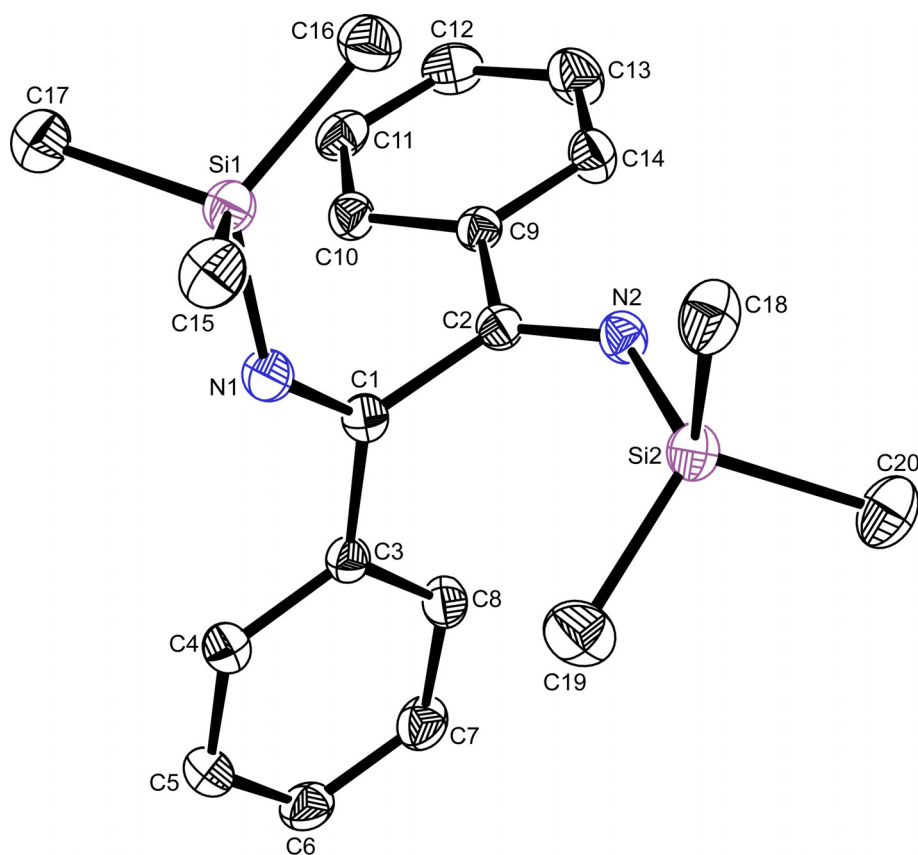
**Figure 27:** Molecular structure of **4**. The thermal ellipsoids are drawn at the 30% probability level. Hydrogen atoms are omitted for clarity.

**Selected bond lengths [Å]**: N(1)−C(1) 1.268(19), N(2)−C(2) 1.270(19), C(1)−C(2) 1.523(2), C(1)−C(3) 1.490(2), C(2)−C(9) 1.493(2), Si(1)−N(1) 1.737(14), Si(2)−N(2) 1.746(13)

**Selected bond angles [°]**: C(1)−N(1)−Si(1) 137.07(11), C(2)−N(2)−Si(2) 133.17(11), N(1)−C(1)−C(3) 120.71(13), N(1)−C(1)−C(2) 123.0(13), C(3)−C(1)−C(2) 116.29(12), N(2)−C(2)−C(9) 121.53(13), N(2)−C(2)−C(1) 122.84(13), C(9)−C(2)−C(1) 115.62(12).

**Torsion angles [°]**: C(3)−C(1)−C(2)−C(9) 86.82(15), N(1)−C(1)−C(2)−N(2) 87.90(19), N(1)−C(1)−C(2)−C(9) −92.81(17), C(3)−C(1)−C(2)−N(2) −92.46(17).

## 2.8.2  Spectroscopic characterisation of 4

**4** has been already characterized by IR, NMR and Mass spectra.[68] The reported values correspond to those found in this work.

## 2.9 Synthesis of the benzildiimine (HBDI) complex of rhodium(III)

*trans*-[bis{(benzildiiminato-*N,N´*)(triphenylphosphine)}rhodium(III)]-chloride
$C_{64}H_{52}ClN_4P_2Rh$ (18)

Reaction of two molar equivalents of **4** with one molar equivalent of $RhCl(CO)(PPh_3)_2$ in $CH_2Cl_2$ at room temperature afforded the cationic rhodium complex $[Rh(PPh_3)_2(HBDI)_2]Cl$ (**18**) with two HBDI ligands within 1 day (scheme 22). Interestingly, it contains one hydrolyzed and one deprotonated nitrogen of each ligand **5** instead of intact $Si_2BDI$ (**4**). Rh(I) is oxidized to Rh(III) after the coordination of two ligands and forms the stable $d^6$ low spin complex **18**. One NH hydrogen atom from each of the ligand **5** is deprotonated and they are reduced to $H_2$. Attempts to obtain the *mono*-$H_2BDI$ rhodium complex (analogous to **19**) from the reaction mixture of 1:1 metal complex:$Si_2BDI$ molar ratio resulted again only in complex **18**. The two $SiMe_3$ groups of **4** were replaced by two H atoms in complex **5**. Probably traces of $H_2O$ in solvent $CH_2Cl_2$ and sterical demands initiated the cleavage of bulky $SiMe_3$ and introduction of the H atoms to the bound ligand. The compound is air stable and soluble in polar solvents and insoluble in non-polar solvents.
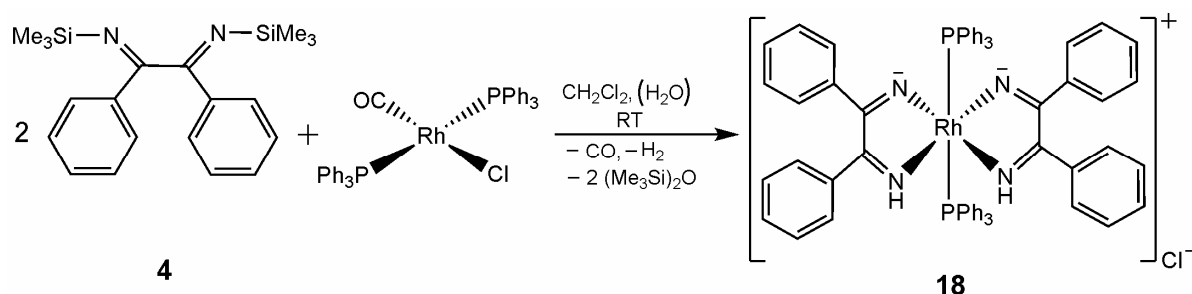


**Scheme 22:** Synthesis of the HBDI complex of rhodium(III) **18**.

## 2.9.1 Molecular structure of 18

Red crystals of the complex suitable for X-ray analysis were grown by slow diffusion of pentane into a solution of **18** in $CH_2Cl_2$ at room temperature. The molecular structure and selected bond lengths and angles of **18** are given in Figure 28. The details of the data collection and refinement are given in **Table 5.7** of the crystallographic appendix. The complex crystallizes in the monoclinic crystal system, space group $P2_1/c$ and with two molecules of disordered dichloromethane as solvate. The coordination sphere of the Rh

center can be described as distorted octahedral. The phosphine ligands are mutually *trans*-disposed with slightly different Rh−P distances (Rh1−P1: 2.351(8), Rh1−P2: 2.367(9) Å). The two chelating $H_2BDI$ ligands also occupy *trans* positions to each other with similar bite angles (N4−Rh1−N3 78.19(11) and N2−Rh1−N1 78.37(11)). The HBDI and the phosphine ligands are placed in axial positions [(P1-Rh1−P2 176.75(3)°, N1−Rh1−N3 177.48(11)° and N4−Rh1−N2 177.90(11)°]. The rest of the angles between the metal atom and the axial and equatorial donor atoms are in the range of 78.19−103.85°. The four Rh−N distances fall within the reported range.[111], two of them (Rh1−N1 and Rh1−N4 2.028(2) Å of two different ligands located on the same side) are almost equal and differ significantly from the other two (Rh1−N3 2.038(3) and Rh1−N2 2.046(3) Å). The bond lengths Rh−P are slightly longer and those of Rh−N are shorter than the bonds observed in complex **13** and other reported values.[106, 112] The bonds N=C (1.279−1.285 Å) of the complex are somewhat longer and those of C1−C2 1.501(5) and C15−C16 1.499(4) Å are slightly shorter compared to the respective bonds of the free ligand **4** (N1−C1 1.268(19), N2−C2 1.270(19), C1−C2 1.523(2) Å). The phenyl rings of $H_2BDI$ are essentially planar (sum of the angle around C3, C9, C17 and C23 is almost near to 360°). One phenyl ring (C17−C22) of $H_2BDI$ and one (C59−C64) of the phosphine ligand are involved in π-π stacking. The distance between the centroids of stacked phenyl rings is 3.62 Å. One molecule of the complex is connected to the chloride anion by N−H···Cl hydrogen bond, involving the two imine hydrogen atoms of one $H_2BDI$ and the chloride ion of another complex.
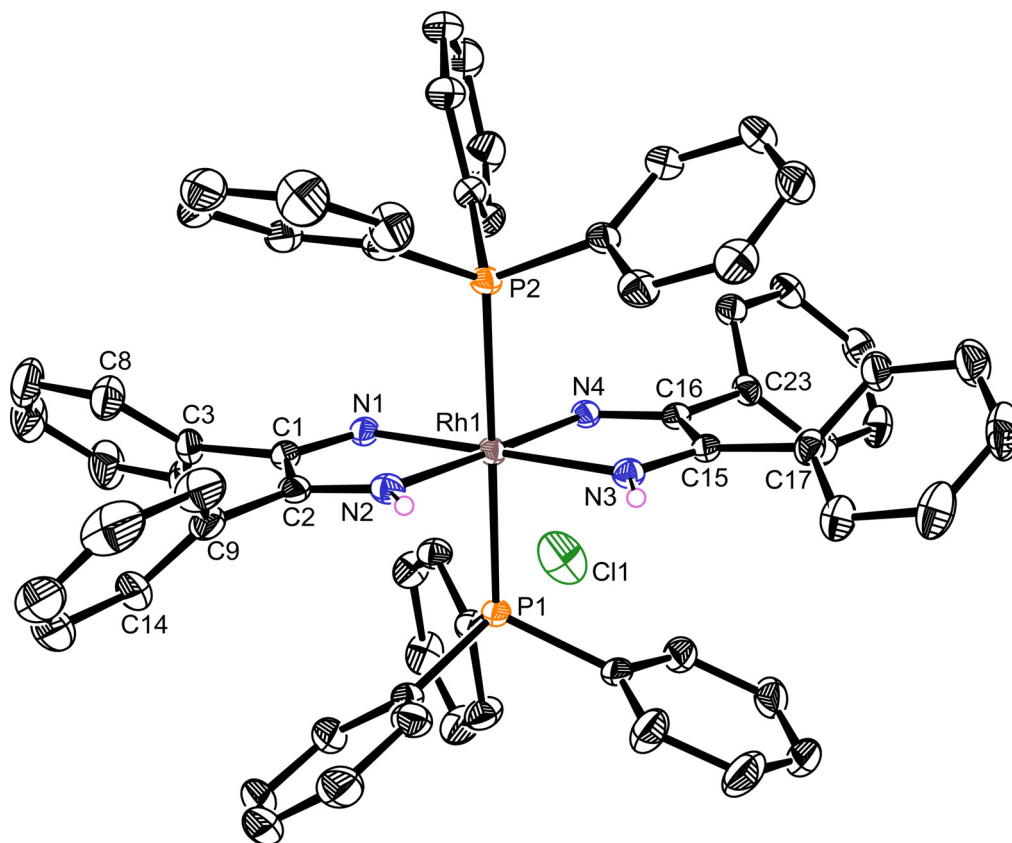
**Figure 28:** Molecular structure of **18**. The thermal ellipsoids are drawn at the 30% probability level. Hydrogen atoms of phenyl groups and disordered $CH_2Cl_2$ solvate molecules are omitted for clarity.

**Selected bond lengths [Å]**: Rh(1)−N(1) 2.028(3), Rh(1)−N(2) 2.046(3), Rh(1)−N(3) 2.038(3), Rh(1)−N(4) 2.028(2), Rh(1)−P(1) 2.351(8), Rh(1)−P(2) 2.367(9), N(1)−C(1) 1.285(4), N(2)−C(2) 1.279(4), N(3)−C(15) 1.284(4), N(4)−C(16) 1.284(4), C(1)−C(2) 1.501(5), C(15)−C(16) 1.499(4), C(2)−C(9) 1.481(5), C(15)−C(17) 1.487(4), C(16)−C(23) 1.498(4), C(1)−C(3) 1.496(5), N(2)−H(2) 0.83(4), N(3)−H(3) 0.86(4).

**Selected bond angles [°]**: N(4)−Rh(1)−N(3) 78.19(11), N(1)−Rh(1)−N(2) 78.37(11), N(1)−Rh(1)−P(1) 88.78(7), N(4)−Rh(1)−P(1) 88.44(7), N(1)−Rh(1)−P(2) 89.07(8), N(4)−Rh(1)−P(2) 89.52(7), N(2)−Rh(1)−P(2) 89.95(8), N(3)−Rh(1)−P(1) 89.96(8), N(2)−Rh(1)−P(1) 92.00(8), N(3)−Rh(1)−P(2) 92.09(8), N(1)−Rh(1)−N(4) 99.59(10), N(3)−Rh(1)−N(2) 103.85(12), P(1)−Rh(1)−P(2) 176.75(3), N(1)−Rh(1)−N(3) 177.48(11), N(4)−Rh(1)−N(2) 177.90(11), C(1)−N(1)−Rh(1) 114.5(2), C(16)−N(4)−Rh(1) 114.5(2), C(2)−N(2)−Rh(1) 117.4(2), C(15)−N(3)−Rh(1) 118.0(2).

**Hydrogen bonds [Å] and angles [°]**:

N(2)−H(2)···Cl(1) 0.83(4), 2.60(4), 3.317(3), 145(3)°; N(3)−H(3)···Cl(1) 0.86(4), 2.38(4), 3.158(3), 151(3)°.

## 2.9.2  Spectroscopic characterisation of 18

The $^1$H NMR spectrum shows distinctive resonance due to imine N–H hydrogen, which is well separated from other parts of the spectrum. The relatively broad N–H resonance is observed at 12.94 ppm, making it simple to determine protonation of the Si$_2$BDI. The spectrum also shows signals in the range 7.89−7.19 ppm and 7.17−5.99 indicating the presence of ring protons of triphenylphosphines and phenyl (H$_2$BDI) ligands respectively.

In the $^{13}$C NMR spectrum all phenyl carbons are well resolved [135.51−128.13 ppm (PPh$_3$) and 134.9 −126.8 ppm (Ph-H$_2$BDI)]. The C=N carbon is observed at 172.37 ppm as a doublet by coupling with $^{103}$Rh ($J$ = 51.9 Hz).

The signals in both $^1$H and $^{13}$C NMR spectra are shifted further upfield as compared to the free ligand (**4**) and other complexes of H$_2$BDI (**20**, **21**, **22**) reported here, which suggests an electron enriched system, because of the more strongly electron donating PPh$_3$ ligands. ($^1$H: 7.80−7.32 ppm, $^{13}$C: 174.2 ppm (CN), 138.28−128.14 (Ph−C) ppm, **4** recorded in CD$_2$Cl$_2$)

The $^{31}$P NMR spectrum exhibits a single doublet at 31.1 ppm with a coupling constant of about 118.5 Hz, indicating *trans* arrangement of the phosphine ligands.

The infrared spectrum (KBr disc) of **18** exhibits weak vibration at 3049 cm$^{-1}$ which is assigned to the $v$(C−H). A significant negative shift in $v$(C=N) stretching mode appearing at 1589 and 1571 cm$^{-1}$ for the complex as compared to free ligand (1652 and 1646 cm$^{-1}$) suggests the involvement of imine nitrogens of the (C=N) groups in coordination with the metal. The aromatic $v$(C=C) absorptions were observed between 1482 and 1432 cm$^{-1}$. The strong bands at 692 and 522 cm$^{-1}$ are indicative of Rh−PPh$_3$ ligation in the complex.[104]

In the positive-ion FAB mass spectrum of **18** the [M$^+$ −Cl] peak was observed at $m/z$ = 1041. Other peaks resulting from the fragmentation of **18** are observed at $m/z$ = 779 and 573, assigned to [M$^+$ −Cl −PPh$_3$] and [Rh(H$_2$BDI)(PPh$_3$)]$^+$ respectively.

## 2.10 Synthesis of the benzildiimine (H₂BDI) complex of iridium(I)

**[Carbonyl-(benzildiimine-*N,N´*)-bis(triphenylphosphine)iridium(I)]-chloride C₅₁H₄₂IrN₂OP₂Cl (19)**

The reaction of equivalent molars of **4** and IrCl(CO)(PPh₃)₂ in benzene at ambient temperature afforded the cationic *mono*-H₂BDI iridium complex **19** within 1 day (scheme 23). Attempts to obtain the *bis*-H₂BDI iridium complex from a 1:2 metal complex:**4** reaction mixture again resulted only in complex **19**. As in the case of **18** two SiMe₃ groups of **4** were replaced by two H atoms in the complex which may be caused by traces of water. The compound is air stable and soluble in polar solvents and insoluble in non polar solvents.
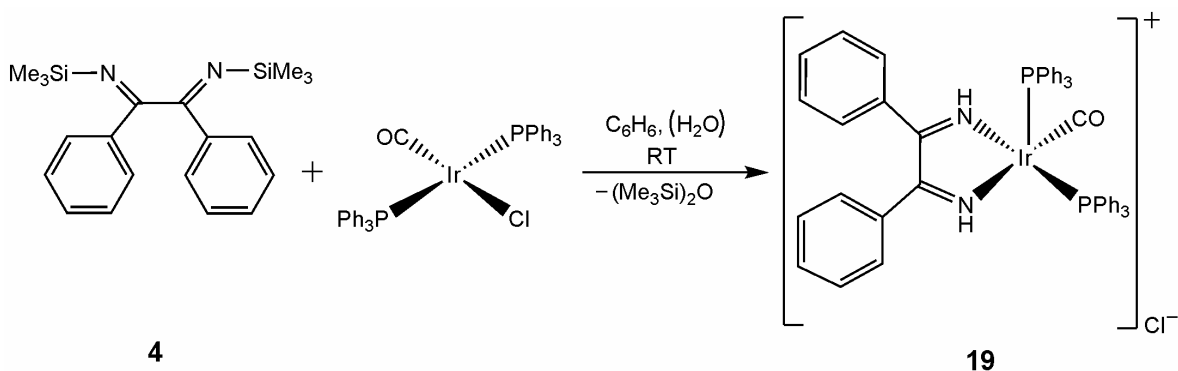


**Scheme 23:** Synthesis of the H₂BDI complex of iridium(I) **19**.

## 2.10.1 Molecular structure of 19

Red crystals of complex **19** suitable for X-ray analysis were grown by slow diffusion of pentane into a solution of **19** in CH₂Cl₂ at room temperature. Complex **19** was isolated as solid red crystals including dichloromethane as solvate. It crystallizes in the triclinic crystal system and space group *P*-1. The molecular structure and selected bond lengths and angles are given in Figure 29. The details of the data collection and refinement are given in **Table 5.8** of the crystallographic appendix. Its geometry could be described as distorted square pyramidal or distorted trigonal bipyramidal as the bond angles around the metal center are in the range of 75.26(9)−160.63(10)°. The arrangement, however, resembles more to a highly distorted square pyramide, caused by the strong steric interactions between the two PPh₃ ligands and the two phenyl rings of H₂BDI. Due to this steric repulsion the phosphine ligands forced from the *trans* position to almost *cis* position [P2−Ir−P1 = 107.96(3)°] and
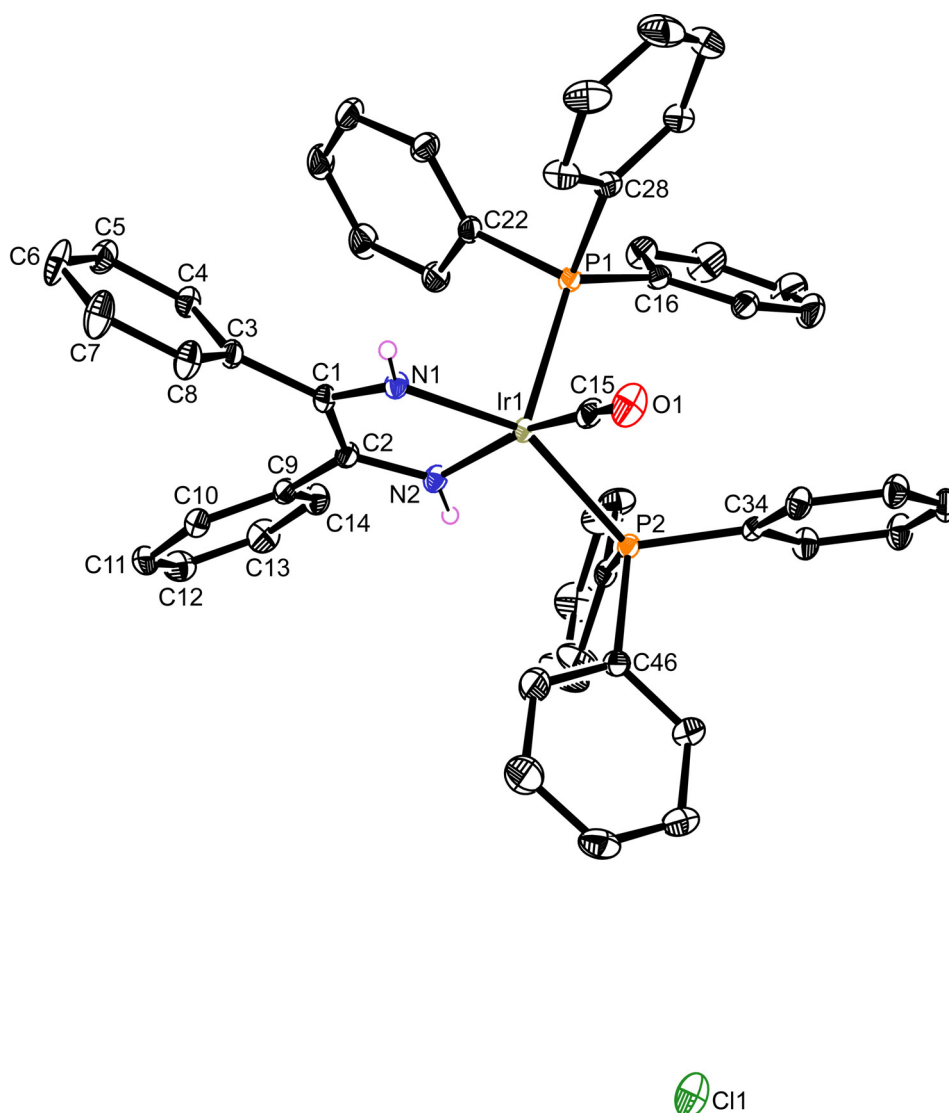
**Figure 29:** Molecular structure of **19**. The thermal ellipsoids are drawn at the 30% probability level. Hydrogen atoms of phenyl groups and $CH_2Cl_2$ solvate molecules are omitted for clarity.

**Selected bond lengths [Å]**: Ir(1)−C(15) 1.872(3), Ir(1)−N(2) 1.994(2), Ir(1)−N(1) 2.032(2), Ir(1)−P(2) 2.327(10), Ir(1)−P(1) 2.350(9), C(15)−O(1) 1.145(3), N(1)−C(1) 1.333(3), N(2)−C(2) 1.340(3), C(1)−C(2) 1.413(3), C(1)−C(3) 1.484(3), C(2)−C(9) 1.481(3), N(1)−H(1) 0.82(3), N(2)−H(2) 0.83(3).

**Selected bond angles [°]**: N(2)−Ir(1)−N(1) 75.26(9), N(2)−Ir(1)−P(2) 88.61(7), N(2)−Ir(1)−P(1) 103.07(7), N(1)−Ir(1)−P(1) 96.68(7), N(1)−Ir(1)−P(2) 153.14(6), C(15)−Ir(1)−P(1) 95.14(9), C(15)−Ir(1)−P(2) 92.06(8), C(15)−Ir(1)−N(1) 96.31(10), C(15)−Ir(1)−N(2) 160.63(10), P(2)−Ir(1)−P(1) 107.96(3), O(1)−C(15)−Ir(1) 177.5(2).

**Hydrogen bonds [Å] and angles [°]**: N(1)−H(1) ⋯Cl(1) 0.82(3), 2.44(3), 3.263(3), 174(2).

the H$_2$BDI ring strained highly to form the small chelate bite angle N2−Ir1−N1 = 75.26(9)°. The N1 and N2 atoms are pseudo *trans* to the CO ligand (C15−Ir1−N2 160.63(10)°) and P2 of one PPh$_3$ ligand (N1−Ir1−P2 153.14(6)°), respectively. As the CO ligand is a better σ-donor-π-acceptor ligand than the PPh$_3$ ligand, the Ir1−N2 distance (1.994(2) Å) *trans* to it is shorter than the Ir1−N1 distance (2.032(2) Å) in *trans* position to the PPh$_3$ ligand. The Ir1−P2 distance (2.327(10) Å) *trans* to the N2 atom is slightly shorter than that of the Ir1−P1 (2.350(9) Å), but both are consistent with reported values [112, 113]. The C=N bond distances (N1−C1 = 1.333(3) and C2−N2 = 1.340(3) Å) are somewhat longer and those of C−C (C1−C2 = 1.413(3), C1−C3 = 1.484(3) Å) and C2−C9 = 1.481(3) Å) are slightly shorter than the expected C=N double and C−C single bonds. However, all the bond distances are in the range observed for similar iridium complexes.[114, 115] Both of the phenyl rings of H$_2$BDI are essentially planar (sum of the angles around C4 and C10 is 359.7 and 359.8° respectively). One molecule of the complex is connected to the chloride anion by N−H···Cl hydrogen bond, involving one imine H atom of one H$_2$BDI and the chloride ligand of another complex.

## 2.10.2 Spectroscopic characterisation of 19

In the $^1$H NMR spectrum the relatively weak N−H resonance is observed at 12.11 ppm. The spectrum also shows signals in the range 7.97−6.75 indicating the presence of phenyl protons of PPh$_3$ and H$_2$BDI ligands.

In the $^{13}$C NMR spectrum overlapped phenyl carbon signals are observed in the range 135.34−126.70 ppm. But, it was not possible to detect the signal of C=N carbon.

The $^{31}$P NMR spectrum exhibits a singlet at 28.5 ppm indicating equivalent phosphine environment.

The infrared spectrum (KBr disc) of **18** exhibits weak vibrations within 3053−2925 cm$^{-1}$ assigned to the $v$(N−H) and $v$C−H) respectively. A significant lower frequency of $v$(C=N) stretching mode appearing at 1597 and 1571 cm$^{-1}$ for the complex as compared to free ligand (1652 and 1646 cm$^{-1}$) suggests the involvement of imine nitrogens of the (C=N) groups in coordination with the metal. The $v$(C=C) absorptions were observed between 1482

and 1432 cm$^{-1}$. The strong bands at 693 and 522 cm$^{-1}$ are indicative of Ir−PPh$_3$ ligation in the complex.

In the positive-ion FAB mass spectrum instead of the molecular peak, the [M$^+$ −2H −CO −Cl] peak was observed at *m/z* = 922. Other peaks resulting from the successive loss of two PPh$_3$ ligands are observed at *m/z* = 660 and 400.

## 2.11 Benzildiimine complexes of iron (II)

The iron complexes [Fe(HL)$_3$](ClO$_4$)$_2$ [HL = benzildiimine, phenanthrenequinonediimine] having nearly same structure of our prepared complexes (**20** and **21**) were synthesized from the corresponding metal salt and alcoholic solutions of HL or of the corresponding 1,2-bis(trimethylsilylimino) analogue (**m**, Figure 8).[74, 78b] Several types of diimine complexes of Ruthenium(II) and Rhodium(III) of 9,10-phenanthrenequinone (phi) were isolated (Scheme 11) which are structurally analogous to our prepared iron complex **20**. Despite of using the Me$_3$Si derivatives as starting material in all syntheses reported in the literature or in this work, the silyl groups were not found in any of the products. They were always substituted against hydrogen forming protonated diimine (**5**) chelate complexes. The reason may be traces of water leading to the formation of disiloxane or silanol ((Me$_3$Si)$_2$O or Me$_3$SiOH) as it was observed by $^1$H-NMR spectroscopy of the reaction solution.

## 2.12 Synthesis of the benzildiimine complex of iron(II)

### [Tris(benzildiimine-*N,N´*)-iron(II)]bis(trifluoromethylsulfonate)
### C$_{44}$H$_{36}$F$_6$FeN$_6$O$_6$S$_2$ (20)

Treatment of CpFe(CO)$_2$Cl and **4** in 1:1 or 1:2 molar ratio at room temperature does not lead to any reaction. After adding, however, some excess of AgOTf to this reaction mixture (or any other molar ratio) a reaction takes place which can be monitored by IR spectroscopy and leads to the formation of iron complex **20** within 1 day (scheme 24). The best yield of **20** is achieved using the molar ratio Fe-complex:**4** = 1:3 and at least 2 moles of AgOTf. It was very surprising, that inspite of the mild reaction conditions CpFe(CO)$_2$Cl was totally decomposed and all former ligands were eliminated to form finally the cationic tris-chelate

complex **20**. The very intensive deep blue complex is air stable and soluble in common solvents ($CH_2Cl_2$, $CHCl_3$, acetone etc) but insoluble in $H_2O$, methanol, pentane, hexane etc.
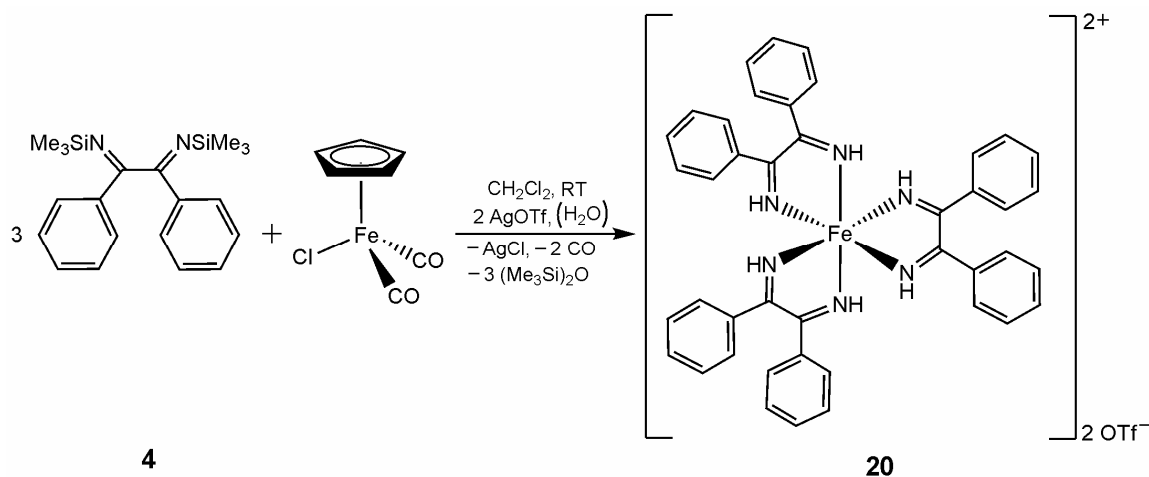


**Scheme 24:** Synthesis of the $H_2BDI$ complex of iron(II) **20**.

## 2.12.1 Molecular structure of 20

Deep blue-black crystals suitable for X-ray analysis were grown by slow isothermic diffusion of *n*-pentane into the solution of **20** in $CH_2Cl_2$ within 2 days. The molecular structure and selected bond lengths and angles of **20** are shown in Figure 30. The complex crystallizes in the trigonal crystal system and space group *R*-3. The details of the data collection and refinement are given in **Table 5.8** of the crystallographic appendix. A hole was found in the unit cell of the complex which was solved by platon squeeze. The Fe(II) centre is hexacoordinated by the six N atoms of three bidentate $H_2BDI$ ligands in a distorted octahedral arrangement. The ligands are coordinated to Fe(II) via loss of all $Si(CH_3)_3$ groups as protonated bidentate *N,N*-donor ligands forming five-membered chelate rings with bite angles 78.3−78.8(10)°. While the remaining cisoid and transoid angles N−Fe−N (89.6(10)−167.7(10)°) fall within the expected range, the Fe−N bond distances (1.903−1.927 Å) are slightly shorter than the M−N distances of complexes **18, 19** and **22** and reported Fe−N distances of similar complexes.[116, 117] The C−C bonds connected with the N atoms and with the phenyl rings and the N−C bonds are in the range 1.471−1.483 and 1.286−1.292 Å, respectively and comparable with those of **18** and of reported values.[80, 81] The three ligands are planar, as expected [sum of the bond angles = 360°] and one ligand plane is
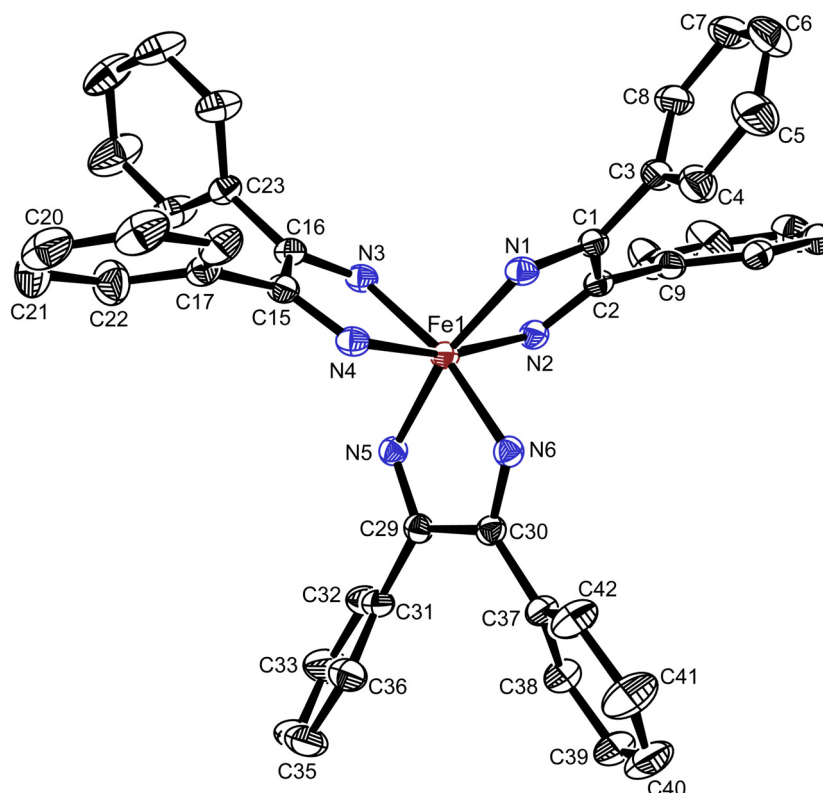
**Figure 30:** Molecular structure of **20**. The thermal ellipsoids are drawn at the 30 % probability level. Hydrogen atoms and two triflate anions are omitted for clarity.

**Selected bond lengths [Å]**: Fe(1)−N(1) 1.903(2), Fe(1)−N(6) 1.909(2), Fe(1)−N(5) 1.910(2), Fe(1)−N(4) 1.912(2), Fe(1)−N(3) 1.913(2), Fe(1)−N(2) 1.927(2), N(1)−C(1) 1.286(3), N(2)−C(2) 1.288(3), N(3)−C(16) 1.286(3), N(4)−C(15) 1.292(3), N(5)−C(29) 1.291(3), N(6)−C(30) 1.288(3), C(1)−C(2) 1.483(4), C(15)−C(16) 1.474(3), C(29)−C(30) 1.479(4), C(1)−C(3) 1.474(4), C(2)−C(9) 1.471(4), C(15)−C(17) 1.480(4), C(16)−C(23) 1.477(3), C(29)−C(31) 1.479(3), C(30)−C(37) 1.480(3), N(1)−H(1) 0.77(3), N(2)−H(2) 0.88(3), N(3)−H(3) 0.73(3), N(4)−H(4) 0.78(3), N(5)−H(5) 0.80(3), N(6)−H(6) 0.70(3).

**Selected bond angles [°]**: N(1)−Fe(1)−N(6) 91.60(10), N(1)−Fe(1)−N(5) 167.60(9), N(6)−Fe(1)−N(5) 78.35(10), N(1)−Fe(1)−N(4) 89.63(10), N(6)−Fe(1)−N(4) 95.86(10), N(5)−Fe(1)−N(4) 98.54(9), N(1)−Fe(1)−N(3) 99.18(9), N(6)−Fe(1)−N(3) 167.71(10), N(5)−Fe(1)−N(3) 91.64(9), N(4)−Fe(1)−N(3) 78.43(10), N(1)−Fe(1)−N(2) 78.84(10), N(6)−Fe(1)−N(2) 95.37(9), N(5)−Fe(1)−N(2) 94.72(9), N(4)−Fe(1)−N(2) 164.11(9), N(3)−Fe(1)−N(2) 92.52(9), N(1)−C(1)−C(3) 122.8(2), N(1)−C(1)−C(2) 111.4(2), C(3)−C(1)−C(2) 125.7(2).

**Torsion angles [°]:** N(6)−Fe(1)−N(2)−C(2) −88.6(2), N(1)−Fe(1)−N(3)−C(16) −86.6(2), N(4)−Fe(1)−N(5)−C(29) −93.3(2), N(6)−Fe(1)−N(1)−C(1) 93.5(2).

**Hydrogen bonds [Å] and angles [°]:** N(1)−H(1)$\cdots$O$_{OTf}$(1) 0.77(3), 2.36(3), 3.105(3), 164(2); N(2)−H(2)$\cdots$O$_{OTf}$(4) 0.88(3), 2.42(3), 3.165(3), 143(2); N(3)−H(3)$\cdots$O$_{OTf}$(5) 0.72(3), 2.34(3), 3.024(3), 158(3); N(5)−H(5)$\cdots$O$_{OTf}$(6) 0.79(3), 2.13(3), 2.906(3), 167(3).

nearly orthogonal to both planes of the other two ligands [the torsion angles: N1−Fe1−N3−C16 = −86.6(2), N4−Fe1−N5−C29 = −93.3(2), N6−Fe1−N1−C1 = 93.5(2), N6−Fe1−N2−C2 = −88.6(2)°].

Among the six N−H bond distances four are shorter than the remaining two [N6−H6: 0.70(3), N3−H3: 0.73(3), N1−H1: 0.77(3), N4−H4: 0.78(3), N5−H5: 0.80(3), N2−H2: 0.88(3) Å]. The H$_2$BDI ligands are connected to the triflate anions by N−H$\cdots$O hydrogen bonds, involving four imine hydrogen atoms and four of the oxygen atoms of the triflates.

## 2.12.2 Spectroscopic characterisation of 20

In the $^1$H NMR spectrum of **20**, a characteristic sharp signal at 12.12 ppm is assigned to the proton resonance of the N−H. Six phenyl groups signals shifted slightly upfield than that of the free ligand (**4**) and form multiplets in the range of 7.52−7.37 ppm.

The $^{13}$C NMR spectrum shows downfield shift of the resonances for the C=N (178.76 ppm) and upfield shift of phenyl carbon (134.7−128.7 ppm) atoms as compared to **4** ($^1$H: 7.80−7.32 ppm, $^{13}$C: 174.2 ppm (CN), 138.28−128.14 (Ph−C) ppm, **4** recorded in CD$_2$Cl$_2$).

The IR spectrum (in KBr) shows the bands characteristic of the imine N−H and C−H stretching vibrations at 3184 and 3064 cm$^{-1}$, respectively, and those for C=C at 1492 and 1445 cm$^{-1}$. It has been further observed that imine nitrogen $v$(C=N) band at 1599 and 1579 cm$^{-1}$ are shifted to lower frequencies than that of the free ligand (1652 and 1646 cm$^{-1}$) upon metal coordination. The stretching and deformation vibrations of the CF$_3$ and SO$_3$ groups of triflates are detected at 1259 cm$^{-1}$ ($v$, sym., CF$_3$), 1166 cm$^{-1}$ ($v$, asym., SO$_3$), 1027 cm$^{-1}$ ($v$, sym., SO$_3$), 765 cm$^{-1}$ ($\delta$, sym., CF$_3$), 639 cm$^{-1}$ ($\delta$, sym., SO$_3$), 575 cm$^{-1}$ ($\delta$, asym., CF$_3$) and 516 cm$^{-1}$ ($\delta$, asym., SO$_3$). The $v$(Fe−N) band appears at 533 cm$^{-1}$.[101]

The FAB$^+$ mass spectrum showed molecular peaks at *m/z* = 829, 680 and 472 which are formed from the molecular ion by gradual loss of the two triflate anions and one H$_2$BDI ligand.

## 2.13   Synthesis of the benzildiimine complex of iron(II)

### *Tris*(benzildiimine-*N,N´*)iron(II)-dichloride, C$_{42}$H$_{36}$Cl$_2$FeN$_6$ (21)

Reaction of **4** (3 moles) with anhydrous FeCl$_2$ (1 mol) in CH$_2$Cl$_2$ without addition of any silver salt produces complex **21** within 2 days (Scheme 25). This complex is almost similar to complex **20**. The only difference between complex **20** and **21** is the anion which is now chloride instead of triflate. The complex is air stable and soluble in common solvents (CH$_2$Cl$_2$, CHCl$_3$, acetone etc), but insoluble in H$_2$O, methanol, pentane, hexane etc. The ink blue crystals grown by slow diffusion of *n*-pentane into a solution of **21** in CH$_2$Cl$_2$ were not suitable for X-ray analysis. Other attempts to crystallise the substance by diffusion of a non-polar solvent into a solution of **21** or by cooling of its solution were not successful. The complex, however was fully characterized by the IR, mass, $^1$H and $^{13}$C NMR spectra and elemental analysis.
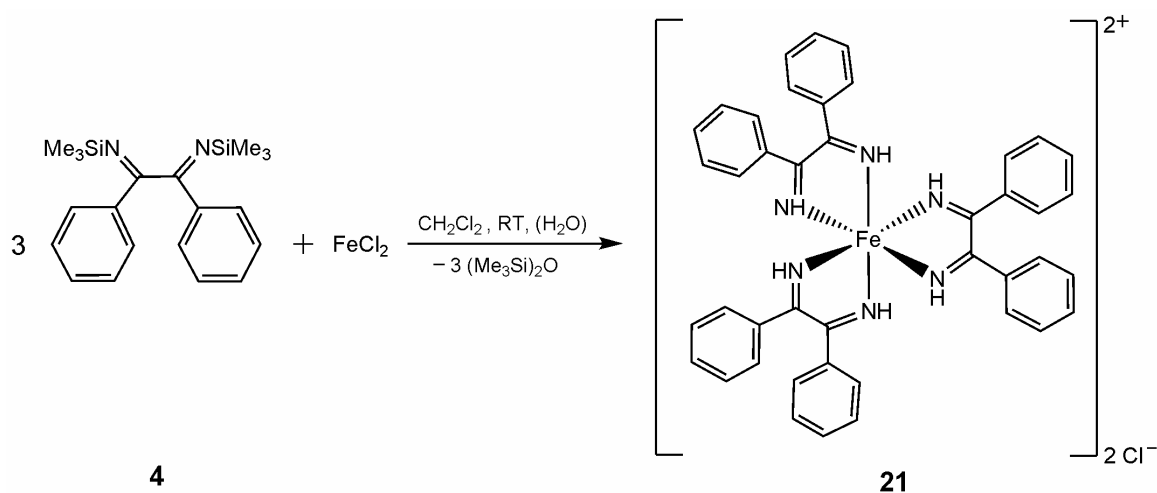


**Scheme 25:** Synthesis of the H$_2$BDI complex of iron(II) **21**.

### 2.13.1  Spectroscopic characterisation of 21

In the $^1$H NMR spectrum of **21**, a characteristic sharp signal at 13.23 ppm is assigned to the proton resonance of the N−H. Six phenyl groups signals shifted slightly upfield than that of the free ligand (**4**) and form multiplets in the range of 7.58−7.36 ppm.

The $^{13}$C NMR spectrum shows downfield shift of the resonances for the C=N (175.3 ppm) and upfield shift of phenyl carbon (134.6−128.6 ppm) atoms as compared to **4**. The resonances observed in the NMR spectrum are quite similar to those found in **20** as expected.

The position and shape of the the imine N−H, C=N, C=C and C−H group bands in the infrared spectrum of **21** are almost same as for the complex **20**, indicating similar coordination of metal and ligand in both complexes. The only difference is that in the spectrum of **21** the stretching and deformation vibrations of the $O_3SCF_3$ groups are absent as expected.

The positive-ion FAB spectra of **21** showed molecular peaks at *m/z* = 715 and 679 that correspond to the successive loss of two Cl anions from the molecular mass. Peaks arising from the additional loss of the two $H_2BDI$ ligands were also observed.

## 2.14  Synthesis of the benzildiimine complex of chromium(III)

**[Bis(benzildiimine-*N,N´*)-$\eta^5$-cyclopentadienyl-chromium(III)]-bis(trifluoromethylsulfonate)**

**$C_{35}H_{29}CrF_6N_4O_6S_2$ (22)**

Treatment of one molar equivalent of $CpCr(NO)_2Cl$ with one molar equivalent of **4** did not show any reaction. However, addition of excess of AgOTf (2.5 molar) in $CH_2Cl_2$ resulted in the formation of **22** within 1 day (scheme 26). The change in the reaction was monitored by IR spectra. The IR of the solution changed only after the addition of excess AgOTf. In the product the CpCr moiety from $CpCr(NO)_2Cl$ remains intact and after elimination of both NO and chloride ligands it is coordinated by two $H_2BDI$ ligands. Probably excess of AgOTf promoted the oxidation of Cr (Cr(0) to Cr(III)). Comparing this reaction of **4** with

CpCr(NO)$_2$Cl and the former reaction of **4** with CpFe(CO)$_2$Cl the resulting products show different formulas in spite of using the same molar ratio. The complex **22** is air stable and soluble in common solvents (CH$_2$Cl$_2$, CHCl$_3$, acetone etc), but insoluble in H$_2$O, methanol, pentane, hexane etc.
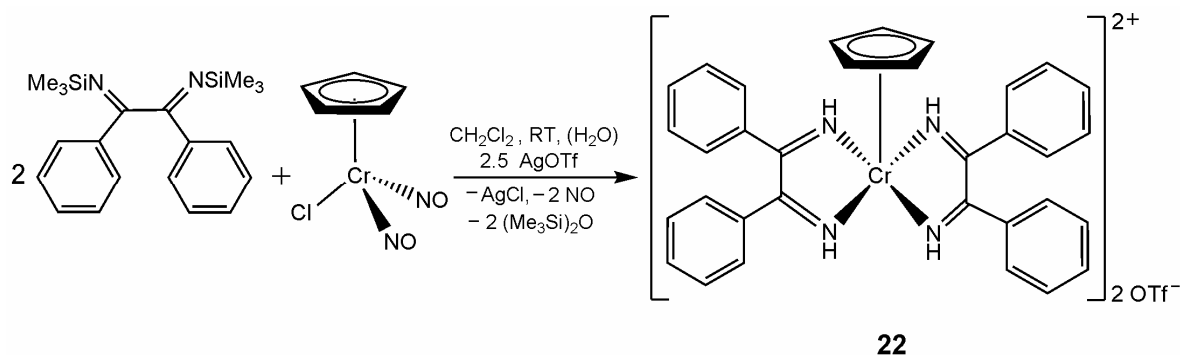


**Scheme 26**: Synthesis of the H$_2$BDI complex of chromium(III) **22**.

## 2.14.1  Molecular structure of 22

Reddish-brown crystals suitable for X-ray analysis were grown by slow isothermic diffusion of *n*-pentane into the solution of **22** in CH$_2$Cl$_2$. The molecular structure and the selected bond lengths and angles are given in Figure 31. The details of the data collection and refinement are given in **Table 5.9** of the crystallographic appendix. It crystallizes in the triclinic crystal system and space group *P*-1, with 1 molecule dichloromethane as solvate. The molecular structure shows a slightly distorted four-legged piano-stool configuration at the chromium(III) centre (N2−Cr1−N4 83.35(17), N3−Cr1−N1 84.18(15), N2−Cr1−N3 124.62(16), N1−Cr1−N4 132.71(15)°), being coordinated to the protonated nitrogen atoms of two bidentate H$_2$BDI ligands. The bite angles of the two H$_2$BDI ligands (N2−Cr1−N1 74.80(17) and N3−Cr1−N474.58(17)°) are nearly equal while Cr1−N1 and Cr1−N4 bonds which are mutually in *trans* position have equal bond lengths (1.993(4) Å), but differ significantly from Cr1−N2 (1.967(4) Å) and Cr1−N3 (1.978(4) Å) bond lengths. The N−C bonds (N2−C7 1.301(6), N1−C6 1.307(5), N3−C20 and N4–C21 1.297(6) Å) are almost the same in both ligands and are shorter than a formal single bond [118] and indicate imine bonds. The distance between Cr atom and the centre of the $\eta^5$-Cp ligand (1.872 Å) and the average distance Cr−C (2.215 Å) are quite close to the compounds of the type CpML$_4$ [119], including complex **6**. The bond lengths and angles observed in complex **22** are comparable with the reported values of similar complexes.[120, 121, 122] The phenyl rings are essentially planar (the

sum of the angles around C8, C14, C22, C28 is 360°). Both of the H₂BDI ligands are connected to the triflate anions by N−H⋯O hydrogen bonds, involving all four imine hydrogen atoms and four of the oxygen atoms of the triflates.
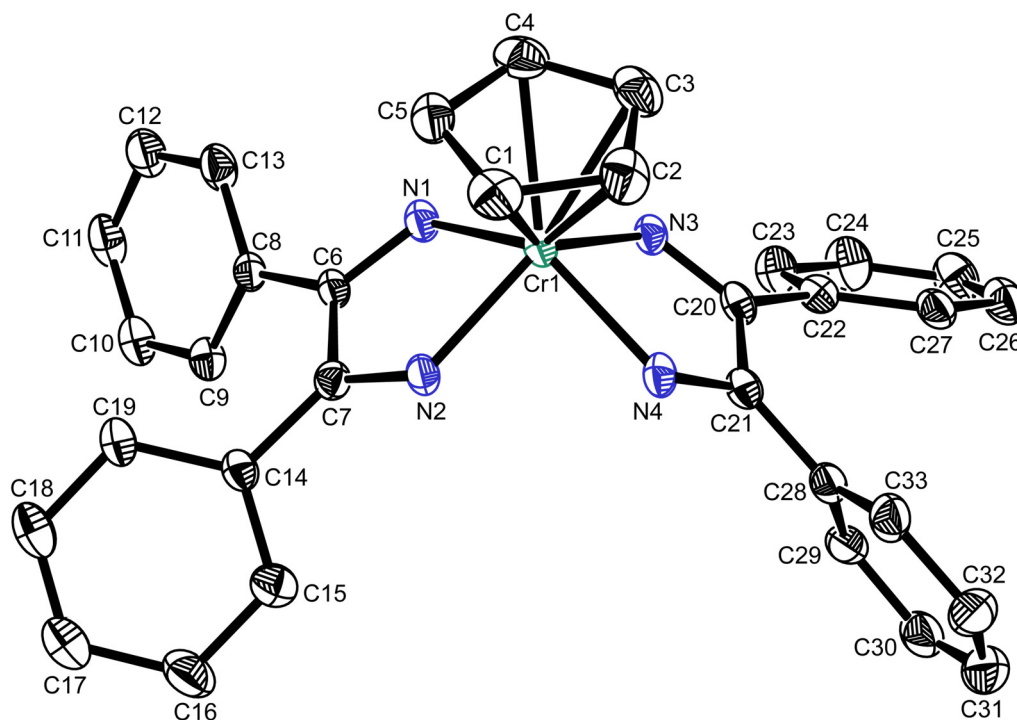


**Figure 31:** Molecular structure of **22**. The thermal ellipsoids are drawn at the 50% probability level. Hydrogen atoms, two triflate anions and the CH₂Cl₂ solvate molecules are omitted for clarity.

**Selected bond lengths [Å]**: Cr(1)−N(2) 1.967(4), Cr(1)−N(3) 1.978(4), Cr(1)−N(1) 1.993(4), Cr(1)−N(4) 1.993(4), Cr(1)−C(1) 2.221(5), Cr(1)−C(2) 2.227(5), Cr(1)−C(3) 2.227(5), Cr(1)−C(4) 2.205(5), Cr(1)−C(5) 2.196(5), N(1)−C(6) 1.307(5), N(2)−C(7) 1.301(6), N(3)−C(20) 1.297(6), N(4)−C(21) 1.297(6), C(6)−C(7) 1.455(6), C(20)−C(21) 1.457(6), C(6)−C(8) 1.478(6), C(7)−C(14) 1.483(6), C(20)−C(22) 1.467(6), C(21)−C(28) 1.471(6), Cr(1) ⋯Ccentroid 1.872.

**Selected bond angles [°]**: N(2)−Cr(1)−N(3) 124.62(16), N(1)−Cr(1)−N(4) 132.71(15), N(2)−Cr(1)−N(1) 74.80(17), N(3)−Cr(1)−N(4) 74.58(17), N(3)−Cr(1)−N(1) 84.18(15), N(2)−Cr(1)−N(4) 83.35(17).

**Hydrogen bonds [Å] and angles [°]**: N(1)−H(1)⋯OOTf(6) 0.88, 2.18, 3.030(5), 161.3; N(2)−H(2)⋯OOTf(3) 0.88, 2.02, 2.869(4), 162.5; N(3)−H(3)⋯OOTf(4) 0.88, 2.08, 2.958(4), 171.7; N(4)−H(4)⋯OOTf (1) 0.88, 2.12, 2.990(4), 169.3.

### 2.14.2 Spectroscopic characterisation of 22

In the ^{1}H NMR spectrum of **22**, a characteristic broad signal at 12.13 ppm is assigned to the proton resonance of N−H. Four phenyl groups signals shifted slightly upfield than that of the free ligand (7.80−7.32 ppm) and form multiplets in the range 7.67−7.20 ppm. The protons of the Cp ring give a singlet at 5.79 ppm.

The ^{13}C NMR spectrum shows downfield shift of the resonances for the C=N (183.10 ppm) and upfield shift of those for phenyl carbons (135.97−128.63 ppm) as compared to **4**. ([1]H: 7.80−7.32 ppm, [13]C: 174.2 ppm (CN), 138.28−128.14 (Ph−C) ppm, **4** recorded in $CD_2Cl_2$). A sharp singlet of Cp carbons is found at 103.24 ppm.

The IR spectrum (in KBr) shows the bands characteristic of the imine N−H and C−H stretching vibrations at 3224 and 3065, 2930 $cm^{-1}$, respectively, and those for C=C at 1488, 1449 and 1419 (Cp) $cm^{-1}$. It has been further observed that imine nitrogen $v$(C=N) bands at 1596, 1578 and 1544 $cm^{-1}$ are shifted to lower frequencies than that of the free ligand (1652 and 1646 $cm^{-1}$) upon metal coordination. The stretching and deformation vibrations of the $CF_3$ and $SO_3$ groups are detected at 1282 $cm^{-1}$ ($v$, asym., $CF_3$), 1244 ($v$, sym., $CF_3$),, 1170 $cm^{-1}$ ($v$, asym., $SO_3$), 1029 $cm^{-1}$ ($v$, sym., $SO_3$), 766 $cm^{-1}$ ($\delta$, sym., $CF_3$), 637 $cm^{-1}$ ($\delta$, sym., $SO_3$), 573 $cm^{-1}$ ($\delta$, asym., $CF_3$) and 516 $cm^{-1}$ ($\delta$, asym., $SO_3$).

The FAB[+] mass spectra of **22** does not show the parent signal, but fragments at $m/z$ = 533 [$M^+$ −2OTf] and 327 [$M^+$ −2OTf −($H_2$BDI)] confirm the molecular structure.

**Table 1:** Comparison of selected bond lengths between **4** and its complexes **18−22**

| Compound | M−N | C−N | C−C (C with N) | C−C (C with Ph) |
|---|---|---|---|---|
| Si$_2$BDI (**4**) | − | 1.268−1.270 | 1.523 | 1.490−1.492 |
| **18** | 2.015−2.047 | 1.281−1.286 | 1.488 | 1.486−1.494 |
| **19** | 1.996−2.033 | 1.333−1.339 | 1.412 | 1.482−1.484 |
| **20** | 1.903−1.927 | 1.286−1.292 | 1.474−1.483 | 1.471−1.480 |
| **22** | 1.967−1.993 | 1.297−1.307 | 1.455−1.457 | 1.467−1.483 |

# 3  EXPERIMENTAL SECTION

## 3.1   Materials and Methods

All reactions were carried out under argon using standard Schlenk and vacuum-line techniques. Solvents were purified by standard procedures; dichloromethane and *n*-pentane were distilled from calcium hydride and sodium, respectively. All solvents were stored under a dry argon atmosphere over 3 Å molecular sieves ($CH_2Cl_2$) or sodium pieces (*n*-pentane). Benzene, $CHCl_3$ and triethylamine were distilled prior to use. The ligand and complexes $Si_2BDI$, [67, 68] $[CpCr(NO)_2Cl]$,[123] $[Re(CO)_5Br]$,[124] [*cis*-$PPh_3Re(CO)_4Br$],[125] *trans*-$[PdCl_2(PPh_3)_2]$,[126] $[(PPh_3)_2CuBH_4]$,[127] $[RhCl(CO)(PPh_3)_2]$,[128] $[IrCl(CO)(PPh_3)_2]$,[128] $Cp*H$, [129] $[IrCl_2(Cp*)]_2$,[130] $[RhCl_2(Cp*)]_2$,[130] [$RuCl_2$(*p*-cymene)]$_2$,[131] and $CpFe(CO)_2Cl$, [132] were prepared and purified according to literature procedures. Other reagents were commercially available (Aldrich, Fluka, Merck and Sigma) and used without further purification.

NMR spectra were measured using a Jeol Eclipse 270, Jeol Eclipse 400 or Jeol EX 400 spectrometer. Chemical shifts ($\delta$) were measured relative to partially deuterated solvent peaks but are reported in ppm relative to tetramethylsilane. $^{31}P$ chemical shifts were measured relative to $H_3PO_4$ (85%). The coupling constants (*J*) are given in Hertz (Hz). NMR multiplicities are abbreviated as follows: s (singlet), d (doublet), t (triplet), q (quartet), sext (sextet), sept (septet) and m (multiplets); broad signals are written as 'br'.

| Solvent | $CD_2Cl_2$ | $CDCl_3$ | $CD_3OD$ | $D_2O$ |
|---|---|---|---|---|
| $^1$H-NMR [ppm] | 5.32 | 7.26 | 3.31 | 4.79 |
| $^{13}$C-NMR [ppm] | 53.5 | 77.16 | 49.0 | − |

Mass spectra were recorded with a Jeol MStation JMS 700, NBA matrix ($FAB^+$). Multi-isotope containing fragments refer to the isotope with the highest abundance.

IR spectra were recorded from KBr pellets or in solutions in a NaCl cell using a Perkin–Elmer Spectrum One FT-IR spectrometer. The absorptions ($\tilde{\nu}$) observed are reported in $cm^{-1}$

and described as very strong (vs), strong (s), medium (m), weak (w), very weak (vw), shoulder (sh), broad (br) etc.

The melting points, obtained with a Büchi Melting Point B-540 device, are uncorrected.

Elemental analyses were performed by the Microanalytical Laboratory of the Department of Chemistry and Biochemistry, LMU, using a Heraeus Elementar Vario El apparatus.

Single crystal X-Ray diffraction data were collected on a Nonius Kappa CCD using graphite-monochromated Mo-Kα radiation. Single crystal X-ray structure analyses were performed by direct methods using the SHELXS software and refined by full-matrix least-squares with SHELXL-97.[133]

## 3.2 Synthesis Procedures and Analytical Data

### 3.2.1 [(5,5-Diethylbarbiturato-*N*)-($\eta^5$-cyclopentadienyl)-dinitrosyl-chromium(0)] (6)
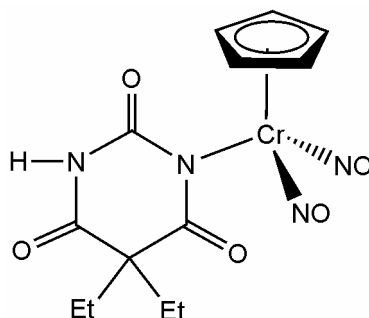


Triethylamine (43 μl, 0.307 mmol) was mixed with H$_2$debarb (**2**) (38.7 mg, 0.21 mmol) in chloroform (10 mL) under stirring. To this clear colourless solution CpCr(NO)$_2$Cl (44.6 mg, 0.21 mmol) was added. The green-brown solution was stirred for 2 days at room temperature and evaporated to dryness under reduced pressure. The residue was extracted with chloroform (30 mL), washed with water (20 mL) and the chloroform layer separated, dried (CaCl$_2$), filtered and the solvent was evaporated. The green solid was dried in vacuo.

**M**(C$_{13}$H$_{16}$CrN$_4$O$_5$):     360.30g/mol.

**Yield**:     31.7 mg (0.088 mmol, 42 %), green powder.

**Melting Point**:     166 °C (decomp.).

**$^1$H-NMR** (399.78 MHz, CD$_2$Cl$_2$):     $\delta$ = 8.14 (br, 1H, NH), 5.66 (s, 5H, Cp−CH), 1.88 (q, $^3J$ = 7.4 Hz, 4H, CH$_2$), 0.75 (t, $^3J$ = 7.4 Hz, 6H, CH$_3$).

**$^{13}$C-NMR** (100.53 MHz, CD$_2$Cl$_2$):     $\delta$ =181.19 (s, CO), 174.79 (s, CO), 156.43 (s, CO), 102.80 (s, Cp−CH), 58.23 (s, CEt$_2$), 32.99 (s, CH$_2$), 9.93 (s, CH$_3$).

**MS**(FAB$^+$):   *m/z* (%) = 361 (38) [MH$^+$], 331(18) [MH$^+$ −NO], 300 (31) [M$^+$−2NO].

**IR** (KBr) [cm$^{-1}$]:   $\tilde{\nu}$ = 3166 (vw), 3125 (w), 3114 (w), 3076 (w), 3027 (w), 2966 (w), 2935 (w), 2876 (vw), 1814 (vs), 1727 (vs), 1714 (sh), 1671 (m), 1620 (s), 1457 (m), 1438 (w), 1429 (w), 1408 (m), 1365 (m), 1324 (s),1317 (s), 1244 (m), 822 (m) (Cp-Cr), 534 (m), 521 (w).

**IR** (CHCl$_3$) [cm$^{-1}$]:   $\tilde{\nu}$ = 3389 (w), 2939 (vw), 2879 (vw), 2820 (vw), 1825 (s), 1720 (vs), 1682 (sh), 1621 (m), 1458 (w), 1443 (vw), 1386 (m), 1324 (w), 1307 (m), 1239 (w), 828 (m).

**Elemental Analysis**:

| | | | |
|---|---|---|---|
| Calculated (%): | C: 43.33 | H: 4.49 | N: 15.55. |
| Found  (%): | C: 43.25 | H: 4.53 | N: 15.52. |

### 3.2.2 *cis*-[(5,5-Diethylbarbiturato-*N*)-tetracarbonyl-(triphenylphosphine)-rhenium(I)] (7)
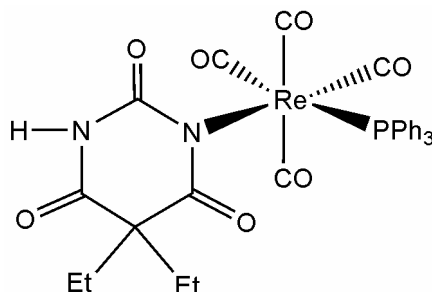


To a stirred solution of [PPh₃Re(CO)₄Br] (96.1 mg, 0.15 mmol) in 20 mL of chloroform, AgOTf (38.5 mg, 0.15 mmol) was added and the solution was stirred for 1 hour until the AgBr had precipitated. After centrifugation and separation of the solution by decantation, **2** (27.6 mg, 0.15 mmol) was added to the solution followed by triethylamine (31 μL, 0.221 mmol) to give a clear pale brown solution which was stirred at room temperature for 2 days and the solvent was removed in vacuo. After crystallization, the colourless crystals were washed with 10 mL methanol, dried in vacuo and used for different analysis.

| | |
|---|---|
| **M**($C_{30}H_{26}N_2O_7PRe$): | 743.71 g/mol. |
| **Yield**: | 55.8 mg (0.075 mmol, 50 %), colourless powder. |
| **Melting Point**: | 180−186°C (decomp.). |
| **¹H-NMR** (399.78 MHz, $CD_2Cl_2$): | $\delta$ =7.76 (br, 1H, NH), 7.47−7.37 (m, 15H, Ar−H), 1.77 (m, 4H, $CH_2$), 0.65 (t, $^3J$ = 7.4 Hz, 6H, $CH_3$). |
| **¹³C-NMR** (100.53 MHz, $CD_2Cl_2$): | $\delta$ = 188.39 (d, $^2J$ (P,C) = 6.7 Hz, Re−CO), 187.16 (d, $^2J$ (P,C) = 9.1 Hz, Re−CO), 184.26 (d, $^2J$ (P,C) = 56.0 Hz, Re−CO), 181.08 (s, Hdebarb−CO), 173.33 (s, Hdebarb−CO), 156.59 (s, Hdebarb−CO), 133.30 (d, $^2J$ (P, C) = 10.54 Hz, o−Ph−C), 131.97 (d, $^1J$ (P, C) = 47.92 Hz, Ph−Cq), 130.87 (d, $^4J$ (P, C) = 1.92 Hz, |

*p*−Ph−C), 128.79 (d, $^3J$ (P, C) = 9.58 Hz, m−Ph−C), 56.17 (s, CEt$_2$), 32.05 (s, CH$_2$), 9.46 (s, CH$_3$).

**$^{31}$P-NMR** (161.83 MHz, CD$_2$Cl$_2$):  $\delta$ = 11.64 (s, PPh$_3$).

**MS**(FAB$^+$):  *m/z* (%) = 745 (MH$_2^{2+}$, 8.5), 743 (M$^+$, 5), 686 (M$^+$ − 2CO −H$^+$, 1.8), 630 (M$^+$ −4CO −H$^+$, 2.3), 262 (PPh$_3$, 53).

**IR** (KBr) [cm$^{-1}$]:  $\tilde{\nu}$ = 3177 (w), 3083 (w), 3053 (w), 2961 (w), 2859 (vw), 2942 (vw), 2880 (vw), 2678 (w), 2106 (s), 2020 (vs), 1999 (sh), 1926 (vs), 1716 (s), 1675 (s), 1615 (vs), 1484 (m), 1452 (w), 1434 (s), 1363 (s), 1316 (m), 1237 (m), 1164 (m), 1030 (s), 746 (s), 692 (s), 692 (s), 639 (s), 577 (s), 526 (s), 458 (m), 411 (m).

**IR** (CHCl$_3$) [cm$^{-1}$]:  $\tilde{\nu}$ = 3390 (w), 3026 (m), 2973 (m), 2880 (w), 2890 (vw), 2105 (s), 2010 (vs), 1946 (s), 1718 (m), 1697 (sh), 1681 (m), 1619 (s), 1483 (w), 1458 (w), 1436 (m), 1392(m), 1298 (s), 1262 (m), 1095 (m), 808 (m).

**Elemental Analysis**:

| | | | |
|---|---|---|---|
| Calculated (%): | C: 48.45 | H: 3.53 | N: 3.77. |
| Found       (%): | C: 47.82 | H: 3.70 | N: 3.94. |

### 3.2.3  [(5,5-Diethylbarbiturato-*N*)-pentacarbonyl-rhenium(I)] (8)
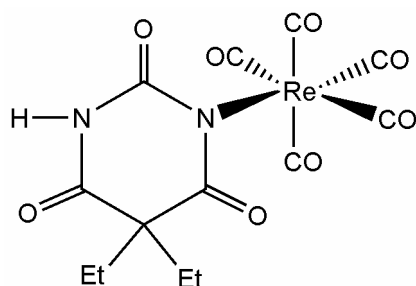


To a stirred solution of Re(CO)$_5$Br (81.3 mg, 0.2 mmol) in 20 mL of chloroform, AgOTf (51.4 mg 0.2 mmol) was added and the solution was stirred for 1 hour until the AgBr had precipitated. After centrifugation and separation of the solution by decantation, **2** (36.8 mg, 0.2 mmol) was added to the solution followed by triethylamine (40 μL, 0.286 mmol) to give a clear pale brown solution which was stirred at room temperature for 2 days and the solvent was removed in vacuo. After crystallization, the crystals were washed with 5 mL methanol. Then the colourless crystals were dried in vacuo and used for different analysis.

| | |
|---|---|
| **M**(C$_{13}$H$_{11}$N$_2$O$_8$Re): | 509.45 g/mol. |
| **Yield**: | 50 mg (0.098 mmol, 49 %), colourless powder. |
| **Melting Point**: | 160−164°C (decomp.). |
| **$^1$H-NMR** (399.78 MHz, CD$_2$Cl$_2$): | $\delta$ = 8.33 (br, 1H, NH), 1.92 (q, $^3J$ = 7.4 Hz, 4H, CH$_2$), 0.74 (t, $^3J$ = 7.4 Hz, 6H, CH$_3$). |
| **$^{13}$C-NMR** (100.53 MHz, CD$_2$Cl$_2$): | $\delta$ = 181.97 (s, Re−CO), 180.67 (s, Re−CO), 180.15 (s, Hdebarb−CO), 174.02 (s, Re−CO), 172.49 (s, Hdebarb−CO), 157.23 (s, Hdebarb−CO), 57.18 (s, CEt$_2$), 33.17 (s, CH$_2$), 9.86 (s, CH$_3$). |
| **MS**(FAB$^+$): | *m/z* (%) = 835 (40) [MH$^+$], 834 (5) [M$^+$], 806 (15) [M$^+$ −CO], 778 (34) [M$^+$ −2CO], 750 (12) [M$^+$ −3CO], 722 |

(26) [M$^+$ −4CO], 694 (11) [M$^+$ −5CO], 453 (27) [M$^+$ −5CO −Re(CO)$_2$H$^+$].

**IR** (KBr) [cm$^{-1}$]:     $\tilde{\nu}$ = 3229 (m), 3098 (w), 2969 (w), 2939 (w), 2880 (w), 2148 (s), 2022 (vs), 1995 (vs), 1726 (s), 1685 (s), 1614 (sh), 1603 (s), 1445 (m), 1423 (w), 1409 (s), 1399 (s), 1373 (s), 1322 (s), 1244 (s), 1039 (w), 947 (w), 818 (w), 801 (w), 693 (m), 645 (w), 595 (s), 540 (m), 496 (w).

**IR** (CHCl$_3$) [cm$^{-1}$]:     $\tilde{\nu}$ = 3386 (w), 2151 (m), 2043 (vs), 1992 (s), 1723 (m), 1683 (m), 1620 (s), 1457 (w), 1398 (m), 1355 (w), 1300 (m), 1237 (s), 1172 (w), 1026 (s).

**Elemental Analysis**:

| | | | |
|---|---|---|---|
| Calculated (%): | C: 30.65 | H: 2.18 | N: 5.50. |
| Found     (%): | C: 30.86 | H: 2.29 | N: 5.67. |

### 3.2.4  [(*μ*-Diethylbarbiturato-*N,N′*)bis(pentacarbonyl-rhenium(I))] (9)
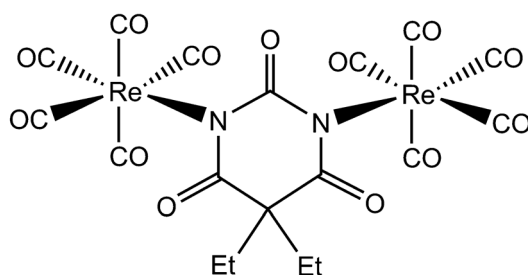


To a stirred solution of Re(CO)$_5$Br (121.8 mg, 0.3 mmol) in 20 mL of chloroform, AgOTf (79.6 mg 0.31 mmol) was added and the solution was stirred for 1 hour until the AgBr had precipitated. After centrifugation and separation of the solution by decantation, **2** (27.6 mg, 0.15 mmol)  was added to the solution followed by triethylamine (72 μL, 0.514 mmol) to give a clear pale brown solution which was stirred at room temperature for 2 days and the

solvent was removed in vacuo. After crystallization, the crystals were washed with 5 mL methanol. Then the colourless crystals were dried in vacuo and used for different analysis.

| | |
|---|---|
| **M**($C_{18}H_{10}N_2O_{13}Re_2$): | 834.70 g/mol. |

**Yield**: 66.36 mg (0.079 mmol, 53 %), colourless powder.

**Melting Point**: 169 °C (decomp.)

**$^1$H-NMR** (270.16 MHz, CDCl$_3$): $\delta = 1.93$ (q, $^3J = 7.4$ Hz, 4H, CH$_2$), 0.75 (t, $^3J = 7.4$ Hz, 6H, CH$_3$).

**$^{13}$C-NMR** (67.93 MHz, CDCl$_3$): $\delta = 181.31-156.22$ (m, Hdebarb−CO and Re−CO), 32.83 (s, CH$_2$), 9.51 (s, CH$_3$).

**MS**(FAB$^+$): *m/z* (%) = 835 (40) [MH$^+$], 834 (5) [M$^+$], 806 (15) [M$^+$ −CO], 778 (34) [M$^+$ −2CO], 750 (12) [M$^+$ −3CO], 722 (26) [M$^+$ −4CO], 694 (11) [M$^+$ −5CO], 453 (27) [M$^+$ −5CO −Re(CO)$_2$H$^+$].

**IR** (KBr) [cm$^{-1}$]: $\tilde{v} = 3228$ (m), 3098 (w), 2968 (w), 2939 (w), 2880 (w), 2148 (m), 2024 (vs), 1994 (vs), 1958 (sh), 1726 (s), 1685 (s), 1614 (s), 1604 (sh), 1584 (sh), 1563 (w), 1445 (m), 1424 (w), 1409 (s), 1398 (s), 1373 (s), 1321 (vs), 1243 (s), 1039 (m), 1032 (sh), 947 (w), 815 (w), 800 (w), 758 (w), 693 (m), 645 (w), 594 (s), 553 (w), 540 (w).

**IR** (CHCl$_3$) [cm$^{-1}$]: $\tilde{v} = 2145$ (m), 2044 (vs), 1987 (s), 1682 (w), 1618 (m), 1586 (m), 1475 (w), 1444 (w), 1393 (w), 1296 (m), 1067 (w), 1026 (s), 928 (m), 638 (s), 595 (s).

**Elemental Analysis**:

| | | | |
|---|---|---|---|
| Calculated (%): | C: 25.89 | H: 1.21 | N: 3.36. |
| Found (%): | C: 25.34 | H: 1.55 | N: 3.25. |

### 3.2.5 *trans*-[Chlorido-(barbiturato-*N*)-bis-(triphenylphosphine)-palladium(II)] (10)
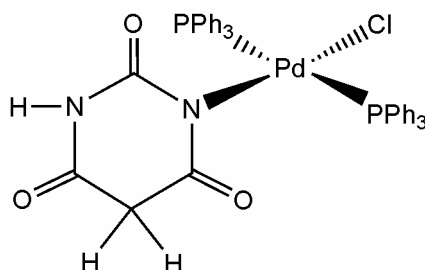


The starting complex (PPh$_3$)$_2$PdCl$_2$ (105.2 mg, 0.15 mmol) was added to a stirring methanol solution (20 mL) of H$_2$barb (**1**) (19.2 mg, 0.15 mmol) and NaOMe (8.1 mg, 0.15 mmol), the resulting colourless solution and yellow precipitate was heated at 50 °C for 1h. The mixture was allowed to cool to room temperature and stirred for 2 days. Then the yellow-coloured product was separated from the solution and was dissolved in dichloromethane (10 mL). The solution was filtered to remove sodium chloride and the solvent was evaporated to give a yellow solid which was dried in vacuo. Yellow colour crystals were obtained by slow isothermic diffusion of *n*-pentane into CH$_2$Cl$_2$ solution of the complex within 1 day. The product was purified from the starting materials by repeated crystallization.

| | |
|---|---|
| **M**(C$_{40}$H$_{33}$ClN$_2$O$_3$P$_2$Pd): | 793.52 g/mol. |
| **Yield**: | 36.5 mg (0.046 mmol, 30.66 %), yellow powder. |
| **Melting Point**: | 245 °C (decomp.). |
| **$^1$H-NMR** (399.78 MHz, CDCl$_3$): | $\delta$ = 8.01 (br, N−H), 7.83−7.36 (m, 30H, Ph−CH), 2.14 (s, CH$_2$). |
| **$^{13}$C-NMR** (100.53 MHz, CDCl$_3$): | $\delta$ = 171.57, 168.18, 154.69 (s, CO−Hbarb), 134.89−128.36 (m, Ph−C), 37.66 (s, CH$_2$). |
| **$^{31}$P-NMR** (161.83 MHz, CDCl$_3$): | $\delta$ = 22.39 (s, PPh$_3$). |

**MS**(FAB$^+$):  $m/z$ (%) = 795 (0.25) [MH$^+$], 757 (0.17) [M$^+$ −Cl −H].

**IR** (KBr) [cm$^{-1}$]:  $\tilde{\nu}$ = 3371 (vw), 3075 (vw), 3053 (w), 3005 (vw), 2986 (vw), 1720 (s), 1683 (s), 1615 (vs), 1584(w), 1572(w) 1480 (s), 1433 (vs), 1409 (s), 1392 (s), 1347 (s), 1251 (s), 1242 (w), 1215 (w), 1184 (m), 1099 (vs), 999 (m), 940 (w), 745 (vs), 708 (vs), 692 (vs), 660 (m), 523 (vs), 512 (vs), 498 (vs).

**IR** (CHCl$_3$) [cm$^{-1}$]:  3399 (vw), 1717 (m), 1689 (s), 1632 (s), 1522 (w), 1482 (w), 1435 (s), 1393 (w), 1340 (w), 1098 (m), 1016 (w), 928 (m), 522 (m).

**Elemental Analysis**:

| | | | |
|---|---|---|---|
| Calculated (%): | C: 60.54 | H: 4.19 | N: 3.53. |
| Found (%): | C: 60.01 | H: 4.10 | N: 3.13. |

### 3.2.6 *trans*-[Chlorido-(5,5-diethylbarbiturato-*N*)-bis-(triphenylphosphine)-palladium(II)] (11)
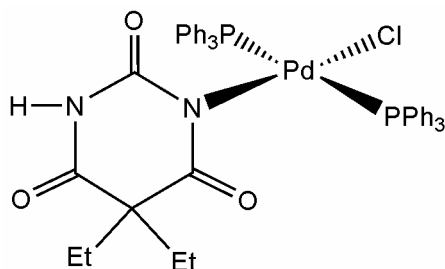


Sodium methoxide (10 mg, 0.18 mmol) and Hdebarb (**2**) (31.3 mg, 0.17 mmol) were added to a suspension of (PPh$_3$)$_2$PdCl$_2$ (119.3 mg, 0.17 mmol) in methanol (15 ml). Then the suspension was heated at 50 °C for 1h. The mixture was allowed to cool to room temperature and stirred at room temperature. After 2 days the solvent was removed under vacuum to leave a yellow solid which was re-dissolved in CH$_2$Cl$_2$ (10 mL). The solution was filtered to remove sodium chloride and the solvent was evaporated and the resulting solid was dried in vacuo. Yellow colour crystals were obtained by slow isothermic diffusion of *n*-pentane into CH$_2$Cl$_2$ solution of the complex within 3 days. The product was purified from the starting materials by repeated crystallization.

**M**(C$_{44}$H$_{41}$ClN$_2$O$_3$P$_2$Pd ):       849.63 g/mol.

**Yield**:       51.4 mg (0.06 mmol, 35.3 %), yellow powder.

**Melting Point**:       251 °C (decomp.).

**$^1$H-NMR** (270.16 MHz, CDCl$_3$):     $\delta$ = 8.2 (br, 1H, N−H), 7.77−7.13 (m, 30 H, Ph−CH), 1.87 (q, $^3J$ = 7.72 Hz, 4H, CH$_2$,), 0.95 (t, $^3J$ = 7.72 Hz, 6H, CH$_3$).

**$^{13}$C-NMR** (67.93 MHz, CDCl$_3$):     $\delta$ =183.9, 175.04, 154.58 (Hdebarb−CO), 134.98−127.92 (m, Ph−CH), 56.8 (s, CEt$_2$), 29.76 (s, CH$_2$), 9.33 (s, CH$_3$).

**$^{31}$P-NMR** (109.36 MHz, CDCl$_3$): $\delta$ = 22.77 (s, PPh$_3$)

**MS**(FAB$^+$): *m/z* (%) = 851 (0.1) [MH$_2$$^{2+}$], 813 (0.6) [M$^+$ −Cl], 551 (0.2) [M$^+$ −Cl −PPh$_3$], 289 (12) [M$^+$ −Cl −2 PPh$_3$].

**IR** (KBr) [cm$^{-1}$]: $\tilde{\nu}$ = (vw), 3156 (vw), 3055 (w), 3023 (w), 2969 (w), 2935 (vw), 2849(w), 1707 (s), 1670 (s), 1613 (vs), 1584 (vw), 1567(vw), 1481 (m), 1459 (w), 1433 (s), 1420 (sh), 1359 (m), 1327 (m), 1252 (m), 1187 (w), 1159 (w), 1098 (s), 1086 (sh), 1028 (w), 998 (w), 859 (w), 754 (m), 740 (s), 701 (sh), 693 (vs), 539 (s), 523 (vs), 512 (w), 493 (m).

**IR** (CHCl$_3$) [cm$^{-1}$]: $\tilde{\nu}$ = 3398 (w), 3061 (w), 3021 (w), 2939(w), 2820 (w), 1714 (m), 1677 (s), 1619 (vs), 1482 (w), 1461(vw), 1438 (s), 1387 (m), 1328 (w), 1308 (w), 1243 (w), 1096 (m), 1068 (w), 1028 (w), 693 (s), 671 (s), 540 (m), 522 (s).

**Elemental Analysis**:

| | | | |
|---|---|---|---|
| Calculated (%): | C: 62.20 | H: 4.86 | N: 3.30. |
| Found      (%): | C: 57.32 | H: 4.27 | N: 3.05. |

### 3.2.7 [5,5-Diethylbarbiturato-*N*-bis(triphenylphosphine)-copper(I)] (12)



To a CHCl$_3$ solution (5 mL) consisting of H$_2$debarb (37.0 mg, 0.201 mmol) and NEt$_3$ (41.0 µL, 0.293 mmol), a solution of (PPh$_3$)$_2$CuBH$_4$ (121.1 mg, 0.201 mmol) in 10 mL of CHCl$_3$ was added under stirring. The resulting colourless reaction mixture was heated at 50 °C for 4 hours and then allowed to cool to room temperature. The mixture was stirred overnight. After this time, the solvent was evaporated under vacuum. The resulting sticky white residues were washed twice with 5 ml of pentane and dried in vacuo for several hours. Colourless crystals were obtained by slow isothermic diffusion of *n*-pentane into chloroform solution of the complex within 1 day. The crystals were washed with methanol and used for analysis. The X-ray structure shows that the compound crystallizes with solvent. The elemental analysis fits if the calculated values include 0.75 CHCl$_3$ molecule as found in the molecular structure.

**M**(C$_{44.75}$H$_{41.75}$Cl$_{2.25}$CuN$_2$O$_3$P$_2$.):      860.83 g/mol.

**M**(C$_{44}$H$_{41}$CuN$_2$O$_3$P$_2$):      771.30 g/mol.

**Yield**:      62.3 mg (0.081 mmol, 40.34%), white powder.

**Melting Point**:      202−205 °C.

**$^1$H-NMR** (399.78 MHz, CDCl$_3$):      $\delta$ = 7.62 (br, 1H, N−H), 7.33−7.18 (m, 30 H, Ph−CH), 1.77 (q, $^3J$ = 7.4 Hz, 4H, CH$_2$), 0.46 (t, $^3J$ = 7.4 Hz, 6H, CH$_3$).

**<sup>13</sup>C-NMR** (100.53 MHz, CDCl<sub>3</sub>):

$\delta$ = 181.09, 176.36, 156.51 (Hdebarb −CO), 133.87, 132.33 (br), 129.96, 128.75 (s, Ph−CH), 57.02 (s, CEt<sub>2</sub>), 32.08 (s, CH<sub>2</sub>), 9.46 (s, CH<sub>3</sub>).

**<sup>31</sup>P-NMR** (161.83 MHz, CDCl<sub>3</sub>):

$\delta$ = −0.85 (s, PPh<sub>3</sub>).

**MS(FAB<sup>+</sup>)**:

$m/z$(%) = 770 (18.5) [M<sup>+</sup> −H], 587 (72) [Cu(PPh<sub>3</sub>)<sub>2</sub>], 509 (4) [M<sup>+</sup> −PPh<sub>3</sub>], 325 (52) [Cu(PPh<sub>3</sub>)], 262 (100) [(PPh<sub>3</sub>)].

**IR** (KBr) [cm<sup>-1</sup>]:

$\tilde{\nu}$ = 3170 (br), 3052 (w), 2969 (w), 2930 (vw), 1711 (w), 1670 (s), 1595 (vs), 1480 (m), 1458 (w), 1435 (s), 1417 (m), 1368 (m), 1316(m), 1252 (w), 1095 (m), 694 (vs), 516 (s), 504 (s).

**IR** (CHCl<sub>3</sub>) [cm<sup>-1</sup>]:

$\tilde{\nu}$ = 3394 (vw), 1707 (w), 1681 (sh), 1670 (m), 1602 (s), 1481 (w), 1459 (w), 1436 (m), 1382 (w), 1311 (w), 1097 (w), 1027 (vw).

**Elemental Analysis**:

| | | | |
|---|---|---|---|
| Calculated (%): | C: 62.43 | H: 4.89 | N: 3.25. |
| Found    (%): | C: 61.14 | H: 4.62 | N: 3.09. |

### 3.2.8 *trans*-[Carbonyl-5,5-diethylbarbiturato-*N*-bis(triphenylphosphine)-rhodium(I)] (13)



A solution of (PPh$_3$)$_2$Rh(CO)Cl (104.3 mg, 0.151 mmol ) in CHCl$_3$ (10 mL) was treated with AgOTf (40 mg, 0.156 mmol) at room temperature and stirred for 1 hour until the AgCl had precipitated. After centrifugation and separation of the solution by decantation, H$_2$debarb (27.8 mg, 0.151 mmol) was added to the solution followed by triethylamine (32 µL, 0.228 mmol) to give a pale yellow solution which was stirred at room temperature for 2 days and the solvent was removed in vacuo.

Yellow crystals obtained by slow isothermic diffusion of *n*-pentane into a solution of the complex in CH$_2$Cl$_2$ were washed with H$_2$O (15 mL) and cold MeOH (5 mL) (to remove unreacted H$_2$debarb and Et$_3$NHO$_3$SCF$_3$) and were dried in vacuo for several hours. The X-ray structure shows that the compound crystallizes with solvent. The elemental analysis fit if the calculated values include one CH$_2$Cl$_2$ molecule as found in the molecular structure.

**M(C$_{45}$H$_{41}$N$_2$O$_4$P$_2$Rh):**  838.67 g/mol.

**M(C$_{45}$H$_{41}$N$_2$O$_4$P$_2$Rh. CH$_2$Cl$_2$):**  923.60 g/mol.

**Yield:**  64.6 mg (0.077 mmol, 51 %), yellow powder.

**Melting Point:**  163 °C.

**$^1$H-NMR** (399.78 MHz, CD$_2$Cl$_2$):  $\delta$ = 7.07 (br, 1H, N−H), 7.72−7.36 (m, 30 H, Ph−CH), 5.29 (s, CH$_2$Cl$_2$), 2.03 (q, $^3J$ = 7.4 Hz, 4H, CH$_2$), 0.22 (t, $^3J$ = 7.4 Hz, 6H, CH$_3$).

**$^{13}$C-NMR** (100.53 MHz, CD$_2$Cl$_2$): $\delta$ = 181.91 (t, $^1J_{Rh-C}$ = 17.7 Hz, Rh−CO), 179.62, 174.79, 155.29 (Hdebarb−CO), 134.42 (t, $J$ = 6.7 and 7.1 Hz, Ph−C)*,* 132.98 (t, $J$ = 22.0 Hz, Ph−Cq)*,* 130.22 (s, Ph−C), 128.35 (t, $J$ = 5.2 Hz, Ph−C), 56.02 (s, CEt$_2$), 27.7 (s, CH$_2$), 8.9 (s, CH$_3$).

**$^{31}$P-NMR** (161.83 MHz, CD$_2$Cl$_2$): $\delta$ = 31.79 (d, $^1J_{Rh-P}$ = 135.5 Hz, PPh$_3$)

**MS**(FAB$^+$): $m/z$ (%) = 839 (4.3) [MH$^+$], 810 (38) [M$^+$ −CO], 548 (6.6) [M$^+$ −CO −PPh$_3$], 286 (26) [M$^+$ −CO −2PPh$_3$].

**IR** (KBr) [cm$^{-1}$]: $\tilde{\nu}$ = 3159 (vw), 3117 (vw), 3055 (w), 3005 (w), 2963 (w), 2931 (w), 2854 (w), 1975 (vs), 1717 (m), 1664 (m), 1601 (s), 1478 (w), 1460 (w), 1435 (s), 1413 (s), 1357 (s), 1312 (w), 1264 (m), 1236 (w), 1096 (s), 797 (w) 741 (m), 692 (s), 584 (m), 518 (s), 505 (m), 496 (w).

**IR** (CHCl$_3$) [cm$^{-1}$]: $\tilde{\nu}$ = 3397 (w), 1981 (s), 1712 (w), 1674 (m), 1611 (m), 1522 (w), 1479 (w), 1435 (m), 1386 (w), 1296 (w), 1096 (w), 1026 (s), 928 (w), 638 (m).

**Elemental Analysis**:

| | | | |
|---|---|---|---|
| Calculated (%): | C: 59.81 | H: 4.70 | N: 3.03. |
| Found    (%): | C: 59.24 | H: 4.70 | N: 3.00. |

### 3.2.9 Bis-(5,5-diethylbarbiturato-*N,O*)-(5,5-diethylbarbiturato-*N*)-($\eta^5$-pentamethylcyclopentadienyl)-rhodium(III)] (14)



A solution of (Cp*RhCl$_2$)$_2$ (41.4 mg, 0.067 mmol) in CHCl$_3$ (5 mL) was heated at 50 °C for 15 min. To this solution Na[Hdebarb] (55.2 mg, 0.268 mmol) was added followed by MeOH (10 mL) and the heating was continued for 4 hours. Then the reaction mixture was allowed to cool down to room temperature stirred for 2 days. During the period the solution colour changed from orange-red to light orange. The solvent was removed under reduced pressure and the residue was dissolved in CH$_2$Cl$_2$. After removal of suspended NaCl by centrifugation and separation of the solution by decantation, the solution was evaporated. The residue was purified by crystallization.

**M**(C$_{26}$H$_{37}$N$_4$O$_6$Rh):  604.50 g/mol.

**Yield**:  36 mg (0.066 mmol, 33 %), yellow powder.

**Melting Point**:  218 °C.

**$^1$H-NMR** (399.78 MHz, CDCl$_3$):  $\delta$ = 7.88, 7.75 (br, 1H, N−H), 2.03 (q, $^3J$ = 7.4, 4H, CH$_2$), 1.86 (br, 4H, CH$_2$), 1.80 (s, 15H, Cp*−CH$_3$), 0.87 (t, $^3J$ = 7.42, 6H, CH$_3$), 0.81 (t, $^3J$ = 7.4, 6H, CH$_3$).

**$^{13}$C-NMR** (100.53 MHz, CDCl$_3$):   $\delta$ = 174.40, 172.38, 151.89, (CO), 93.70 (d, $^1J_{Rh–C}$ = 9.58 Hz, Cp*−Cq), 57.59 (s, CEt$_2$), 32.10, 29.68 (s, CH$_2$), 9.89, 9.73 (s, CH$_3$), 9.64 (s, Cp*−CH$_3$).

**MS**(FAB$^+$):   $m/z$ (%) = 421 (26) [M$^+$ −Hdebarb].

**IR** (KBr) [cm$^{-1}$]:   $\tilde{\nu}$ = 3185 (br), 3133 (vw), 3085 (vw), 2965(w), 2935 (w), 2878 (w), 2847 (w), 1723 (m), 1684 (m), 1630 (s), 1569 (m), 1483 (w), 1459 (m), 1407 (w), 1363 (w), 1357 (m), 1312 (m), 1242 (w), 1031 (w), 941 (w), 690 (w), 545 (w).

**IR** (CHCl$_3$) [cm$^{-1}$]:   $\tilde{\nu}$ = 3388 (w), 2400 (w), 1716 (s), 1695 (sh), 1629 (m), 1527 (m), 1459 (vw), 1382 (w), 1341 (vw), 1312 (m), 1024 (w), 928 (m), 849 (vw), 629 (vw).

**Elemental Analysis**:

| | | | |
|---|---|---|---|
| Calculated (%): | C: 51.65 | H: 6.18 | N: 9.27. |
| Found      (%): | C: 50.79 | H: 6.17 | N: 8.44. |

### 3.2.10 Chlorido-($\eta^5$-pentamethylcyclopentadienyl)-(5,5-diethylbarbiturato-*N,O*)-iridium(III) (15)



A solution of (Cp*IrCl$_2$)$_2$ (79.6 mg, 0.1 mmol) in CHCl$_3$ (5 mL) was heated at 50 °C for 15 min. To this solution Na[Hdebarb] (41.2 mg, 0.2 mmol) was added followed by MeOH (10 mL) and the heating was continued for 4 hours. Then the reaction mixture was allowed to cool down to room temperature and stirred for 2 days. During the period the solution colour changed from orange-red to light orange. The solvent was removed under reduced pressure and the residue was dissolved in CH$_2$Cl$_2$. After removal of suspended NaCl by centrifugation and separation of the solution by decantation, the solution was evaporated. Two sets of crystals were obtained. The orange crystals of **15** were separated physically from the red crystals of (Cp*IrCl$_2$)$_2$.

The residue was washed with 5 mL of water and then dried to eliminate half molecule or excess Hdebarb from the product.

| | |
|---|---|
| **M**(C$_{18}$H$_{26}$ClN$_2$O$_3$Ir. C$_5$H$_6$N$_1$O$_2$): | 657.91 g/mol. |
| **M**(C$_{18}$H$_{26}$ClN$_2$O$_3$Ir): | 545.85 g/mol |

**Yield**: 36 mg (0.066 mmol, 33 %), yellow powder.

**Melting Point**: 216 °C.

**$^1$H-NMR** (399.78 MHz, CDCl$_3$): $\delta$ = 8.14, 7.96 (br, 1H, N−H), 2.03 (q, 4H, CH$_2$, $^3J$ = 7.42,), 1.74 (s, 15H, Cp*−CH$_3$), 0.88 (t, 6H, $^3J$ = 7.42, CH$_3$,).

**<sup>13</sup>C-NMR** (100.53 MHz, CDCl$_3$):  $\delta$ = 173.48, 172.03, 151.78, 148.03 (Hdebarb−CO), 88.92 (s, Cp*−Cq), 59.13, 58.13 (s, CEt$_2$), 32.10 (s, CH$_2$), 9.93 (s, CH$_3$), 9.36 (s, Cp*−CH$_3$).

**MS(FAB$^+$):**  *m/z* (%) = 511 (39) [M$^+$ −Cl, $^{193}$Ir], 509 (22) [M$^+$ −Cl, $^{191}$Ir], 363 (8.5) [IrCp*Cl$^+$] .

**IR** (KBr) [cm$^{-1}$]:  $\tilde{\nu}$ = 3192 (w), 3098 (w), 2968 (w), 2940 (w), 2876 (vw), 1707 (s), 1679 (s), 1591(w), 1525 (m), 1456 (w), 1387 (m), 1343 (w), 1312 (s), 1268 (m), 1184 (w), 1080 (w), 1034 (m), 948 (vw), 803 (w), 757 (vw), 645 (w), 494 (w).

**IR** (CHCl$_3$) [cm$^{-1}$]:  $\tilde{\nu}$ = 3386 (w), 2922 (w), 2878 (w), 1701 (s), 1636 (m), 1525 (w), 1504 (w), 1458 (w), 1382 (m), 1341 (w), 1313 (m), 1251 (m), 1080 (vw), 1031 (w), 955 (vw), 813 (vw), 639 (vw).

**Elemental Analysis**:

(C$_{18}$H$_{26}$ClN$_2$O$_3$Ir)

| | | | |
|---|---|---|---|
| Calculated (%): | C: 39.59 | H: 4.80 | N: 5.13. |
| Found     (%): | C: 36.98 | H: 4.67 | N: 4.09. |

Despite repeated attempts no better and reproducible C values were obtained.

### 3.2.11 Bis-(5,5-diethylbarbiturato-*N,O*)-(5,5-diethylbarbiturato-*N*)-($\eta^6$-*p*-isopropyl(methyl)benzene)-ruthenium(II) (16)



A solution of {(*p*-cymene)RuCl$_2$}$_2$ (42.9 mg, 0.07 mmol) in CHCl$_3$ (5 mL) was heated at 50°C for 15 min. To this solution NaHdebarb (57.7 mg, 0.28 mmol) was added followed by MeOH (10 mL) and the heating was continued for 5 hours. Then the reaction mixture was allowed to cool down to room temperature stirred for 2 days. During the period the solution colour changed from orange-red to light orange. The solvent was removed under reduced pressure and the residue was dissolved in CH$_2$Cl$_2$. After removal of suspended NaCl by centrifugation and separation of the solution by decantation, the solution was evaporated.
The residue was washed with 5 mL of water and then dried to eliminate excess Hdebarb from the product.

| | |
|---|---|
| **M**(C$_{26}$H$_{36}$N$_4$O$_6$Ru): | 453.93 g/mol. |
| **M**(C$_{26}$H$_{36}$N$_4$O$_6$Ru.C$_8$H$_{12}$N$_2$O$_3$): | 785.85 g/mol. |

**Yield**: 34.2 mg (0.057 mmol, 40.6 %), orange powder.

**Melting Point**: 190 °C (decomp).

**$^1$H-NMR** (399.78 MHz, CDCl$_3$): $\delta = 8.4$ (br, 2H, NH), 5.75 (d, $^3J_{H-H} = 5.7$ Hz, 2H, Ar$_{p\text{-cym}}$), 5.65 (d, $^3J_{H-H} = 5.5$ Hz, 2H, Ar$_{p\text{-cym}}$), 2.94 (sept, $^3J_{H-H} = 6.9$ Hz, 1H, CH(CH$_3$)$_2$), 2.25 (s, 3H, *p*-cym CH$_3$), 1.85 (br, 8H, Hdebarb-CH$_2$), 1.32 (d, $^3J_{H-H} =$

6.8 Hz, 6H, CH(CH$_3$)$_2$), 0.83 (m, 9H, Hdebarb-CH$_3$), 0.53 (t, $^3J$ = 7.4 Hz, 3H, Hdebarb-CH$_3$).

**$^{13}$C-NMR** (100.53 MHz, CDCl$_3$):   $\delta$ = 174.1, 172.8, 154.9 (s, CO), 103.0, 95.8 (s, Ar$_{p\text{-}}$$_{cym}$-Cq), 78.4, 78.1 (s, Ar$_{p\text{-cym}}$-$C$H), 57.5, 57.4 (s, $C$Et$_2$), 31.5, 31.3 (s, Hdebarb-CH$_2$), 29.6 (s, $C$H(CH$_3$)$_2$), 22.2 (s, CH($C$H$_3$)$_2$), 19.1 (s, 3H, $p$-cym CH$_3$), 9.6, 9.4 (s, Hdebarb-CH$_3$).
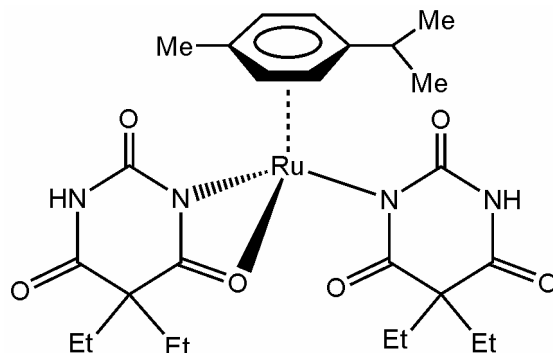
**MS**(FAB$^+$):   $m/z$ (%) = 418 (80) [MH$^{2+}$ −Hdebarb].

**IR** (KBr) [cm$^{-1}$]:   $\tilde{\nu}$ = 3191 (w), 3076 (w), 2966 (m), 2935 (w), 2877 (w), 1714 (vs), 1685 (sh), 1627 (s), 1496 (vs), 1458 (w), 1429 (m), 1381 (w), 1312 (m), 1253 (m), 1184 (vw), 1036 (w), 949 (w), 869 (w), 802 (m), 532 (vw), 493 (w), 401 (w).

**IR** (CHCl$_3$) [cm$^{-1}$]:   $\tilde{\nu}$ = 3387 (w), 2941 (w), 2880 (w), 2833 (w), 1717 (sh), 1700 (s), 1629 (s), 1496 (s), 1458 (w), 1444 (w), 1383 (m), 1311 (m), 1254 (w), 1089 (vw), 1038 (vw), 949 (vw), 869 (w), 643 (w).

**Elemental Analysis**:
(C$_{26}$H$_{36}$N$_4$O$_6$Ru)

| | | | |
|---|---|---|---|
| Calculated (%): | C: 51.89 | H: 6.04 | N: 9.31. |
| Found      (%): | C: 50.05 | H: 6.14 | N: 8.04. |

### 3.2.12  Chlorido-($\eta^6$-*p*-isopropyl(methyl)benzene)-(5,5-diethylbarbiturato-*N,O*)-ruthenium(II) (17)
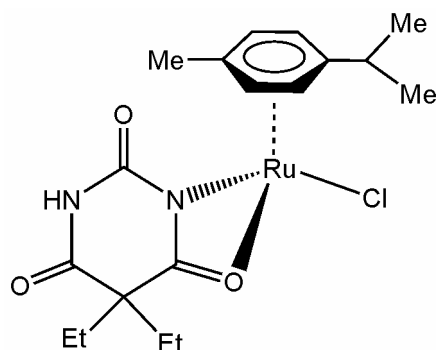


A solution of {(*p*-cymene)RuCl$_2$}$_2$ (44.1 mg, 0.072 mmol) in CHCl$_3$ (5 mL) was heated at 50 °C for 15 min. To this solution NaHdebarb (29.6 mg, 0.144 mmol) was added followed by MeOH (10 mL) and the heating was continued for 5 hours. Then the reaction mixture was allowed to cool down to room temperature and stirred for 2 days. During the period the solution colour changed from orange-red to light orange. The solvent was removed under reduced pressure and the residue was dissolved in CH$_2$Cl$_2$. After removal of suspended NaCl by centrifugation and separation of the solution by decantation, the solution was evaporated. The residue was purified by crystallization.

| | |
|---|---|
| **M**(C$_{64}$H$_{54}$ClN$_4$P$_2$Rh): | 453.93 g/mol. |
| **Yield**: | 33.1 mg (0.073 mmol, 50.7 %), orange powder. |
| **Melting Point**: | 180 °C (decomp). |
| **$^1$H-NMR** (270.16 MHz, CDCl$_3$): | $\delta$ = 7.9 (br, 1H, NH), 5.71 (d, $^3J$ = 7.4 Hz, 1H, Ar$_{p\text{-cym}}$), 5.64 (t, $^3J$ = 5.3 Hz, 2H, Ar$_{p\text{-cym}}$), 5.56 (d, $^3J$ = 6.4 Hz, 1H, Ar$_{p\text{-cym}}$), 2.96 (sept, $^3J$ = 6.8 and 7.1 Hz, 1H, CH(CH$_3$)$_2$), 2.28 (s, 3H, *p*-cym CH$_3$), 1.82 (m, 4H, Hdebarb-CH$_2$), 1.35 (d, $^3J_{\text{H-H}}$ = 6.8 Hz, 3H, CH(CH$_3$)$_2$), 1.30 (d, $^3J$ = 7.1 Hz, 3H, CH(CH$_3$)$_2$), 0.77 (m, 6H, Hdebarb-CH$_3$). |

**$^{13}$C-NMR** (67.93 MHz, CDCl$_3$):  $\delta$ = 173.16, 152.9 (s, CO), 101.1, 94.4 (s, Ar$_{p\text{-cym}}$-Cq), 79.3, 79.0, 78.6, 78.1 (s, Ar$_{p\text{-cym}}$-*C*H), 57.8 (s, *C*Et$_2$), 32.1, 31.6 (s, CH$_2$-Hdebarb), 30.9 (s, *C*H(CH$_3$)$_2$), 22.5, 22.4 (s, CH(*C*H$_3$)$_2$), 19.2 (s, *p*-cym CH$_3$), 9.9, 9.2 (s, Hdebarb-CH$_3$).

**MS(FAB$^+$):**  *m/z* (%) = 1041 (1.4) [M$^+$ −3H −Cl], 779 (3.8) [M$^+$ −3H −Cl −PPh$_3$], 573 (16) [Rh(H$_2$BDI)(PPh$_3$)]$^+$.

**IR** (CHCl$_3$) [cm$^{-1}$]:  $\tilde{\nu}$ = 3385 (m), 2941 (w), 2880 (w), 2839 (vw), 1701 (vs), 1630 (m), 1582 (w), 1565 (w), 1517 (m), 1492 (vs), 1460 (vw), 1442 (w), 1389 (m), 1342 (m), 1313 (s), 1250 (m), 1089 (w), 1057 (w), 1016 (m), 956 (vw), 873 (m), 804 (m), 643 (w), 572 (vw).

**Elemental Analysis**:

| | | | |
|---|---|---|---|
| Calculated (%): | C: 47.62 | H: 5.56 | N: 6.16. |
| Found      (%): | C: 46.91 | H: 5.48 | N: 6.37. |

### 3.2.13  *trans*-[bis{(benzildiiminato-*N,N´*)(triphenylphosphine)} rhodium(III)]-chloride (18)
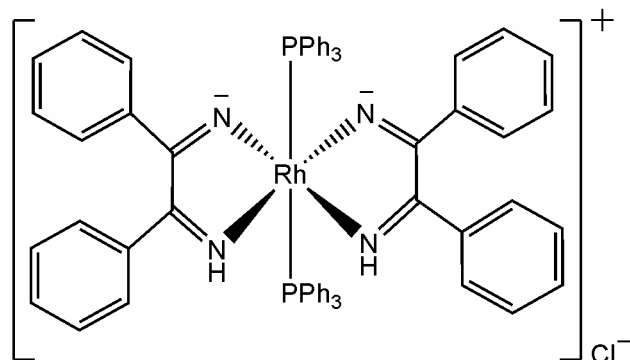


A solution of $(PPh_3)_2Rh(CO)Cl$ (51.8 mg, 0.075 mmol) in 10 mL of dichloromethane was added to a dichloromethane solution (10 mL) of $Si_2BDI$ (**1**) (52.8 mg, 0.15 mmol). The resulting yellow mixture was heated at 45 °C for 30 min forming a clear yellow solution which was allowed to cool down to room temperature and stirred continued for 1 day at room temperature. Then the solution colour changed from yellow to reddish brown. The solvent was removed in vacuo. The solid product was washed with pentane and dried under vacuum.

| | |
|---|---|
| **M**($C_{64}H_{52}ClN_4P_2Rh$): | 1077.39 g/mol. |
| **Yield**: | 40 mg (0.037 mmol, 49.3 %), reddish brown powder. |
| **Melting Point**: | 240 °C (decomp.). |
| **$^1$H-NMR** (270.17 MHz, $CD_2Cl_2$): | $\delta$ = 12.94 (br, 2H, N–H), 7.89−7.81 (m, 12H, Rh−Ph), 7.24−7.19 (m, 18H, Rh−Ph), 7.17−5.99 (m, 20H, $H_2BDI$−Ph). |
| **$^{13}$C-NMR** (67.93 MHz, $CD_2Cl_2$): | $\delta$ = 172.37 (d, $^2J_{Rh-C}$ = 51.9 Hz, C=N), 135.51 (t, $^nJ$= 5.2 Hz, $PPh_3$−CH), 131.89 (br, $PPh_3$−CH), 129.95 (s, $PPh_3$−CH), 128.13 (t, $^nJ$= 5.2 Hz, $PPh_3$−CH), 134.93−126.88 ($H_2BDI$−CH). |

**$^{31}$P-NMR** (109.36 MHz, CD$_2$Cl$_2$):  $\delta$ = 31.1 (d, $^1J_{\text{Rh–P}}$ =118.5 Hz, PPh$_3$)

**MS**(FAB$^+$):  *m/z* (%) = 1041 (1.4) [M$^+$ −Cl], 779 (3.8) [M$^+$ −Cl −PPh$_3$], 573 (16) [Rh(H$_2$BDI)(PPh$_3$)]$^+$.

**IR** (KBr) [cm$^{-1}$]:  $\tilde{\nu}$ = 3049 (w), 1589 (w), 1571 (w), 1482 (s), 1432 (s), 1226 (m), 1190 (vw), 1096 (m), 1071 (w), 961 (vw), 938 (m), 789 (m), 769 (m) 745 (m), 735 (m), 692 (vs), 522 (s), 512 (m), 491 (w).

**Elemental Analysis**:

| | | | |
|---|---|---|---|
| Calculated (%): | C: 71.34 | H: 4.87 | N: 5.20. |
| Found     (%): | C: 70.31 | H: 4.63 | N: 4.80. |

### 3.2.14  [Carbonyl-(benzildiimine-*N,N´*)-bis(triphenylphosphine)-iridium(I)]-chloride (19)
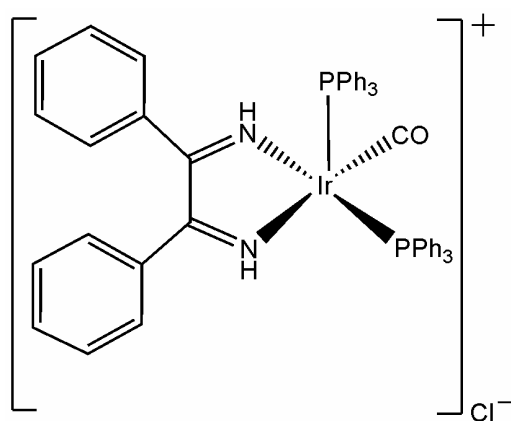


A solution of (PPh$_3$)$_2$Ir(CO)Cl (195 mg, 0.25 mmol) in benzene (15 mL) was added to a benzene solution (5 mL) of Si$_2$BDI (88.16 mg, 0.25 mmol). After 30 min the solution color changed from yellow to reddish–brown. The resulting solution was stirred at room temperature for 2 days. The solvent was then removed under reduced pressure and the resulting residue was washed with pentane (20 mL) and dried under vacuum.

**M**($C_{51}H_{42}IrN_2OP_2Cl \cdot CH_2Cl_2$):    1073.40 g/mol.

**M**($C_{51}H_{42}IrN_2OP_2Cl$):    988.48 g/mol.

**Yield**:    75 mg (0.076 mmol, 30.4 %), light red powder.

**Melting Point**:    175 °C (decomp.).

**¹H-NMR** (270.16 MHz, $CD_2Cl_2$):    $\delta$ = 12.11 (br, 2H, NH), 7.97−6.75 (m, 40H, CH−Ph).

**¹³C-NMR** (67.93 MHz, $CD_2Cl_2$):    $\delta$ = 135.34−126.70 (m, CH−Ph).

**³¹P-NMR** (109.36 MHz, $CD_2Cl_2$):    $\delta$ = 28.5 (s, $PPh_3$).

**MS**($FAB^+$):    $m/z$ (%) = 922 (1.6) [$M^+$ −2H −CO −Cl], 660 (6) [$M^+$ −2H −CO −Cl −$PPh_3$], 400 (10) [$M^+$ −2H −CO −Cl − $2PPh_3$].

**IR** (KBr) [$cm^{-1}$]:    $\tilde{\nu}$ = 3053 (m), 2957 (w), 2925 (w), 1962, 1597 (m), 1571 (w), 1483 (s), 1435 (vs), 1384 (w), 1188 (s), 1118 (s), 1094 (vs), 1072 (w),1027 (m), 998 (m), 942 (w), 790 (w), 747 (s), 721 (m), 693 (vs), 540 (s), 522 (s), 515 (sh), 458 (w).

**Elemental Analysis**:

| | | | |
|---|---|---|---|
| Calculated (%): | C: 58.18 | H: 4.14 | N: 2.61 |
| Found     (%): | C: 59.05 | H: 4.51 | N: 2.68 |

### 3.2.15 [Tris(benzildiimine-*N,N´*)-iron(II)]bis(trifluoromethylsulfonate) (20)
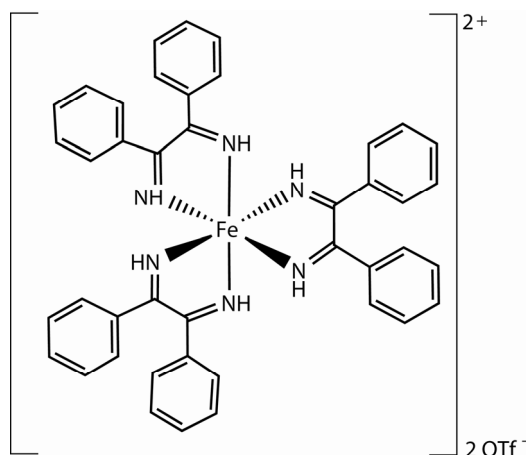


A solution of CpFe(CO)$_2$Cl (21.2 mg, 0.1 mmol ) in CH$_2$Cl$_2$ (10 mL) was treated with AgOTf (51.3 mg, 0.2 mmol) at room temperature and stirred for 1 hour until the AgCl had precipitated. After centrifugation and separation of the solution by decantation, **4** (105.8 mg, 0.3 mmol) was added to the solution. On addition of Si$_2$BDI, the solution colour immediately changed from red to deep blue. The mixture was stirred at room temperature for 1 day and the solvent was removed in vacuo. The deep blue solid was washed with n-pentane and was dried in vacuo for several hours.

**M**(C$_{44}$H$_{36}$F$_6$FeN$_6$O$_6$S$_2$):            978.76 g/mol.

**Yield**:            49.9 mg (0.051 mmol, 51 %), deep blue powder.

**Melting Point**:            250 °C.

**$^1$H-NMR** (399.78 MHz, CD$_2$Cl$_2$):    $\delta$ = 12.12 (s, 6H, NH), 7.52−7.37 (m, 30H, Ph−CH).

**$^{13}$C-NMR** (100.53 MHz, CD$_2$Cl$_2$):    $\delta$ = 178.76 (s, C=N), 134.70, 131.80, 128.77, 128.72 (s, Ph−CH).

**MS**(FAB⁺):  *m/z* (%) = 829 (3.8) [M²⁺ −OTf], 680 (1.2) [M²⁺ −2OTf], 472 (6.9) [M²⁺ −2OTf −H₂BDI].

**IR** (KBr) [cm⁻¹]:  $\tilde{\nu}$ = 3184 (m), 3064 (vw), 1599 (w), 1579 (w), 1492 (w), 1445 (m), 1392 (vs), 1259 (vs), 1166 (s), 1027 (vs), 1000 (vw), 935 (vw), 789 (vw), 765 (s), 745 (m), 699 (s), 639 (s), 594 (m), 575 (w), 533 (s), 516 (w).

**Elemental Analysis**:

| | | | |
|---|---|---|---|
| Calculated (%): | C: 53.99 | H: 3.71 | N: 8.59. |
| Found (%): | C: 53.97 | H: 3.89 | N: 7.91. |

## 3.2.16 Tris(benzildiimine-*N,N´*)-iron(II)-dichloride (21)
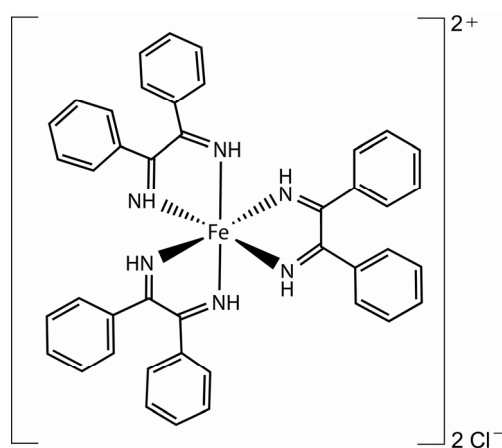


A solution of **4** (137.2 mg, 0.388 mmol) in 5 mL CH₂Cl₂ was added to a stirred suspension of anhydrous FeCl₂ (16.4 mg, 0.129 mmol) in 5 mL of CH₂Cl₂ at room temperature. After the reaction mixture was stirred for 2 day, the yellow colour solution changed to ink blue. The solvent was removed in vacuo to leave an ink blue solid. Crystals were grown by slow diffusion of *n*-pentane into a CH₂Cl₂ solution of the blue solid were not suitable for X-ray analysis. The elemental analysis fits if the calculated values include two CH₂Cl₂ molecules.

| | |
|---|---|
| **M**($C_{42}H_{36}Cl_2FeN_6$): | 751.52 g/mol. |
| **M**($C_{42}H_{36}Cl_2FeN_6 \cdot 2\ CH_2Cl_2$): | 836.45 g/mol. |

**Yield**:  55.6 mg (0.074 mmol, 57.3 %), ink blue powder.

**Melting Point**:  240 °C.

**$^1$H-NMR** (400.18 MHz, $CD_2Cl_2$):  13.23 (s, 6H, NH), 7.58−7.36 (m, 30H, Ph−CH).

**$^{13}$C-NMR** (100.63 MHz, $CD_2Cl_2$):  $\delta$ = 175.33 (s, CN), 134.62, 131.34, 128.69, 128.63 (s, Ph−CH).

**MS**(FAB$^+$):  $m/z$ (%) = 715 (3.1) [M$^{2+}$ −Cl −H], 679 (10.1) [M$^{2+}$ −2Cl −H], 472 (22.1), [M$^{2+}$ −2Cl −H$_2$BDI], 265 (8.2) [Fe$^{2+}$H$_2$BDI +H], 209 (7.2) [H$_2$BDI+H].

**IR** (KBr) [cm$^{-1}$]:  $\tilde{\nu}$ = 3060 (vw), 1597 (vw), 1490 (sh), 1444 (m), 1391 (vs), 1328 (sh), 1238 (m), 1020 (m), 931 (vw), 788 (w), 766 (m), 698 (s), 592 (w), 532 (s), 381(vw).

**Elemental Analysis**:

| | | | |
|---|---|---|---|
| Calculated (%): | C: 57.36 | H: 4.38 | N: 9.12. |
| Found      (%): | C: 56.86 | H: 4.57 | N: 9.02. |

## 3.2.17 [Bis(benzildiimine-*N,N´*)-*η*$^5$-cyclopentadienyl-chromium(III)] bis(trifluoromethylsulfonate) (22)
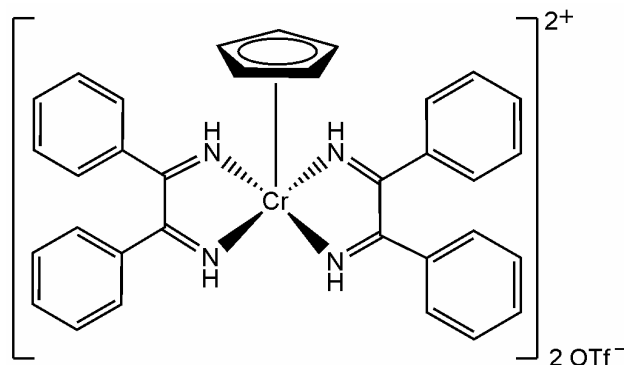


A solution of CpCr(NO)$_2$Cl (31.8 mg, 0.15 mmol) in CH$_2$Cl$_2$ (10 mL) was treated with AgOTf (96.3 mg, 0.38 mmol) at room temperature and stirred for 1 hour until the AgCl had precipitated. After centrifugation and separation of the solution by decantation, **4** (105.8 mg, 0.3 mmol) was added to the solution. The solution was stirred at room temperature for 1 day and the solvent was removed in vacuo. The reddish-brown solid was washed with n-pentane (15 mL) and dried in vacuo for several hours.

| | |
|---|---|
| **M**(C$_{35}$H$_{29}$CrF$_6$N$_4$O$_6$S$_2$.CH$_2$Cl$_2$): | 916.68 g/mol. |
| **M**(C$_{35}$H$_{29}$CrF$_6$N$_4$O$_6$S$_2$): | 832.65 g/mol. |

**Yield**:          40 mg (0.048 mmol, 32 %), reddish brown powder.

**Melting Point**:          217 °C (decomp.).

**$^1$H-NMR** (399.78 MHz, CD$_2$Cl$_2$):    $\delta$ = 12.13 (s, 4H, NH), 7.67−7.20 (m, 20H, Ph−CH), 5.79 (s, Cp−CH).

**$^{13}$C-NMR** (100.53 MHz, CD$_2$Cl$_2$):    $\delta$ = 183.10 (s, C=N), 135.97−128.63 (m, Ph−CH), 103.24 (s, Cp−CH).

**MS**(FAB$^+$):          *m/z* (%) = 533 (0.7) [M$^+$ −2OTf], 403 (6) [M$^+$ −2OTf −C$_{10}$H$_{10}$], 327 (7) [M$^+$ −2OTf −(H$_2$BDI)].

**IR** (KBr) [cm$^{-1}$]:      $\tilde{\nu}$ = 3224 (w), 3065 (w), 2930 (w), 1596 (m), 1578 (w), 1544 (w), 1488 (w), 1449 (m), 1419 (w), 1282 (s), 1244 (vs), 1225 (sh), 1170 (s), 1029 (vs), 914 (w), 876 (w), 766 (m), 697 (s), 637 (s), 573 (w), 516 (m).

**Elemental Analysis**:

($C_{36}H_{31}Cl_2CrF_6N_4O_6S_2$)

| | | | |
|---|---|---|---|
| Calculated (%): | C: 47.16 | H: 3.41 | N: 6.11. |
| Found     (%): | C: 46.58 | H: 3.68 | N: 6.26. |

# 4 SUMMARY

The synthesis and characterisation of some new transition metal complexes of barbituric acid (**1**), 5,5-diethylbarbituric acid (**2**), sodium salt of diethylbarbituric acid (**3**) and benzildiimine (**5**) are presented in this dissertation. As metal centres act selected $d^n$-systems with n = 3, 6, 8 and 10, e.g. Cr(0/III), Re(I), Pd(II), Cu(I), Rh(I/III), Ir(I/III), Ru(II) and Fe(II) monomeric and dimeric metal complexes such as $CpCr(NO)_2Cl$, $CpFe(CO)_2Cl$, $Re(CO)_5Br$, $(PPh_3)Re(CO)_4Br$, $[PdCl_2(PPh_3)_2]$, $[(PPh_3)_2CuBH_4]$, $[RhCl(CO)(PPh_3)_2]$, $[IrCl(CO)(PPh_3)_2]$, $[RhCl_2Cp^*]_2$, $[IrCl_2Cp^*]_2$, $[RuCl_2(p\text{-cymene})]_2$, and $FeCl_2$ which were used to prepare the complexes **6-22**.
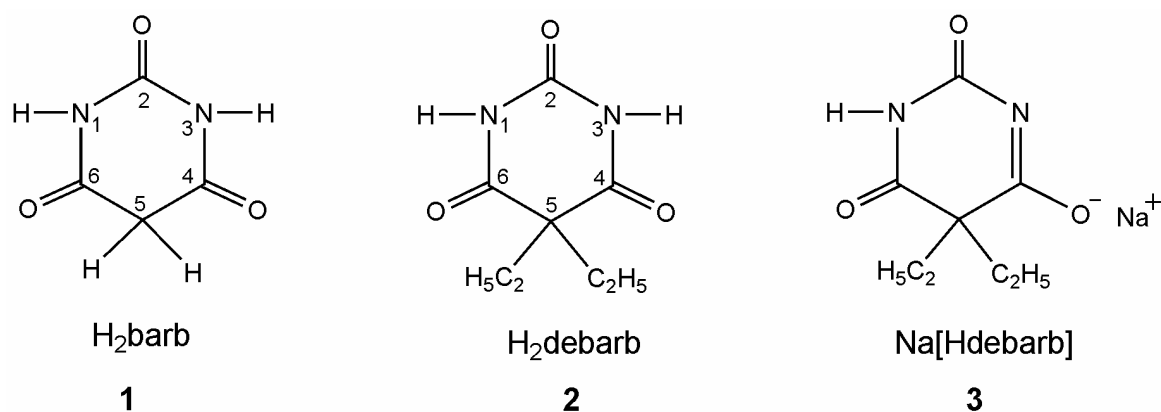


**Fig. I.** Barbiturate ligands used in this study.

All of the complexes were fully characterized by the IR, mass, $^1H$, $^{13}C$, $^{31}P$ NMR spectra and elemental analysis. In addition, except complex **21** their solid-state structures were determined by single crystal X-ray diffraction studies.

The addition of ($H_2$debarb) (**2**) to $CpCr(NO)_2Cl$, $Re(CO)_5Br$ or $(PPh_3)Re(CO)_4Br$ in the presence of triethylamine and AgOTf respectively, resulted the *mono*-barbiturato-*N* complexes $CpCr(NO)_2(Hdebarb)$ (**6**), $PPh_3Re(CO)_4(Hdebarb)$ (**7**) and $Re(CO)_5(Hdebarb)$ (**8**) (Fig II). The bis-barbiturato complex $\{(CO)_5Re\}_2(debarb)$ (**9**) with the double deprotonated barbiturate dianion formed when the metal complex to ligand molar ratio used was 2:1. AgOTf must be used additionally with rhenium metal complexes to cleave off bromide. The compounds isolated contain distorted pseudo tetrahedral (**6**) and octahedral (**7-9**) configurations around the metal centre.

**a)**
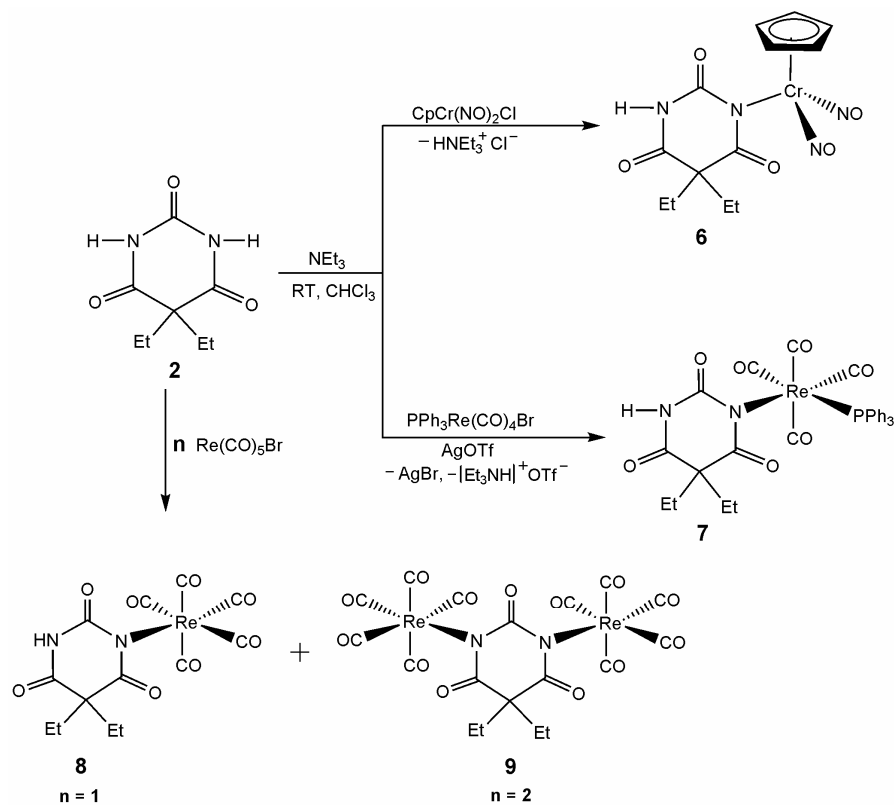


**b)**
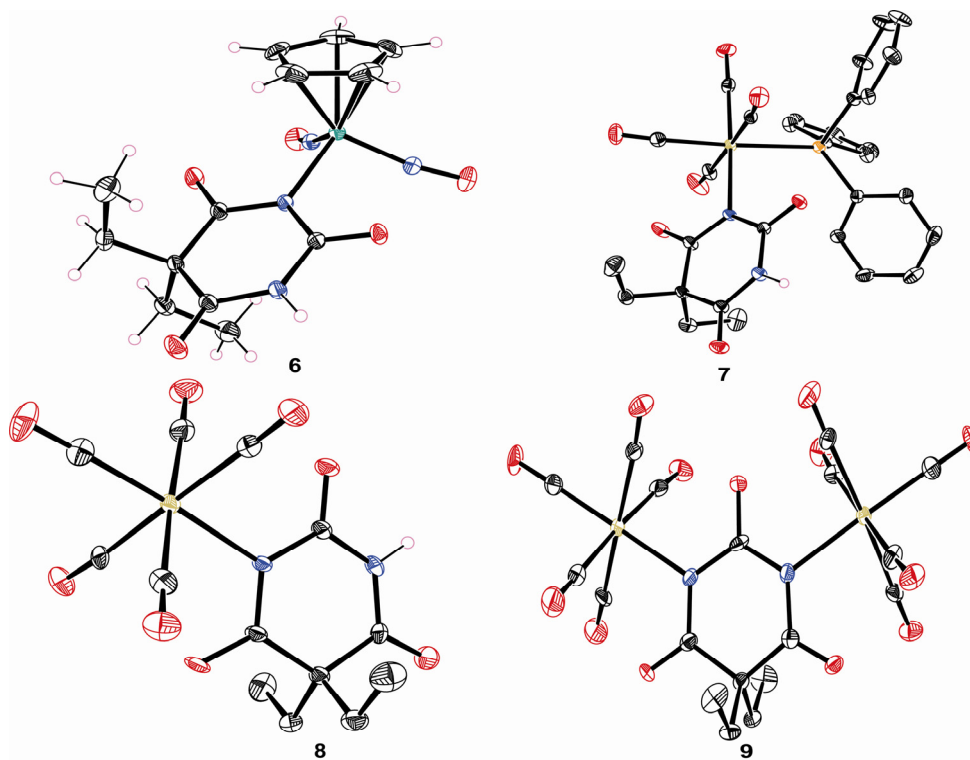


**Fig. II.** Reaction schemes (a) and molecular structures (b) of **6-9**.

119

Neutral *mono*-barbiturato-*N* complexes **10-13** were synthesized by the reactions of $H_2$debarb and $H_2$barb with the respective $(PPh_3)_2MX_2$ complexes (M = Pd (**10**, **11**), Cu (**12**) or Rh (**13**) and X = Cl (**10**, **11**), $BH_4$ (**12**) or CO and Cl (**13**)). **10**, **11** and **13** show slightly distorted square planar and **12** shows trigonal planar geometry around the metal centre (Fig III). In all these complexes metal atoms are coordinated to the deprotonated nitrogen atom of **1** and **2**. Deprotonated Hdebarb and Hbarb are generated in situ by the addition of $Et_3N$ (**12-13**) or NaOMe (**10-11**). To prepare complex **13** additionally AgOTf was added to eliminate Cl anion from $RhCl(CO)(PPh_3)_2$.

The reactions of the dinuclear complexes $[\{(\eta^5\text{-}C_5Me_5)MCl_2\}_2]$ (M = Rh, Ir) and $[\{(\eta^6\text{-}p\text{-}cymene)RuCl_2\}_2]$ with either two molar or four molar equivalents of Na[Hdebarb] (**3**) in $CHCl_3$/MeOH mixture afforded neutral complexes $[(\eta^5\text{-}C_5Me_5)Rh(Hdebarb)_2]$ (**14**), $[(\eta^5\text{-}C_5Me_5)IrCl(Hdebarb)]$ (**15**) (Fig. IV), and the arene ruthenium complexes $[(p\text{-}cymene)Ru(Hdebarb)_2]$ (**16**) and $[(p\text{-}cymene)RuCl(Hdebarb)]$ (**17**) (Fig. V). In complex **14** one molecule of Hdebarb is coordinated with Rh as *N,O*-chelate and the other molecule as monodentate *N*-ligand. But, in **15** only one chelating *N,O*-ligand is bonded with Ir.

**a)**
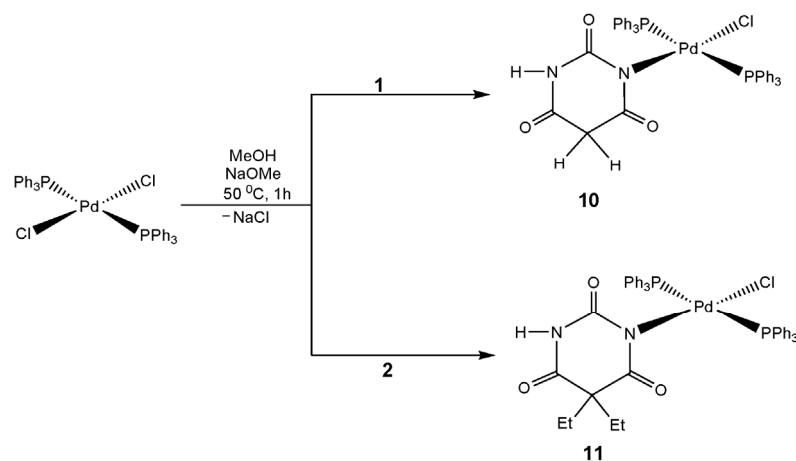


**b)**
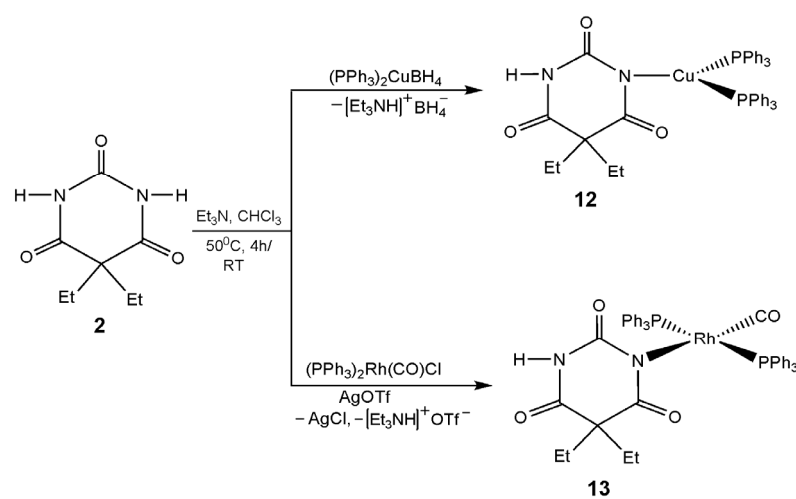


**c)**
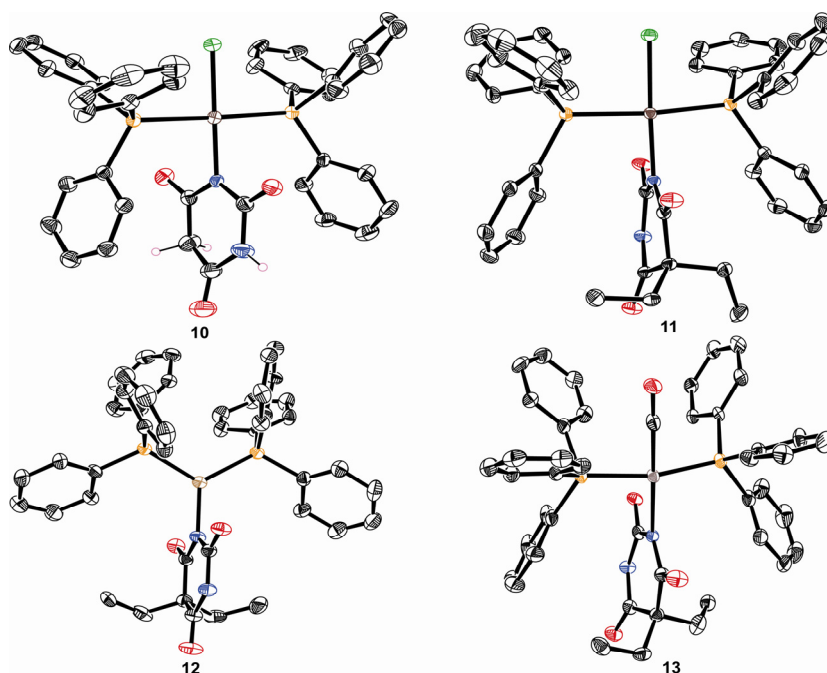


**Fig. III.** Reaction schemes (a, b) and molecular structures (c) of **10-13**.

121

**a)**
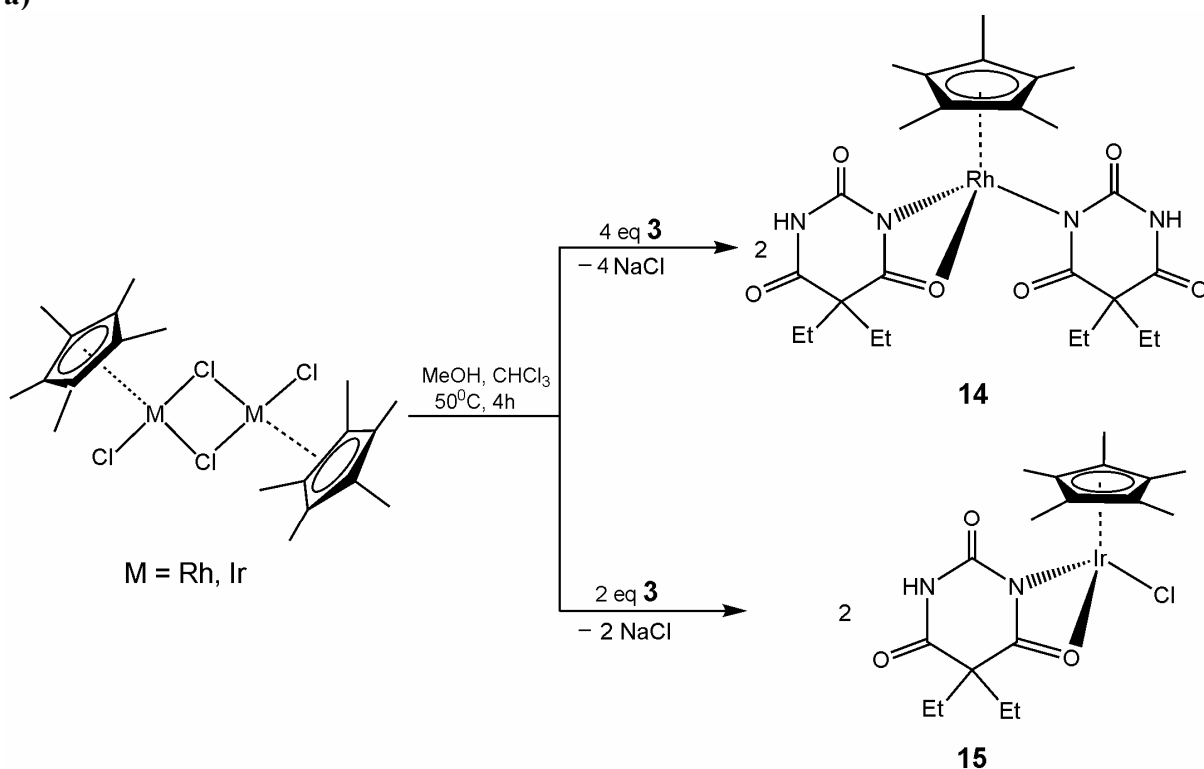


**b)**
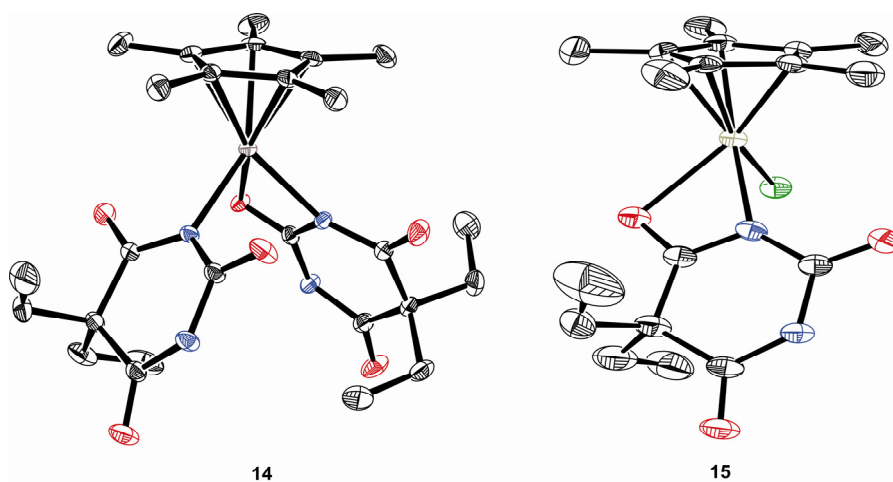


**Fig. IV:** Reaction scheme (a) and molecular structures (b) of **14** and **15**.

In the case of {($\eta^6$-arene)RuCl$_2$}$_2$ synthesis of two different types of complexes (**16**, **17**) using different molar ratios (1:1 and 1:2) of metal complex and **3** was successful. In one of the two complexes (**16**) the coordination mode is similar to complex **14** with one *N,O*- chelating and one *N*-bonded ligand and the coordination in the second complex **17** resembles to **15** with only one *N,O*-chelating ligand. Notably, the syntheses of the above mentioned complexes starting from H$_2$debarb were unsuccessful. Hdebarb anions were generated after the formation

of NaCl in the reaction mixture. All the complexes possess slightly distorted octahedral or piano stool coordination geometry around the metal centers.

**a)**
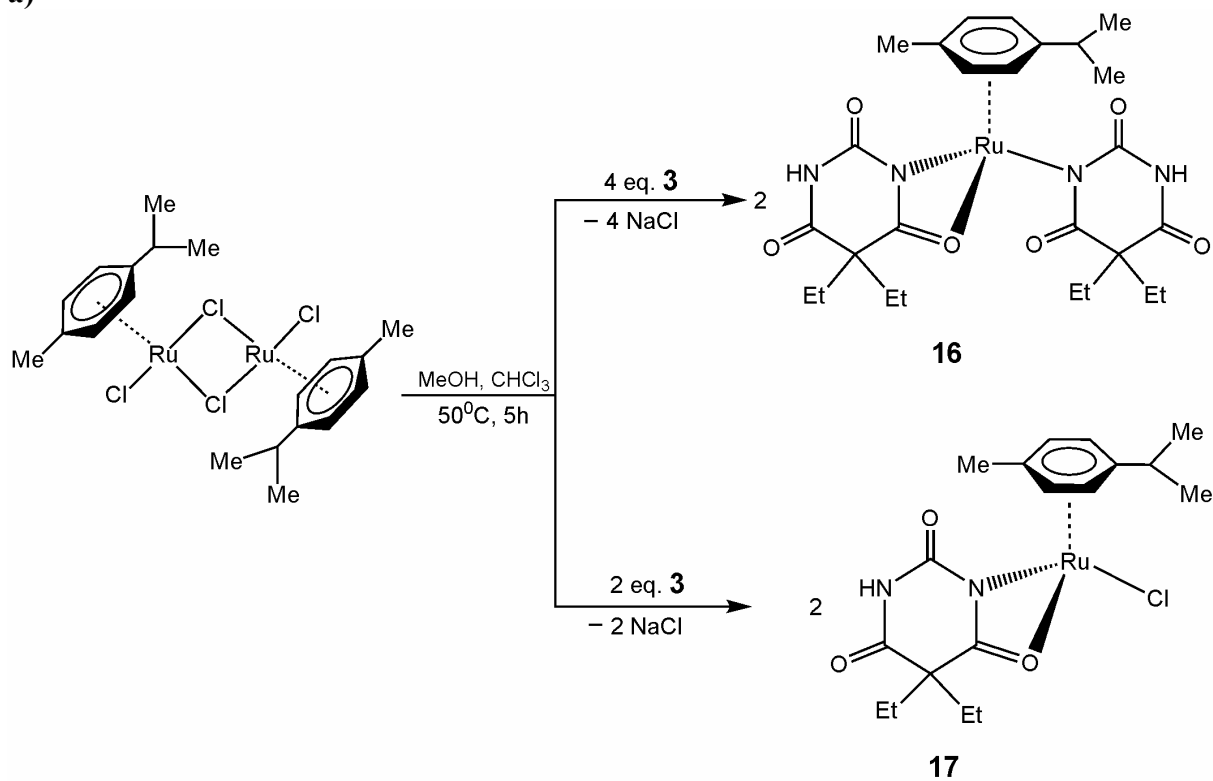


**b)**
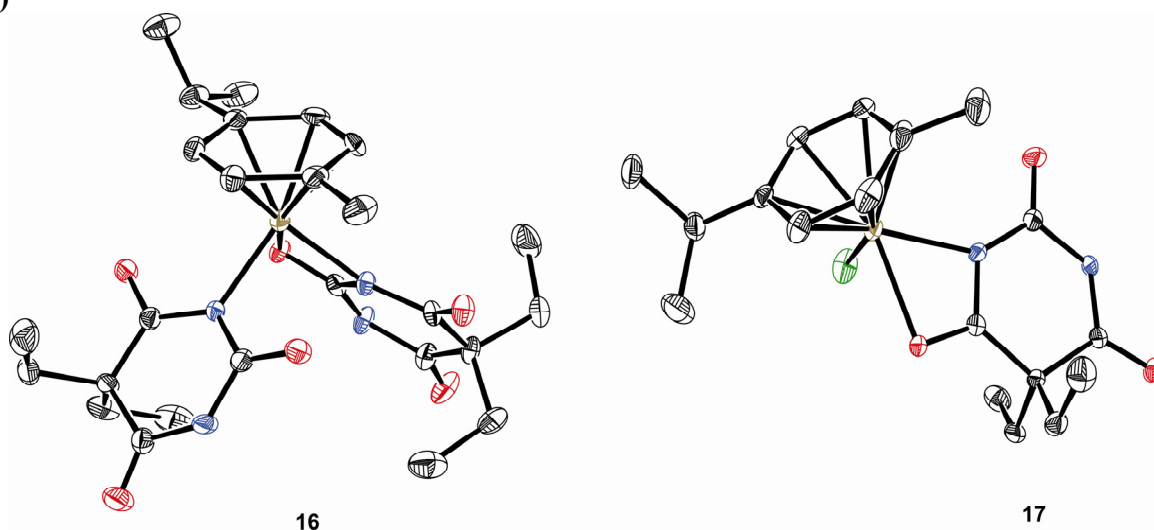


**Fig. V**: Reaction scheme (a) and molecular structures (b) of **16** and **17**.

$H_2$debarb and Hbarb ligands retain their planar structure while coordinated with the metals in all the complexes.

In the second part of this study the series of rhodium(III), iridium(I), Fe(II), and Cr(III) complexes containing one or two benzildiimine ligands (H$_2$BDI, **5**) derived from benzil-bis(trimethylsilyl) diimine (Si$_2$BDI, **4**) ligand have been prepared and characterized. The molecular structure of **4** is reported here for the first time. In all the reactions of **4** presented here, the two SiMe$_3$ groups were replaced by two H atoms in the complex as it was already reported in the literature. Probably traces of H$_2$O or CH$_2$Cl$_2$ initiated the cleavage of SiMe$_3$ in **4** and introduce the H atoms to the ligand to form the new ligand H$_2$BDI, **5**.
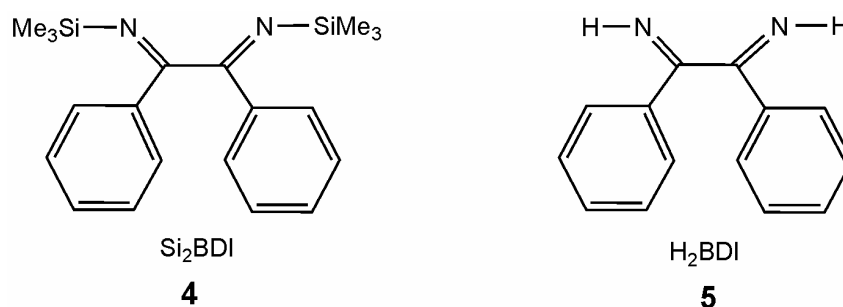


**Fig. VI.** Benzil-bis(trimethylsilyl)diimine (**4**) and Benzildiimine (**5**).

The reaction of *trans*-[RhCl(CO)(PPh$_3$)$_2$] with 2 molar equivalents of **4** afforded the cationic *bis*-HBDI rhodium complex **18** by the loss of CO, H$_2$ and the elimination of Cl$^-$ (Fig. VII). In contrast, the reactions between equivalent molars of **4** and *trans*-IrCl(CO)(PPh$_3$)$_2$ in benzene yielded the cationic *mono*-H$_2$BDI iridium complex **19** where CO remains coordinated to Ir(I) and Cl$^-$ is found as anion like complex **18** (Fig. VII). Their structures displayed distorted octahedral (**18**) and square pyramidal (**19**) configuration respectively around the cationic metal centre.

**a)**



**b)**
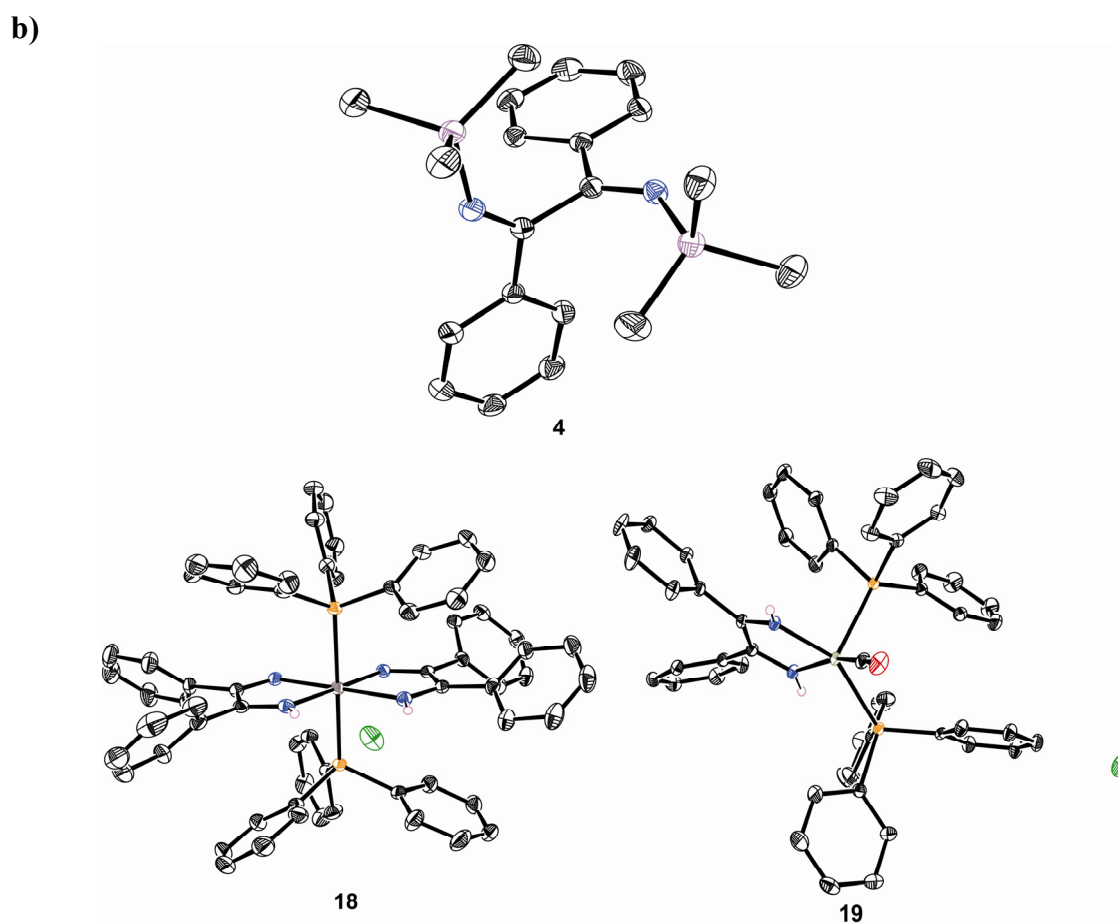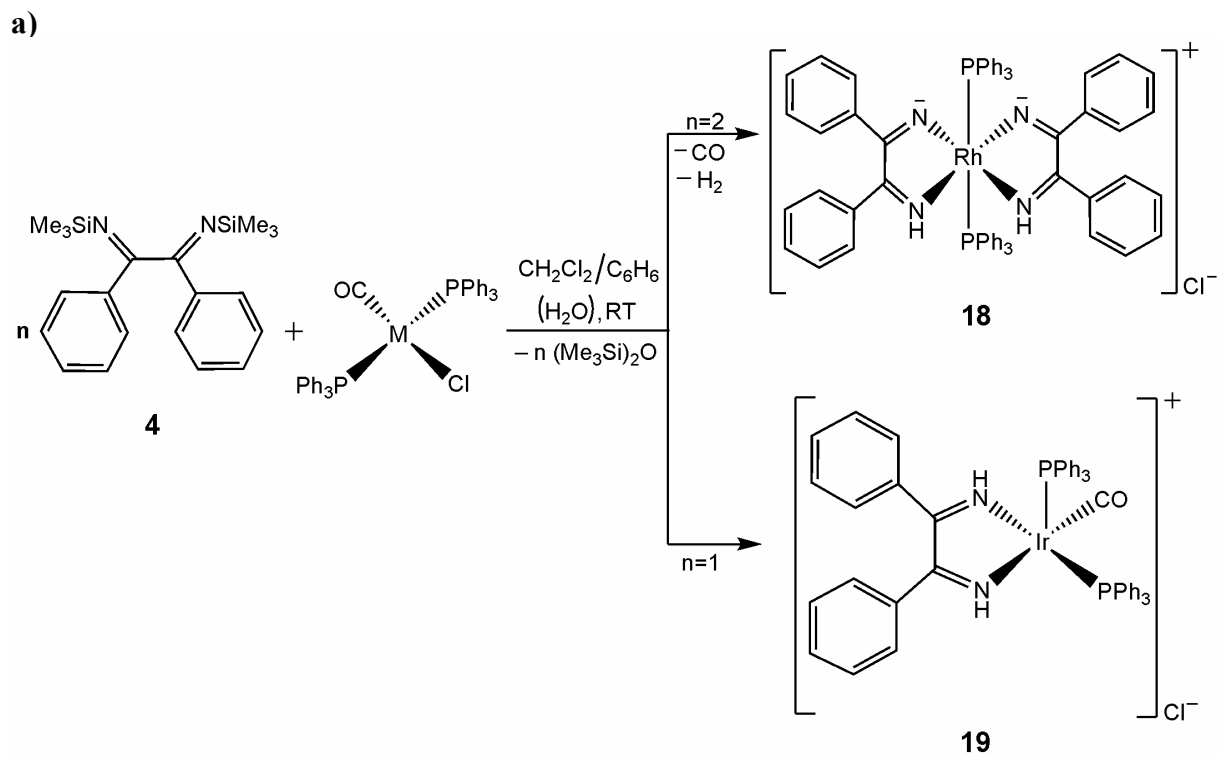


**Fig. VII.** Reaction scheme (a) and molecular structures (b) of **4**, **18** and **19**.

125

Treatment of CpFe(CO)$_2$Cl and CpCr(NO)$_2$Cl with **4** in 1:3 and 1:2 molar ratio, respectively, in the presence of excess AgOTf afforded surprisingly the complexes **20** and **22** (Fig. VIII). Without the addition of excess AgOTf no reactions were observed. Surprisingly, inspite of the mild reaction conditions CpFe(CO)$_2$Cl was totally decomposed and all former ligands were eliminated to form finally the cationic tris-chelate complex **20**.

**a)**



**b)**



**c)**
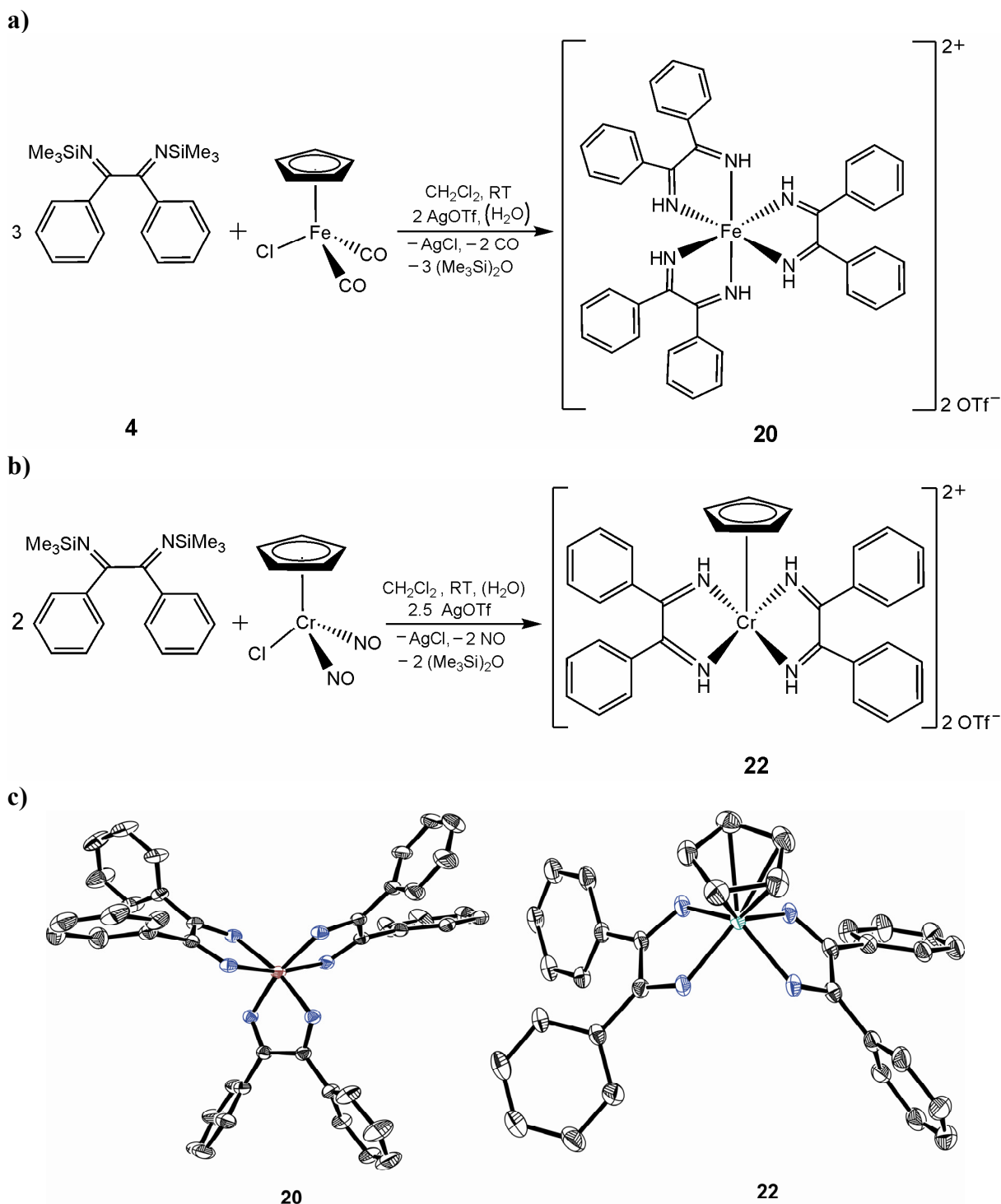


**Fig. VIII.** Reaction schemes (a, b) and molecular structures (c) of **20** and **22**.

126

Also in the case of **22** only the CpCr moiety from CpCr(NO)$_2$Cl remains intact and after elimination of both NO and the chloride ligands it is coordinated with two H$_2$BDI ligands. Probably the excess AgOTf not only initiated the cleavage of chloride anion in both complexes but also promoted the oxidation of Cr (Cr(0) to Cr(III)). Their molecular structures show a slightly distorted octahedral (**20**) and four-legged piano-stool (**22**) configuration at the metal centres.

Reaction of **4** (3 moles) with anhydrous FeCl$_2$ (1 mol) in CH$_2$Cl$_2$ without addition of any silver salt produces complex **21** which is almost similar to complex **20**. The only difference between complex **20** and **21** is the anion which is now chloride instead of triflate. The crystals grown by slow diffusion of *n*-pentane into a solution of **21** in CH$_2$Cl$_2$ were not suitable for X-ray analysis. Other attempts to crystallize this substance by diffusion of a non-polar solvent into a solution of **21** or by cooling of its solution were not successful. The complex, however was fully characterized by IR, mass, $^1$H and $^{13}$C NMR spectra and elemental analysis.

This study focused on the exploration of new transition metal complexes of barbituric acid, its diethyl derivatives and benzildiimine. Synthesis and characterization of similar transition metal complexes of other derivatives of barbituric acid can also be investigated in the near future. Furthermore, the study of the reactions of different types of Rh, Ir, Ru and Pd metal complexes with **1**-**5** can be undertaken to determine their coordination properties. Most importantly, investigation of the biological activity of the synthesized complexes in the present work would be an important set of data to determine the cytotoxicity and other relevant properties which can contribute to the development of new metal-based chemotherapeutic agents.

# 5 CRYSTALLOGRAPHIC APPENDIX

**Table 5.1** Crystal data and details of structural refinement for complexes **6** and **7**

| | 6 | 7 |
|---|---|---|
| Empirical formula | $C_{13}H_{16}CrN_4O_5$ | $C_{30}H_{26}N_2O_7PRe$ |
| Formula weight | 360.30 | 743.71 |
| Temperature [K] | 200(2) | 200(2) |
| Wavelength [Å] | 0.71073 | 0.71073 |
| Crystal system | triclinic | triclinic |
| Space group | *P*-1 | *P*-1 |
| *a*/Å | 8.0472(16) | 9.5486(19) |
| *b*/Å | 10.061(2) | 10.974(2) |
| *c*/Å | 10.825(2) | 13.998(3) |
| α/° | 63.84(3) | 92.29(3) |
| β/° | 85.62(3) | 91.41(3) |
| γ/° | 85.11(3) | 95.91(3) |
| *V*/Å$^3$ | 783.1(3) | 1457.0(5) |
| *Z* | 2 | 2 |
| calc. density/g cm$^{-3}$ | 1.5282(6) | 1.6953(6) |
| μ/mm$^{-1}$ | 0.761 | 4.274 |
| F(000) | 372 | 732 |
| Crystal size [mm$^3$] | 0.21 x 0.16 x 0.09 | 0.19 x 0.14 x 0.09 |
| θ range [°] | 3.23 to 27.52 | 3.26 to 27.48 |
| Index ranges | -10 ≤ h ≤ 10, | -12 ≤ h ≤ 12, |
| | -13 ≤ k ≤ 13, | -14 ≤ k ≤ 14, |
| | -14 ≤ l ≤ 14 | -18 ≤ l ≤ 18 |
| Reflections collected | 6812 | 8977 |
| Independent reflections | 3595 | 4648 |
| $R_{int}$ | 0.0234 | 0.0204 |
| Completeness to θ | 99.7 % | 99.7 % |
| Refinement method | Full-matrix least squares on $F^2$ | Full-matrix least squares on $F^2$ |
| Data / restraints / parameters | 3595 / 0 / 208 | 6652 / 0 / 370 |
| *S* on F$^2$ | 1.072 | 1.064 |
| Final R indices [I>2 σ (I)] | $R_1 = 0.0342$, $wR_2 = 0.0778$ | $R_1 = 0.0223$, $wR_2 = 0.0499$ |
| R indices (all data) | $R_1 = 0.0450$, $wR_2 = 0.0872$ | $R_1 = 0.0265$, $wR_2 = 0.0515$ |
| Largest difference peak/hole | 0.393 and -0.414 e.Å$^{-3}$ | 1.156 and -1.364 e.Å$^{-3}$ |
| Absolute structure parameter | - | - |

**Table 5.2** Crystal data and details of structural refinement for complexes **8** and **9**

| | 8 | 9 |
|---|---|---|
| Empirical formula | $C_{13}H_{11}N_2O_8Re$ | $C_{18}H_{10}N_2O_{13}Re_2$ |
| Formula weight | 509.45 | 834.70 |
| Temperature [K] | 200(2) | 200(2) |
| Wavelength [Å] | 0.71073 | 0.71073 |
| Crystal system | monoclinic | triclinic |
| Space group | $P2_1/c$ | $P1$ |
| $a$/Å | 12.468(3) | 7.0648(14) |
| $b$/Å | 6.7750(14) | 13.593(3) |
| $c$/Å | 20.018(4) | 14.288(3) |
| $\alpha$/° | 90 | 109.38(3) |
| $\beta$/° | 103.81(3) | 91.36(3) |
| $\gamma$/° | 90 | 98.92(3) |
| $V$/Å$^3$ | 1642.1(7) | 1274.5(5) |
| $Z$ | 4 | 2 |
| calc. density/g cm$^{-3}$ | 2.061(8) | 2.1749(7) |
| $\mu$/mm$^{-1}$ | 7.444 | 9.552 |
| F(000) | 967 | 772 |
| Crystal size [mm$^3$] | 0.30 x 0.25 x 0.22 | 0.25 x 0.09 x 0.06 |
| $\theta$ range [°] | 3.37 to 27.48 | 3.23 to 27.44 |
| Index ranges | $-16 \leq h \leq 16$, | $-9 \leq h \leq 9$, |
| | $-8 \leq k \leq 8$, | $-17 \leq k \leq 17$, |
| | $-25 \leq l \leq 25$ | $-18 \leq l \leq 18$ |
| Reflections collected | 12028 | 10571 |
| Independent reflections | 3743 | 10571 |
| $R_{int}$ | 0.0849 | 0.0000 |
| Completeness to $\theta$ | 99.4 % | 99.3 % |
| Refinement method | Full-matrix least squares on $F^2$ | Full-matrix least squares on $F^2$ |
| Data / restraints / parameters | 3743 / 0 / 217 | 10571 / 3 / 632 |
| $S$ on F$^2$ | 1.059 | 1.048 |
| Final R indices [I>2 σ (I)] | $R_1 = 0.0366$, $wR_2 = 0.0945$ | $R_1 = 0.0473$, $wR_2 = 0.1250$ |
| R indices (all data) | $R_1 = 0.0445$, $wR_2 = 0.0995$ | $R_1 = 0.0491$, $wR_2 = 0.1274$ |
| Largest difference peak/hole | 1.185 and -1.753 e.Å$^{-3}$ | 2.712 and -2.272 e.Å$^{-3}$ |
| Absolute structure parameter | - | 0.121(12) |

**Table 5.3** Crystal data and details of structural refinement for complexes **10** and **11**

| | **10** | **11** |
|---|---|---|
| Empirical formula | $C_{40}H_{33}ClN_2O_3P_2Pd$ | $C_{44}H_{41}ClN_2O_3P_2Pd$ |
| Formula weight | 793.47 | 849.58 |
| Temperature [K] | 200(2) | 200(2) |
| Wavelength [Å] | 0.71073 | 0.71073 |
| Crystal system | orthorhombic | monoclinic |
| Space group | *Pbca* | *P*2$_1$/*n* |
| *a*/Å | 12.0517(3) | 12.2439(2) |
| *b*/Å | 23.3292(5) | 17.6363(3) |
| *c*/Å | 25.1866(5) | 18.8963(3) |
| α/° | 90 | 90 |
| β/° | 90 | 103.5673(10) |
| γ/° | 90 | 90 |
| *V*/Å$^3$ | 7081.4(3) | 3966.55(11) |
| *Z* | 8 | 4 |
| calc. density/g cm$^{-3}$ | 1.489(6) | 1.42276(4) |
| μ/mm$^{-1}$ | 0.732 | 0.658 |
| F(000) | 3232 | 1744 |
| Crystal size [mm$^3$] | 0.10 × 0.09 × 0.09 | 0.22 × 0.22 × 0.05 |
| θ range [°] | 3.22 to 26.37 | 3.20 to 26.38 |
| Index ranges | -15 ≤ h ≤ 15, | -15 ≤ h ≤ 15, |
| | -29 ≤ k ≤ 27, | -20 ≤ k ≤ 22, |
| | -30 ≤ l ≤ 30 | -22 ≤ l ≤ 23 |
| Reflections collected | 43070 | 27540 |
| Independent reflections | 7205 | 8096 |
| R$_{int}$ | 0.0891 | 0.0338 |
| Completeness to θ | 99.7 | 99.7 |
| Refinement method | Full-matrix least squares on $F^2$ | Full-matrix least squares on $F^2$ |
| Data / restraints / parameters | 7205/ 0 / 443 | 8096 / 0 / 484 |
| *S* on F$^2$ | 1.052 | 1.046 |
| Final R indices [I>2 σ (I)] | R$_1$ = 0.0528, $w$R$_2$ = 0.1224 | R$_1$ = 0.0282, $w$R$_2$ = 0.0631 |
| R indices (all data) | R$_1$ = 0.1013, $w$R$_2$ = 0.1468 | R$_1$ = 0.0392, $w$R$_2$ = 0.0683 |
| Largest difference peak/hole | 2.161 and −0.864 e.Å$^{-3}$ | 0.481 and −0.534 e.Å$^{-3}$ |
| Absolute structure parameter | - | - |

**Table 5.4** Crystal data and details of structural refinement for complexes **12** and **13**

| | 12 | 13 |
|---|---|---|
| Empirical formula | $C_{44.75}H_{41.75}Cl_{2.25}CuN_2O_3P_2$ | $C_{46}H_{43}Cl_2N_2O_4P_2Rh$ |
| Formula weight | 860.79 | 923.57 |
| Temperature [K] | 200(2) | 200(2) |
| Wavelength [Å] | | 0.71073 |
| Crystal system | triclinic | triclinic |
| Space group | $P$-1 | $P$-1 |
| $a$/Å | 12.8298(5) | 12.26470(10) |
| $b$/Å | 18.8256(9) | 12.39940(10) |
| $c$/Å | 20.4567(9) | 28.5778(3) |
| $\alpha$/° | 102.114(2) | 84.1302(7) |
| $\beta$/° | 107.373(2) | 88.6380(7) |
| $\gamma$/° | 103.428(2) | 85.9100(7) |
| $V$/Å$^3$ | 4374.2(3) | 4311.58(7) |
| $Z$ | 4 | 4 |
| calc. density/g cm$^{-3}$ | 1.307(9) | 1.423 |
| $\mu$/mm$^{-1}$ | 0.750 | 0.639 |
| F(000) | 1782 | 1896 |
| Crystal size [mm$^3$] | $0.20 \times 0.16 \times 0.11$ | $0.19 \times 0.16 \times 0.11$ |
| $\theta$ range [°] | 3.14 to 24.11 | 3.15 to 25.35 |
| Index ranges | $-14 \leq h \leq 14$, | $-14 \leq h \leq 14$, |
| | $-21 \leq k \leq 21$, | $-14 \leq k \leq 14$, |
| | $-23 \leq l \leq 23$ | $-34 \leq l \leq 34$ |
| Reflections collected | 26227 | 30097 |
| Independent reflections | 8371 | 15726 |
| $R_{int}$ | 0.0583 | 0.0340 |
| Completeness to $\theta$ | 99.6 | 99.7 |
| Refinement method | Full-matrix least-squares on $F^2$ | Full-matrix least-squares on $F^2$ |
| Data / restraints / parameters | 8371 / 9 / 989 | 15726 / 4 / 1002 |
| $S$ on F$^2$ | 1.036 | 1.104 |
| Final R indices [I>2 σ (I)] | $R_1 = 0.0935$, $wR_2 = 0.2634$ | $R_1 = 0.0859$, $wR_2 = 0.2310$ |
| R indices (all data) | $R_1 = 0.1411$, $wR_2 = 0.3092$ | $R_1 = 0.1058$, $wR_2 = 0.2415$ |
| Largest difference peak/hole | 2.179 and -0.923 e.Å$^{-3}$ | 2.385 and -1.594 e.Å$^{-3}$ |
| Absolute structure parameter | - | - |

**Table 5.5** Crystal data and details of structural refinement for complexes **14** and **15**

| | 14 | 15 |
|---|---|---|
| Empirical formula | $C_{26}H_{37}N_4O_6Rh$ | $C_{44}H_{64}Cl_2Ir_2N_6O_9$ |
| Formula weight | 604.501 | 1276.353 |
| Temperature [K] | 195(2) | 95(2) |
| Wavelength [Å] | 0.71073 | 0.71073 |
| Crystal system | Monoclinic | Monoclinic |
| Space group | *C*2/*c* | *C*2/*c* |
| *a*/Å | 24.643(5) | 24.557(5) |
| *b*/Å | 12.147(2) | 8.8469(18 |
| *c*/Å | 18.299(4) | 22.628(5) |
| α/° | 90 | 90° |
| β/° | 97.19(3) | 100.72(3) |
| γ/° | 90 | 90 |
| *V*/Å$^3$ | 5434.4(19) | 4830.2(17) |
| *Z* | 8 | 4 |
| calc. density/g cm$^{-3}$ | 1.4777(5) | 1.7552(6) |
| μ/mm$^{-1}$ | 0.675 | 5.674 |
| F(000) | 2512 | 2520 |
| Crystal size [mm$^3$] | 0.14 x 0.12 x 0.06 | 0.16 x 0.14 x 0.09 |
| θ range [°] | 3.32 to 26.38 | 3.15 to 26.00 |
| Index ranges | -27<=h<=30, | -30<=h<=29, |
| | -15<=k<=15, | -10<=k<=10 |
| | -22<=l<=22 | 0<=l<=27 |
| Reflections collected | 18273 | 9137 |
| Independent reflections | 5536 | 4731 |
| R$_{int}$ | 0.0252 | 0.0320 |
| Completeness to θ | 99.7 % | 99.8 % |
| Refinement method | Full-matrix least-squares on $F^2$ | Full-matrix least-squares on $F^2$ |
| Data / restraints / parameters | 5536 / 0 / 347 | 4731 / 0 / 294 |
| *S* on F$^2$ | 1.117 | 1.060 |
| Final R indices [I>2 σ (I)] | R1 = 0.0308, *w*R2 = 0.0715 | R1 = 0.0281, *w*R2 = 0.0705 |
| R indices (all data) | R1 = 0.0379, *w*R2 = 0.0749 | R1 = 0.0368, *w*R2 = 0.0741 |
| Largest difference peak/hole | 0.696 and -0.903 e.Å$^{-3}$ | 1.206 and -1.316 |
| Absolute structure parameter | - | - |

**Table 5.6** Crystal data and details of structural refinement for complexes **16** and **17**

| | 16 | 17 |
|---|---|---|
| Empirical formula | $C_{34}H_{48}N_6O_9Ru$ | $C_{18}H_{25}ClN_2O_3Ru$ |
| Formula weight | 785.85 | 453.93 |
| Temperature [K] | 195(2) | 195(2) |
| Wavelength [Å] | 0.71073 | 0.71073 |
| Crystal system | Monoclinic | Triclinic |
| Space group | $P2_1/c$ | $P$-1 |
| $a$/Å | 13.870(3) | 7.1875(14) |
| $b$/Å | 26.646(5) | 12.265(3) |
| $c$/Å | 12.839(3) | 12.339(3) |
| $\alpha$/° | 90 | 103.91(3) |
| $\beta$/° | 112.90(3) | 103.43(3) |
| $\gamma$/° | 90 | 106.57(3) |
| $V$/Å$^3$ | 4371.1(19) | 957.6(5) |
| $Z$ | 4 | 2 |
| calc. density/g cm$^{-3}$ | 1.1942(4) | 1.5743(5) |
| $\mu$/mm$^{-1}$ | 0.409 | 0.977 |
| F(000) | 1640 | 464 |
| Crystal size [mm$^3$] | 0.12 x 0.05 x 0.03 | 0.19 x 0.12 x 0.05 |
| θ range [°] | 3.16 to 23.57 | 3.46 to 26.38 |
| Index ranges | -15<=h<=14, | -8<=h<=8, |
| | -29<=k<=29, | -15<=k<=15, |
| | 0<=l<=14 | -15<=l<=15 |
| Reflections collected | 12476 | 7432 |
| Independent reflections | 6467 | 3897 |
| $R_{int}$ | 0.0637 | 0.0213 |
| Completeness to θ | 99.0 % | 99.8 % |
| Refinement method | Full-matrix least-squares on $F^2$ | Full-matrix least-squares on $F^2$ |
| Data / restraints / parameters | 6467 / 0 / 451 | 3897 / 0 / 230 |
| $S$ on F$^2$ | 0.923 | 1.068 |
| Final R indices [I>2 σ (I)] | R1 = 0.0533, $w$R2 = 0.1090 | R1 = 0.0258, $w$R2 = 0.0607 |
| R indices (all data) | R1 = 0.0933, $w$R2 = 0.1196 | R1 = 0.0308, $w$R2 = 0.0631 |
| Largest difference peak/hole | 1.998 and -0.452 e.Å$^{-3}$ | 0.503 and -0.481 e.Å$^{-3}$ |
| Absolute structure parameter | - | - |

**Table 5.7** Crystal data and details of structural refinement for complexes **4** and **18**

| | 4 | 18 |
|---|---|---|
| Empirical formula | $C_{20}H_{28}N_2Si_2$ | $C_{66}H_{56}Cl_5N_4P_2Rh$ |
| Formula weight | 352.62 | 1247.29 |
| Temperature [K] | 200(2) | 195(2) |
| Wavelength [Å] | 0.71073 | 0.71073 |
| Crystal system | Triclinic | Monoclinic |
| Space group | $P$-1 | $P2_1/n$ |
| $a$/Å | 9.202(18) | 11.698(2) |
| $b$/Å | 10.195(2) | 30.177(6) |
| $c$/Å | 12.093(2) | 17.812(7) |
| $\alpha$/° | 82.22(3) | 90 |
| $\beta$/° | 85.44(3) | 108.33(3) |
| $\gamma$/° | 69.06(3) | 90 |
| $V$/Å$^3$ | 1049.2(4) | 5968.98(13) |
| $Z$ | 2 | 4 |
| calc. density/g cm$^{-3}$ | 1.1162(4) | 1.3879(6) |
| $\mu$/mm$^{-1}$ | 0.173 | 0.608 |
| F(000) | 380 | 2560 |
| Crystal size [mm$^3$] | 0.28 x 0.16 x 0.09 | 0.23 x 0.11 x 0.10 |
| $\theta$ range [°] | 3.27 to 26.00 | 3.15 to 26.00 |
| Index ranges | -11<=h<=11, | -14<=h<=14, |
| | -12<=k<=11, | -37<=k<=37, |
| | -14<=l<=14 | -21<=l<=21 |
| Reflections collected | 7694 | 23106 |
| Independent reflections | 4116 | 11706 |
| $R_{int}$ | 0.0197 | 0.0382 |
| Completeness to $\theta$ | 99.8 % | 99.8 % |
| Refinement method | Full-matrix least-squares on $F^2$ | Full-matrix least-squares on $F^2$ |
| Data / restraints / parameters | 4116 / 0 / 223 | 11706 / 0 / 747 |
| $S$ on F$^2$ | 1.047 | 1.028 |
| Final R indices [I>2 $\sigma$ (I)] | R1 = 0.0343, $w$R2 = 0.0894 | R1 = 0.0463, $w$R2 = 0.1106 |
| R indices (all data) | R1 = 0.0433, $w$R2 = 0.0947 | R1 = 0.0733, $w$R2 = 0.1234 |
| Largest difference peak/hole | 0.223 and -0.220 e.Å$^{-3}$ | 1.222 and -0.865 e.Å$^{-3}$ |
| Absolute structure parameter | ? | ? |

**Table 5.8** Crystal data and details of structural refinement for complexes **19** and **20**

|  | **19** | **20** |
|---|---|---|
| Empirical formula | $C_{105}H_{90}Cl_8Ir_2N_4O_2P_4$ | $C_{49}H_{48}F_6FeN_6O_6S_2$ |
| Formula weight | 2231.81 | 1050.91 |
| Temperature [K] | 195(2) | 200(2) |
| Wavelength [Å] | 0.71073 | 0.71073 |
| Crystal system | Triclinic | Trigonal |
| Space group | $P$-1 | $R$-3 |
| $a$/Å | 9.827(2) | 27.874(4) |
| $b$/Å | 13.190(3) | 27.874(4 |
| $c$/Å | 19.791(4) | 32.590(7) |
| $\alpha$/° | 86.22(3) | 90 |
| $\beta$/° | 84.70(3) | 90 |
| $\gamma$/° | 71.72(3) | 120 |
| $V$/Å$^3$ | 2423.6(10) | 21929(6) |
| $Z$ | 1 | 18 |
| calc. density/g cm$^{-3}$ | 1.5292(5) | 1.4324(4) |
| $\mu$/mm$^{-1}$ | 3.081 | 0.474 |
| F(000) | 1114 | 9792 |
| Crystal size [mm$^3$] | 0.12 x 0.10 x 0.06 | 0.30 x 0.25 x 0.19 |
| $\theta$ range [°] | 3.24 to 27.00 | 3.15 to 24.00 |
| Index ranges | -12<=h<=12, | -31<=h<=15 |
|  | -16<=k<=16, | 0<=k<=31 |
|  | -25<=l<=25 | -37<=l<=36 |
| Reflections collected | 21056 | 15199 |
| Independent reflections | 10576 | 7620 |
| $R_{int}$ | 0.0218 | 0.0192 |
| Completeness to $\theta$ | 99.8 % | 99.6 % |
| Refinement method | Full-matrix least-squares on $F^2$ | Full-matrix least-squares on $F^2$ |
| Data / restraints / parameters | 10576 / 0 / 585 | 7620 / 0 / 610 |
| $S$ on F$^2$ | 1.056 | 1.086 |
| Final R indices [I>2 $\sigma$ (I)] | R1 = 0.0242, $w$R2 = 0.0526 | R1 = 0.0427, $w$R2 = 0.1187 |
| R indices (all data) | R1 = 0.0293, $w$R2 = 0.0547 | R1 = 0.0519, $w$R2 = 0.1265 |
| Largest difference peak/hole | 1.595 and -0.898 e.Å$^{-3}$ | 0.731 and -0.504 e.Å$^{-3}$ |
| Absolute structure parameter | ? | ? |

**Table 5.9** Crystal data and details of structural refinement for complex **22**

| | **22** |
|---|---|
| Empirical formula | $C_{36}H_{31}Cl_2CrF_6N_4O_6S_2$ |
| Formula weight | 916.679 |
| Temperature [K] | 293(2) |
| Wavelength [Å] | 0.71073 |
| Crystal system | Triclinic |
| Space group | $P$-1 |
| $a$/Å | 12.324(3) |
| $b$/Å | 13.279(3) |
| $c$/Å | 14.257(3) |
| $\alpha$/° | 83.17(3) |
| $\beta$/° | 67.31(3) |
| $\gamma$/° | 68.09(3)° |
| $V$/Å$^3$ | 1996.3(10) |
| $Z$ | 2 |
| calc. density/g cm$^{-3}$ | 1.5250(6) |
| $\mu$/mm$^{-1}$ | 0.603 |
| F(000) | 934 |
| Crystal size [mm$^3$] | 0.16 x 0.06 x 0.02 |
| $\theta$ range [°] | 3.18 to 24.15 |
| Index ranges | -14<=h<=14, |
| | -15<=k<=15, |
| | -16<=l<=16 |
| Reflections collected | 11935 |
| Independent reflections | 6356 |
| $R_{int}$ | 0.0253 |
| Completeness to $\theta$ | 99.5 % |
| Refinement method | Full-matrix least-squares on $F^2$ |
| Data / restraints / parameters | 6356 / 0 / 557 |
| $S$ on $F^2$ | 1.045 |
| Final R indices [I>2 σ (I)] | R1 = 0.0500, $w$R2 = 0.1304 |
| R indices (all data) | R1 = 0.0661, $w$R2 = 0.1399 |
| Largest difference peak/hole | 0.530 and -0.606 e.Å$^{-3}$ |
| Absolute structure parameter | ? |

# 6 References

[1] F. Hueso-Urena, N. A. IIIan-Cabeza, M. N. Moreno-Carretero, J. M. Martinez-Martos, M. J. Ramirez-Exposito, *J. Inorg. Biochem.* **2003**, *94*, 326–334.

[2] M. S. Refat, S. A. El-Korashy, A. S. Ahmed, *Spetrochim. Acta*, **2008**, *71A*, 1084–1094.

[3] A. Tsunoda, M. Shibisawa, Y. Yasuda, N. Nakao, K. Kusano, *Anticancer Res.* **1994**, *14*, 2637–2642.

[4] E. S. Raper, *Coord. Chem. Rev.*, **1985**, *61*, 115–184.

[5] J. S. Casas, E. E. Castellans, M. D. Louce, J. Ellena, A. Sanchez, J. Sordo, C. Taboada, *J. Inorg. Biochem.* **2006**, *11*, 1858–1860.

[6] M. J. Campbell*, Coord. Chem. Rev.* **1975**, *15*, 279–319.

[7] M. C. Rodriguez-Argüelles, M. B. Ferrari, G. G. Fava, C. Pelizzi, P. Tarasconi, R. Albertini, P. P. Dall'Aglio, P. Lunghi, S. Pinelli, *J. Inorg. Biochem.* **1995**, *58*, 157–175.

[8] J. S. Casas, M. S. Garcia-Tasende, C. Maichel-Mossmer, M.C. Rodriguez-Argüelles, A. Sanchez, J. Sordo, A. Vazquez-Lopez, S. Pinelli, P. Lunghi, R. Albertini, *J. Inorg. Biochem.* **1996**, *62*, 41–55.

[9] M. B. Ferrari, G. G. Fava, G. Tarasconi, R. Albertini, S. Pinelli, R. Starcich, *J. Inorg. Biochem.* **1994**, *53*, 13–25.

[10] U. Koch, B. Attenni, S. Malancona, S. Colarusso, I. Conte, M. D. Filippo, S. Harper, B. Pacini, C. Giomini, S. Thomas, I. Incitti, L. Tomei, R. D. Francesco, S. Altamura, V.G. Matassa, F. Narjes, *J. Med. Che*m. **2006**, *49*, 1693–1705.

[11] W. Beck, N. Kottmair, *Chem. Ber.* **1976**, *109*, 970–993.

[12] N. Kottmair, W. Beck, *Inorg. Chim. Acta* **1979**, *34*, 137-144.

[13] A. Ashnagar, N. G. Naseri, B. Sheeri, *Chin. J. Chem.* **2007**, *25*, 382−384.

[14] J. N. Delgado, W. A. Remers, J. B. Lippincott (Eds.), *Wilson and Gisvold's Textbook of Organic Medicinal Pharmaceutical Chemistry*, 9th. ed., L. Williams & Wilkins, Philadelphia, **1991**, pp. 39, 341, 376.

[15] L. Fillaut, I. de los Rios, D. Masi, A. Romerosa, F. Zanobini, M. Peruzzini, Eur. *J. Inorg. Chem.* **2002**, *4*, 935-942.

[16] O. T-Arpaci, A. Ozdemir, I. Yalcin, I. Yildiz, E. Aki-Sener, N. Altanlar, *Arch. Pharm.* **2005**, *338*, 105-111.

[17] Merck index 13th

[18] T. W. G. Solomons, C. B. Fryhle, *Organic Chemistry*, 9th ed. John Wiley & Sons, Inc., NJ, **2008**, p. 867-868.

[19] J. H. Block, J. M. Beale, *Wilson and Gisvold's Textbook of Organic Medicinal and Pharmaceutical Chemistry*, 11th. ed., Lippincott Williams & Wilkins, Philadelphia, **2004**, pp. 493-494.

[20] W. O. Foye, T. L. Lemke, D. A. Williams, *Principles of Medicinal Chemistry*, 4th ed. Williams & Wilkins, Philadelphia, **1995**, pp 88, 89, 154-180.

[21] A. Kar, *Medicinal Chemistry*, Anshan Ltd. **2006**, pp-117-121.

[22] D. A. Williams, T. L. Lemke, Foye's *Principles of Medicinal Chemistry*, 5th ed. Lippincott Williams & Wilkins, Philadelphia, **2002**, pp 377-378.

[23] F. Sandberg, *Acta Physiol Scand*. **1951**, *24*, 7–26.

[24] T. C. Butler, *J. Am. Chem. Soc.* **1955**, *77*, 1486–1488.

[25] A. Baeyer, *Ann. Phys.* **1863**, *127*, 199.

[26] G. A. Jeffrey, S. Ghose, J. O. Warwicker, *Acta Cryst.* **1961**, *14*, 881–887.

[27] W. Bolton, *Acta Cryst.* **1963**, *16*, 166–173.

[28] T. C. Lewis, D. A. Tocher, S. L. Price, *Cryst. Growth Des*. **2004**, *4*, 979–987.

[29] E. Sinn, C. M. Flynn, R. B. Martin, *J. Am. Chem. Soc.* **1978***, 2,* 489-492.

[30] (a) M. S. Masoud, A. M. Heiba, F. M. Ashmawy, *Transition Met. Chem*. **1983**, *8*, 124–126.

(b) M. S. Masoud, A. M. Heiba, *Transition Met. Chem*. **1989**, *14*, 175-180.

[31] Y. Xiong, C. He, T. -C. An, C.-H. Cha, X. -H. Zhu, *Transition Met. Chem.* **2003**, *28*, 69-73.

[32] F. Bonati, A. Burini, B. R. Pietroni, B. Bovio, *J. Organomet. Chem*. **1986**, *317*, 121−135.

[33] B. M. Craven, E. A. Vizzini, M. M. Rodrigues, *Acta Crystallogr.* **1969**, *B25*, 1978.

[34] B. Berking, B. M. Craven, *Acta Crystallogr.* **1971**, *B27*, 1107−1115.

[35] B. Berking, *Acta Crystallogr.* **1972**, *B28*, 98–113.

[36] W. J. Doran, *Medicinal chemistry*, **1959**, Vol. 4, John Wiley, New York.

[37] B. C. Wang, B. M. Craven, *Chem. Commun*. **1971**, 290−291.

[38] L. R. Nassimbeni, A. Rodgers, *Acta Crystallogr*. **1974**, *30*, 2593−2602.

[39] G. V. Fazakerley, P. W. Linder, L. R. Nassimbeni, A. L. Rodgers, *Inorg. Chim. Acta* **1974**, *9*, 193−201.

[40] L. Nassimbeni, A. Rodgers, *Acta Crystallogr*. **1974**, *30*, 1953−1961.

[41] F. Yilmaz, V. T. Yilmaz, E. Bicer, O. Büyükgüngör, *J. Coord. Chem.* **2007**, *60*, 777−784.

[42] F. Yilmaz, V. T. Yilmaz, C. Kazak, *Z. Anorg. Allg. Chem.* **2005**, *631*, 1536−1540.

[43] Z.-D. Liu, H.-L. Zhu, *Acta Cryst*. **2004**, *60*, 1883−1885.

[44] M. S. Masoud, M. F. Amira, A. M. Ramadan, G. M. El-Ashry, *Spectrochim. Acta*. **2008**, *69*, 230−238.

[45] J. Fawcett, W. Henderson, R. D. W. Kemmitt, D. R. Russel, A. Upreti, *J. Chem. Soc. Dalton Trans.* **1996**, *9*, 1897−1903.

[46] B. Rudolf, J. Zakrzewski, *J. Organomet. Chem*. **2000**, *597,* 17−19.

[47] A. Bult, H. B. Klasen, *Spectorscopy Lett*. **1976**, *9*, 81−94.

[48] G. E. Damsma, A. Alt, F. Brueckner, T. Carell, P. Cramer, *Nature* **2007**, *14*, 1127−1133.

[49] A. Romanelli, R. Iacovino, G. Piccialli, F. Ruffo, L. De Napoli, C. Pedone, B. Di Blasio, A. Messere, *Organomet.* **2005**, *24*, 3401–3406.

[50] L. D. Pettit, M. Bezer, *Coord. Chem. Rev.* **1985**, *61*, 97–114.

[51] D. J. Nelson, P. L Yeagle, T. L. Miller; R. B. Martin, *Bioinorg. Chem.* **1976**, *5*, 353–358.

[52] M. C. Lim, R. B. Martin, *J. Inorg. Nucl. Chem.* **1976**, *38*, 1915–1918.

[53] J. Kuduk-Jaworska, A. Puszko, M. Kubiak, M. Pelczynska, *J. Inorg. Biochem.* **2004**, *98*, 1447–1456.

[54] G. Zhao, L. Huakuan, P. Yu, H. Sun, S. Zhu, X. Su, Y. Chen, *J. Inorg. Biochem.* **1999,** *73*, 145–149.

[55] E. Budzisz, U. Krajewska, M. Rozalski, A. Szulawska, M. Czyz, B. Nawrot, *Eur. J. Pharm.* **2004**, *502*, 59–65.

[56] D. S. Dwyer, K. Gordon, B. Jones, *Int. J. Immunopharmacology*. **1995**, *17*, 931–940.

[57] (a) T. W. Hayton, P. Legzdins, W. B. Sharp, *Chem. Rev.* **2002**, *102*, 935.–992

(b) N. A. Davies, M. T. Wilson, E. Slade, S. P. Fricker, B.A. Murrer, N.A. Powell, G.R. Henderson, *Chem. Commun*. **1997**, 47–48.

[58] (a) B. Cetinkaya, E. Cetinkaya, H. Kucukbay, R. Durmaz, *Arzneimittel-Forschung,* **1996**, *46*, 821–823.

[59] C. S. Allardyce , P. J. Dyson, D. J. Ellis, P. A. Salter, R. Scopelliti, *J. Organomet. Chem.* **2003**, *668*, 35–42.

[60] R. E. Morris, R. E. Aird, P. del Socorro Murdoch, H. Chen, J. Cummings, N. D. Hughes, S. Parsons, A. Parkin, G. Boyd, D. I. Jodrell, P. J. Sadler, *J. Med. Chem*. **2001**, *22*, 3616−3621.

[61] H. Chen, J. A. Parkinson, R. E. Morris, P. J. Sadler, *J. Am. Chem. Soc*. **2003**, 125(1), 173−186.

[62] R. E. Aird, J. Cummings, A. A. Ritchie, M. Muir, R. E. Morris, H. Chen, P. J. Sadler, D. I. Jodrell, *Brit. J. Cancer.* **2002**, *86*, 1652−1657.

[63] (a) T. W. Johann, J. K. Barton, *Philos. Trans*. *R*. *Soc*. *Lond*. **1996**, *354*, 299−324.

(b) K. E. Erkkila, D. T. Odom, J. K. Barton, *Chem. Rev.* **1999**, *99*, 2777−2795.

[64] S. Schäfer, W. S. Sheldrick, *J. Organomet. Chem.* **2007**, *692*, 1300−1309.

[65] D. Herebian, W. S. Sheldrick, *J. Chem. Soc. Dalton Trans*., **2002**, *6*, 966−974.

[66] T. K. Schoch, J. L. Hubbard, C. R. Zoch, G.-B. Yi, M. Sørlie, *Inorg. Chem.*, **1996**, *35*, 4383−4390.

[67] G. Tuchtenhagen, K. Rühlmann, *Liebigs Ann. Chem*. **1968**, *711*, 174−183.

[68] B. N. Diel, T. L. Hubler, W. G. Ambacher, *Heteroatom. Chem*. **1999**, *10*, 423−429.

[69] J. Sundermeyer, H. W. Roesky, M. Noltemeyer, *Can. J. Chem*. **1989**, *67*, 1785−1787.

[70] N. Weis, H. Pritzkow, W. Siebert, *Eur. J. Inorg. Chem*. **1999**, *1*, 7−9.

[71] I. Matsuda, T. Takahashi, Y. Ishii, *Chem. Lett*. **1977**, *12*, 1457−1460.

[72] R. Neidlein, D. Knecht, *Helv. Chim. Acta*, **1987**, *70*, 1076−1078.

[73] (a) D. Walther; M. Teutsch, *Z. Chem*. **1976**, *16*, 118−19.

(b) D. Walther; *Z. Anorg*. Allg. Chem. **1974**, *405*, 8−18.

[74] K. Schlosser, E. Hoyer, *Z. Chem.* **1970***, 10,* 439−440.

[75] K. Schlosser, E. Hoyer, *Z. Anorg. Allg. Chem.* **1972***, 387,* 91−106.

[76] G. Van Koten, K. Vrieze, *Adv. Organomet. Chem.* **1982**, *21,* 151−239, and references cited therein.

[77] G. Van Koten, K. Vrieze, *Recl. Trav. Chim. Pays-Bas.* **1981**, *100*, 129−142, and references cited therein.

[78] (a) A. H. Krotz, L. Y. Kuo, J. K. Barton, *Inorg. Chem.* **1993**, *32,* 5963−5974.

(b) A. M. Pyle, M. Y Chiang, J. K. Barton, *Inorg. Chem.* **1990***, 29,* 4487−4495.

(c) A. M. Pyle, J. K. Barton, *Inorg. Chem.* **1987**, *26,* 3820−3823.

[79] B. N. Diel, P. J. Deardorff, C. M. Zelenski, *Tetrahedron Lett.* **1999**, *40*, 8523−8527.

[80] A. K. Das, S.-M. Peng, S. Bhattacharya, *Polyhedron*, **2001**, *20*, 327-335.

[81] A. M. Pyle, J. P. Rehmann; R. Meshoyrer; C. V. Kumar; N. J. Turro, J. K. Barton, *J. Am. Chem. Soc.* **1989**, *111 ,* 3051-3058.

[82] A. M. Pyle, E. C. Long; J. K. Barton, *J. Am. Chem. Soc*. **1989**, *111*, 4520−4522.

[83] S. J. Berners-Price, P. J. Sadler, *Coord. Chem. Rev*. **1996**, *151*, 1–40.

[84] Y. Inouye, T. Kanamori, T. Yoshida, X. Bu, M. Shionoya, T. Koike, E. Rimura, *Biol. Pharm. Bull*. **1994,** *17*, 243–250.

[85] H. Mitsuya, S. Broder, *Nature*, **1987**, *325*, 773–778.

[86] Y. X. Wang, P. Legzdins, J. S Poon, C. C. Y. Pang, J. *Cardiovasc. Pharmacol*. **2000**, *35*, 73–77.

[87] F. A. Cotton, L. R. Falvello, W. Schwotzer, C A. Murillo, G. Valle-Bourrouet, *Inorg. Chim. Acta*, **1991**, *190,* 89−95.

[88] T. J. Greenhough, B. W. S. Kolthammer, P. Legzdins, J. Trotter, *Acta Crystallogr.* 1980, *B36*, 795−799.

[89] R. Wilberger, H. Piotrowski, M. Warchhold, I.-P. Lorenz, *Z. Anorg. Allg. Chem.* **2003**, *629*, 2485−2492.

[90] M. Limmert, I.-P. Lorenz, J. Neubauer, H. Nöth, T. Habereder, *Eur. J. Inorg. Chem.* **2001,** *6*, 1593−1597.

[91] O. E. Woisetschläger, K. Sünkel, W. Weigand, W. Beck , *J. Organomet. Chem.* **1999**, *584*, 122–130.

[92] S. M. O. Quintal, H. I. S. Nogueira, V. Fe ̀lix, M. G. B. Drew, *Polyhedron*, **2002**, *21*, 2783–2791.

[93] P. Gruhlke, C. G. Seipelt, A. Dolle, M. D. Zeidler, P. Zaderenko, P. Ballesteros, S. Cerdan, *J. Chem. Soc*. **1995**, *2*, 2191–2194.

[94] L. Levi, C. E. Hubley, *Anal. Chem.* **1956**, *28*, 1591-1605.

[95] M. R. Caira, G. V. Fazakerley, P. W. Linder, L. R. Nassimbeni, *Acta Crystallogr.* **1973**, *B29,* 2898−2904.

[96] M. R. Caira, G. V. Fazakerley, P. W. Linder, L. R. Nassimbeni, *Inorg. Nucl. Chem. Lett*. **1973**, *9,* 1101−1104.

[97] M. F. Mahon, K. C. Molloy, M. M. Venter, I. Haiduc., *Inorg. Chim. Acta*., **2003,** *348* 75-81.

[98] C. Pettinari, G. G. Lobbia, G. Sclavi, D. Leonesi, *Polyhedron*, **1995**, *14*, 1709- 1723.

[99] J. T. Gill, J. J. Mayerle, P. S. Welcker, D. F. Lewis, D. A. Ucko, D. J. Barton, D. Stowens, S. J. Lippard, *Inorg. Chem.,* **1976**, *15*, 1155-1168.

[100] V. G. Albano, P. L. Bellon, G. Ciani and M. Manassero, *J. Chem. Soc., Dalton Trans.,* **1972**, *2*, 171-175.

[101] R. Bobka, *Dissertation*, **2007**, LMU München, 57.

[102] L. Dahlenburg, M. Kühnlein**,** *Eur. J. Inorg. Chem.* **2000**, *9*, 2117–2125.

[103] J. Wagler, A. F. Hill, *Organometallics,* **2008,** *27,* 2350–2353.

[104] M. Shakir, S. Khatoon, S. Parveen, Y. Azim, *Transition Met. Chem.* **2007**, *32*, 42–46.

[105] P. Govindaswamy, B. Therrien, G. Suess-Fink, P. Stepnicka, J. Ludvik. *J. Organomet. Chem.* **2007**, *692*, 1661–1671.

[106] M. T. Youinou, R. Ziessel, *J. Organomet. Chem.* **1989**, *363*, 197–208.

[107] D. F. Kennedy, B. A. Messerle, M. K. Smith, *Eur. J. Inorg. Chem.* **2007**, *(1)*, 80−89.

[108] D. Belli Dell' Amico, F. Calderazzo, L. Labella, F. Marchetti, E. Sbrana, *J. Organomet. Chem*. **2002**, *651*, 52–59.

[109] B. N. Diel, P. J. Deardorff, C. M. Zelenski, *Tetrahedron Lett.*, **1999**, *40*, 8523–8527.

[110] S. Nishigaki, H. Yoshioka, K. Nakatsu, *Acta Cryst*. **1978**, *34*, 857–879.

[111] A. Alvarez, R. Macias, M. J. Fabra, M. L. Martin, F. J. Lahoz, L. A. Oro, *Inorg. Chem*. **2007**, *46*, 6811-6826.

[112] L. Dahlenburg, M. Kuhnlein, *Eur.J. Inorg Chem*. **2000**, *9*, 2117–2125.

[113] R. D. Gilbertson, T. L. S. Lau, S. Lanza, H. P. Wu, T. J. R. Weakley, M. M. Haley, *Organomet*. **2003**, *22*, 3279–3289.

[114] A. Tiripicchio, M. T. Camellini, M. Ghedini, G. Dolcetti, *Transition Met. Chem.* **1980**, *5*, 102–105.

[115] P. Dapporto, G. Denti, G. Dolcetti, M. Ghedini, *J. Chem. Soc*., **1983**, *4,* 779–782.

[116] L. L. Koh, Y. Xu, L. Ji, *Acta Cryst*. **1994**, *50*, 884–886.

[117] S. Kammer, H. Müller, N. Grunwald, A. Bellin, A. Kelling, U. Schilde, W. Mickler, C. Dosche, H. J. Holdt, *Eur. J. Inorg. Chem.* **2006**, *8*, 1547–1551.

[118] S. Leelasubcharoen, K.-C. Lam, T. E. Concolino, A. L. Rheingold, K. H. Theopold *Organomet.* **2001,** *20*, 182–187.

[119] O. M. Heigl, E. Herdtweck, S. Grasser, F. H. Köhler, W. Strauss, H. Zeh, *Organomet.* **2002,** *21*, 3572–3579.

[120] J. C. Fettinger, S. P. Mattamana, R. Poli, R. D. Rogers, *Organomet.* **1996,** *15*, 4211–4222.

[121] A. A. Danopoulos, G. Wilkinson, T. K. N. Sweet, M. B. Hursthouse, *J. Chem. Soc., Dalton Trans.* **1996***, 3,* 271–281.

[122] V. W. L. Ng, W. K. Leong, L. L. Koh, G. K. Tan, L. Y. Goh, *J. Organomet. Chem.* **2004**, *689*, 3210–3217.

[123] P. Legzdins, J. T. Malito, *Inorg. Chem.* **1975**, *14*, 1875−1878.

[124] G. Brauer, *Handbuch der Präparativen Anorganischen Chemie*, 3rd. ed., vol 3, F. Enke, Stuttgart, **1981**, pp. 1951–1952.

[125] J. G. Stack, J. J. Doney, R. G. Bergman, C. H. Heathcock, *Organometallics*, **1990**, *9*, 453−466.

[126] G. Brauer, *Handbuch der Präparativen Anorganischen Chemie*, 3rd. ed., vol 3, F. Enke, Stuttgart, **1981**, pp. 2014–2015.

[127] M. J. Bhanushali, N. S. Nandurkar, M. D. Bhor, B. M. Bhanage, *Tetrahedron Lett.* **2007**, *48*, 1273–1276.

[128] P. Serp, M. Hernandez, B. Richard, P. Kalck, *Eur. J. Inorg. Chem.* **2001**, *9*, 2327–2336.

[129] C. M. Fendrick, L. D. Schertz, E. A. Mintz, T. J. Marks, T. E. Bitterwolf; P. A. Horine, T. L. Hubler, J. A. Sheldon, D. D. Belin, *Inorg. Synth.* **1992**, *29*, 193–198.

[130] C. White, A. Yates, P. M. Maitlis, D. M. Heinekey, *Inorg. Synth.* **1992**, *29*, 228–234.

[131] M. A. Bennett, T.-N. Huang, T. W. Matheson, A. K. Smith, *Inorg Synth.* **1982**, *21*, 74–78.

[132] G. Brauer, *Handbuch der Präparativen Anorganischen Chemie*, 3rd. ed., vol 3, F. Enke, Stuttgart, **1981**, pp. 1953–1955.

[133] (a) G. M. Sheldrick, *SHELXL-97, An Integrated System for Solving and Refining Crystal Structures from Diffraction Data*, University of Göttingen, Germany, **1997**.
(b) G. M. Sheldrick, *Acta Crystallogr.,* Sec. A: Found. Crystallogr. **2008**, *A64*, 112–122.

# CURRICULUM VITAE

## Personal Details

Date of Birth            06.08.1977

Place of Birth           Dhaka, Bangladesh

Nationality              Bangladeshi

Marital Status           Married

## Education

01/2006-09/2009    PhD in Inorganic Chemistry (Department of Chemistry and Biochemistry), Ludwig Maximilans-Universität München (LMU)

Supervisor: Prof. I.-P. Lorenz

**Title:** Coordination Chemistry of Barbituric Acid, its Diethyl Derivative and Benzildiimine with Transition Metals.

1997-98            M.Sc. in Chemistry (Physical-Inorganic), University of Dhaka, Bangladesh (Exam held in 2000) Grade: 1$^{st}$ Class

**Title:** A study of the interaction of 5,5-diphenylhydantoin and 1,5-diphenylcarbazone with Cd(II) and Zn(II) ions in mixed solvent

Supervisor: Prof. A. M. Shafiqul Alam

| 1995-97 | B.Sc. (Hons.) in Chemistry, University of Dhaka, Bangladesh |
| | (Exam Held in 1999) Grade: $2^{nd}$ Class |

| 1992-94 | Higher Secondary Certificate |
| | Viqarunnisa Noon College, Dhaka, Bangladesh |
| | Grade: $1^{st}$ Division |

| 1982-92 | Secondary School Certificate |
| | Pallabi M. I. Model High School, Dhaka, Bangladesh |
| | Grade: $1^{st}$ Division |

## Award

| 5/2008-4/2009 | Recipient of scholarship from the Bayerische Forschungsstiftung München. |

## Experiences

| 5/2001- 6/2002 | Teacher at the Cherry Blossoms International School, Dhaka, Bangladesh. |
| 7/2002-12/2004 | Teacher at the Adamjee Cantonment College, Dhaka, Bangladesh |

| **Language** | English (Excellent: Reading, Writing and Speaking) |
| | German (Weak) |

| **Computer Skill** | Ms Word, Ms Power Point, ChemDraw, Delta, ORTEP, Adobe Illustrator, ResView, SciFinder Scholar. |
| | Operating System: MSWindows. |

# List of publications

1.  Synthesis, Crystal Structure and Spectroscopic Characterisation of Mono- and Dinuclear 5,5-Diethylbarbiturato Complexes of Chromium(0) and Rhenium(I).
    **N. Haque**, J. N. Roedel, I.-P. Lorenz, *Z. Anorg. Allg. Chem.* **2009**, *635*, 496−502.

2.  Synthesis, structures, and characterization of benzildiimine complexes of rhodium(III) and iridium(I).
    **N. Haque**, B. Neumann, J. N. Roedel, I.-P. Lorenz, *Inorg. Chim. Acta.* **2010**, *363*, 723−728.

3.  Formation of the Complexes $[Fe(H_2BDI)_3]X_2$ and $[CpCr(H_2BDI)_2]X_2$ (X = OTf) from the Unusual Reactions of Benzil-bis(trimethylsilyl)diimine with $CpML_2Cl$ (M = Fe, L = CO; M = Cr, L = NO).
    **N. Haque**, B. Neumann, I.-P. Lorenz, *Z. Naturforsch.* **2010**, *65b*, 101−106.

4.  Mono- and bidentate function of 5,5-Diethylbarbiturato ligand towards some $d^n$ transition metals (n = 6, 8, 10).
    **N. Haque**, B. Neumann, P. Mayer, I.-P. Lorenz, *J. Organomet. Chem.* **2010**, manuscript in preparation.

5.  Ligandendesign und Katalysepool: Neue *N,N'*- und *N,P*-Komplexe.
    **N. Haque**, B. Köhler, B. Neumann, I.-P. Lorenz, *Industrietag* 05.10.**2006***,* München (**Poster**)